CHAPTER IV

RESULTS AND DISCUSSION

The preservation of heritage textiles is a crucial aspect of cultural heritage conservation. The deterioration of textiles is often caused by microbial and insect infestation, which can result in permanent damage or loss of historical and cultural artifacts. Therefore, the development of effective preservation methods for textiles is of paramount importance.

The aim of this study was to develop a preservative fabric for the long-term conservation of heritage textiles from microbes and insects. The development of the preservative fabric involved the use of traditional practices as a foundation, but with a scientific approach to overcome the limitations of those practices. Thereby, providing more effective preservation environment over a larger surface area, for a longer period of time.

In the results and discussion chapter of this study, a thorough analysis of the data collected from the experiments is presented. The chapter comprehensively interprets and showcases the findings, emphasizing the important results, their significance, and their implications for the cultural heritage conservation field. Moreover, the efficacy of the preservative fabric in preventing microbial and insect damage, as well as its long-term effectiveness, will be examined in detail within this chapter.

The findings have been presented and analyzed in the subsequent sub-sections:

4.1 Studying the preservative practices followed at the museums and by the individuals at home

4.2 Studying the micro flora of the preserved cellulosic and protein textiles

- 4.2.1 Selection of the degraded textile
- 4.2.2 Isolating and identifying the microorganisms present on the preserved cellulosic and protein fabrics undergone deterioration
- 4.2.3 Characterization and identification of bacterial isolates:
  - 4.2.3.1 Morphological characterization
  - 4.2.3.2 Biochemical characterization
  - 4.2.3.3 Identification of fungal isolates

4.3 Preparation of nanoparticles (NPs)

4.3.1 Selection of core and wall material

4.3.2 Preparation of essential oil chitosan nanoparticles (CNPs)

4.3.2.1 Pilot work

4.3.2.1.1 Screening the parameters for developing neem essential oil nanoparticles

4.3.2.1.2 Screening the parameters for developing cinnamon essential oil nanoparticles

4.3.2.1.3 Screening the parameters for developing clove essential oil nanoparticles

4.3.2.1.4 Screening the parameters for developing carom essential oil nanoparticles

4.4 Optimizing nanoparticle formulation and process parameters to maximize the Entrapment Efficiency

4.4.1 Effect of Chitosan concentration on the entrapment efficiency, loading capacity, and nanoparticle size

4.4.2 Effect of % surfactant on the entrapment efficiency, loading capacity, and the size of the nanoparticles

4.4.3 Effect of oil concentration on entrapment efficiency, loading capacity, and the size of the nanoparticles

4.4.4 Impact of % TPP on the entrapment efficiency, loading capacity, and the size of the nanoparticles

4.5 Characterization of the nanoparticles

4.5.1 Determining the calibration curve of the essential oils

4.5.2 Determining the particle size and the polydispersity index (PDI) of the prepared nanoparticles

4.5.3 Determining the minimum inhibitory concentrations of the NPs (MIC)

4.5.4 Surface analysis of the prepared NPs using Scanning electron microscope (SEM)

4.6 Application of the optimized essential nanoparticles on the substrate

4.7 Assessment of the treated fabrics

4.7.1 Assessment of Antibacterial activity of the treated cotton and polyester fabric using standard AATCC 147

4.7.2 Determination of Antifungal test using standard AATCC 30: Antifungal Assessment and Mildew Resistance Test

4.7.3 Surface analysis of the coated cotton and polyester fabrics using Energy dispersive X-ray spectroscopy (EDX)

4.7.4 Determining the physicochemical stability of the nanoparticles over time and storage conditions

4.7.5 Determination of resistance to insects using standard ISO 3998:1977

4.8 SWOC analysis of the developed preservative fabric

4.1 Studying the preservative practices followed at the museums and by the individuals at home

The aim of this objective was to understand and study the preservative practices that are currently being used at museums and by individuals at home in order to develop an effective preservative environment for heritage textiles. This approach provided valuable insights into the existing preservation methods and highlighted the limitations and challenges of these methods. By understanding the weaknesses of these methods, researcher created a preservative fabric that is not only effective but also practical and feasible to use in the museums and also by individuals at home.

In order to achieve this objective, the researcher visited several textile museums to gather primary data by interacting with museum conservators and curators. The following museums were included in the study:

- The Textile Art Museum at the Department of Clothing and Textiles, The Maharaja Sayajirao University of Baroda, Vadodara
- Baroda Museum and Picture Gallery, Vadodara
- Calico Museum in Ahmedabad
- Raja Dinkar Kelkar Museum in Pune
- National Museum in New Delhi

- Crafts Museum in New Delhi
- Anne Lambert Clothing and Textile Collection at the University of Alberta in Edmonton, Canada

Table 4.1 Preservative practices followed by the Museums

Name of the Museum	**Preservative practices followed**
The Textile Art Museum Department of Clothing and Textiles, The Maharaja Sayajirao University of Baroda, Vadodara	Large artifacts were mounted between pixel glass frames to enhance their preservation by protecting them from direct light, dust particles and insects. Tobacco leaves that have been dried are placed between muslin fabric that has had its starch removed. This is used as a foundation layer in museum shelves or drawers. The museum textiles are then placed on top of this flat surface.
Baroda Museum and Picture Gallery, Vadodara	The museum used Incandescent and LED lights because they emit low levels of ultraviolet and blue light, which helps to reduce the negative impact of light on textiles such as fading, discoloration, and brittleness. Ceiling fans were used to maintain a consistent temperature and air circulation within the museum, which help prevent the buildup of heat and humidity that can damage textiles. By circulating the air, ceiling fans also help to distribute cool air from air conditioning units throughout the space more effectively. Exhaust fans were used to remove excess moisture and pollutants from the air, which can also help to prevent damage to textiles. High humidity levels can lead to mold growth, which can cause irreparable damage to textiles, and pollutants in the air can also cause discoloration and deterioration of the fabrics. Exhaust fans help to remove these harmful elements from the museum environment, promoting a healthier and safer environment for the textiles.

	Naphthalene balls were typically employed to protect their collections from moth damage. A small bag of mulmul fabric was placed in the corners of the display and storage areas, which was filled with dried crushed leaves of neem and cloves.
Calico Museum in Ahmedabad	The Calico Museum also utilized Incandescent and LED lights because they reduce the impact of photochemical degradation. Additionally, the museum preferred to on the lights and keep them dimmed until visitors arrived at the display, and then turn them off again. The museum also implemented the use of ceiling fans and exhaust fans to prevent the air from becoming overly humid by removing excess moisture and to promote air circulation. Small bag of mulmul fabric at the corner of the display and storage area (boxes, cabinets, etc.) in a small glass dish which contains dried crushed leaves of neem and tobacco. Some textiles were also sandwiched between two sheets of clear plastic film, which were then sealed together by weaving them using needle and thread which creates small holes, which allow air to circulate around the textile. The plastic film provides a barrier to protect the textile from environmental factors such as light, dust, and humidity, which can cause damage over time. Naphthalene balls were used to protect the textiles from moth damage. Scoured muslin treated with tea extracts was used as a backing material as it provides natural antibacterial property.
Raja Dinkar Kelkar Museum in Pune	The museum also practiced using LED and Incandescent lights along with ceiling fans, exhaust fans and dehumidifiers. Fumigation was practiced once a year especially during monsoons. Use of Naphthalene balls was done to prevent damage caused by insects

National Museum in New Delhi	Practice of incandescent and LED lights, as well as ceiling and exhaust fans was found to be common. During the monsoon season, a dehumidifier was used if necessary. Naphthalene balls was used as an insect repellent. Use of coarse, de-starched muslin fabric was implemented as a backing material to provide extra support for delicate and fragile fabrics. Additionally, silica gel was used for preserving cottons, and pyridine chlorobenzene was used for preserving wools and silk. These preservation materials were stored in muslin bags placed below the storage paper in shelves and cupboards. Finally, when any new textiles were added to the museum collection, fumigation was done to prevent infestations.
Crafts Museum in New Delhi	Crafts museum also practiced the use of incandescent and LED lights, as well as ceiling and exhaust fans. A dehumidifier may be used during the monsoon season if needed, and naphthalene balls are utilized to protect against insects. Coarse, de-starched cotton fabric was used as a backing material for additional support. Unbleached, sterilized knitted cotton fabric (typically used in medical field) were used on rollers and as a padding material on hangers. In addition, the curator recommended to use carom seed, and dried cannabis (bhang) leaves for preservation purposes against microbes and insects.
Anne Lambert Clothing and Textile Collection at the University of Alberta in Edmonton, Canada	The museum utilizes mobile shelving systems to store their textile collection. These shelves are opened for inspection or for museum visitors and are designed to protect the textiles from dust and light. The textiles are laid on acid-free paper and stored in acid-free containers, sometimes wrapped in acid-free tissue paper to prevent acid migration.

	Textiles are flat laid, and the sturdy ones are hung on a padded hangers. Larger textiles are rolled for storage. The dry climate in Alberta means that the museum does not encounter insect problems. New textiles brought into the museum are typically fumigated to prevent any potential infestations. The climate is carefully controlled to maintain a temperature range of 18-22°C and relative humidity level between 40-50%. For 3D storage of textiles such as hats and shoes, they are stuffed with acid-free tissue paper to help maintain their shape.

Table 4.1 represents the preservative practices followed the museums that were visited by the researcher. In addition to the pointers listed in the table, all the museums had common ways of storing fragile and sturdy artifacts. Small, delicate items were typically laid flat in display cases, while sturdier items were hung on padded hangers. Sarees, big carpets and rugs were often rolled and displayed along walls, depending on their condition. Every museum used light and soft brushing, and vacuuming to surface clean the textiles being the safest method to clean aged textiles.

According to the responses collected from the textile collectors, the greatest threats to textiles were considered to be dust, followed by light, insects, microorganisms, temperature, and relative humidity. Respondents stored their textiles in metal trunks and wooden wardrobes, and wrapped them in washed mull fabric before storage. They tried to minimize the number of folds when storing, with most using four to six folds, and stacked them on top of each other. Two respondents separated their Zari artifacts. Respondents also changed the folds of their textiles yearly, and some exposed the textiles to sunlight for a few hours once a year to aerate and kill microbes. While being aware that the exposure to sunlight can be effective for microbial control, it can also cause fading and damage to textiles over time, so caution should be taken when using this method. Each of the participants utilized naphthalene balls as a means of preservation. A total of three individuals opted to use a sachet comprised of a cotton bag containing cloves and cinnamon stick, which acted as a deterrent to both insects and microbes. Another participant employed a sachet containing sandalwood and lavender as an insect repellent. The sachets were expected to be replaced biannually or according to a predetermined schedule, but adherence to this practice was not consistently followed. Overall, the respondents'

methods demonstrated a good understanding of the factors that can affect textile preservation and satisfactory commitment to preserving their keepsakes.

The most common preservative observed at the museums and by the textile collectors was the use of natural herbs and spices which has a spectrum of antimicrobial and insect repellent property. The reason tobacco leaves are used is because they act as a natural preservative, preventing the growth of insects and fungi that can damage the textiles. Dried tobacco leaves contain nicotine, which has antimicrobial properties and acts as a natural insect repellent. When placed in an enclosed space, such as a museum storage shelf or drawer, the nicotine from the tobacco leaves will evaporate and create a protective atmosphere that inhibits the growth of bacteria, fungi, and insects. This makes tobacco leaves an effective and natural way to preserve textiles. However, it's worth noting that the use of tobacco leaves for preservation purposes is not without controversy due to the health risks associated with tobacco use. Dried neem leaves contain compounds such as azadirachtin, nimbin, and nimbidin, which have antimicrobial and insecticidal properties. Neem leaves are a popular alternative to tobacco leaves, particularly in regions where tobacco use is not acceptable. Additionally, neem leaves are non-toxic and do not pose any health risks, making them a safer option for preservation purposes. Clove and Cinnamon were also used as a natural preservative for textiles as it is a safe and effective way to protect textiles from damage and preserve them for longer periods of time. Eugenol from clove and cinnamaldehyde and proanthocyanidins from Cinnamon has shown to inhibit the growth of bacteria, fungi and also repel insects because of its strong pungent aroma.

Lavender and sandalwood are commonly used as natural preservatives for textiles due to their insect-repellent properties and pleasant aroma. Lavender contains compounds, such as linalool and linalyl acetate, which are known to repel insects, including moths, and can help protect textiles from damage caused by insect infestation (Medha et al., 2021). Similarly, sandalwood also has insect-repellent properties, and its oil has been shown to be effective against a variety of insects, including termites and cockroaches. In addition to their insect-repellent properties, lavender and sandalwood are valued for their pleasant aroma, which can help to freshen up textiles and keep them smelling good. The fragrance of lavender and sandalwood has also been shown to have a calming effect, which may help to reduce stress and promote relaxation.

Naphthalene balls were also commonly used by everyone as an effective moth repellent and to protect the textiles from other insect damage. But, one of the most significant risks is

that naphthalene balls can leave behind oily stains on fabrics and textiles, particularly if the naphthalene balls come into direct contact with the textile. These stains can be difficult to remove and may require professional cleaning to fully remove. Additionally, they can cause discoloration or yellowing of the fabric over time. This is especially true for delicate or light-colored fabrics. It is important to handle naphthalene balls with care to minimize the risk of exposure and adverse effects or use alternative source of preservatives.

As suggested by the curator of Crafts Museum, Delhi, carom seed as a natural preservative against microbes and insects. It contains thymol, which is a powerful antiseptic and antimicrobial agent. When applied to textiles, it can help repel microorganisms that can cause damage or decay. In addition to its antimicrobial properties, carom seed oil is also believed to have insecticidal properties that can help to deter moths and other pests that can damage textiles. Another advantage of using carom seed oil is that it has a pleasant, spicy aroma that can help to mask musty or unpleasant odours that may be present in textiles. This can be particularly beneficial for antique textiles that may have been stored for long periods of time and may have developed an unpleasant odour. The idea behind recommending dried Cannabis leaves as a preservative was the leaves of the cannabis plant contain a variety of compounds, including cannabinoids and terpenes, that can help to protect textiles from decay and damage from microbes and insects. One of the advantages of using cannabis leaves as a natural preservative is that they are non-toxic and environmentally friendly. However, it is important to note that the use of cannabis leaves as a textile preservative may be illegal in some jurisdictions due to the legal status of cannabis.

Conservators also mentioned, however, these preservation methods are not always effective or practical, especially when it comes to preserving large collections of heritage textiles over extended periods. Sachets containing herbs and spices may only provide limited protection against insects and microbes. They may not be effective against all types of pests or may only be effective for a limited period of time. Sachets are typically small and may not provide complete coverage for larger textiles. Insects and microbes may still be able to access areas that are not covered by the sachet. While, some herbs and spices may contain pigments or oils that can stain textiles. This can be particularly problematic for delicate or valuable textiles. Additionally, layering a bed of dried neem and tobacco leaves below the textiles can be a tedious process and may also cause damages to textiles if contaminated by its small particles.

Considering the pros and cons of the use of traditional preservative practices, the researcher decided to apply the principles of traditional practices in combination with a more scientific approach, by developing a preservative fabric that provides a better preservation environment over a larger surface area for a longer time. By taking this approach, the researcher addressed all of the limitations of traditional practices, resulting in a preservation method that is both effective and practical, with no adverse side effects.

4.2 Studying the micro flora of the preserved cellulosic and protein textiles

One of the primary issues that can be caused by microorganisms is degradation. Certain types of bacteria and fungi can break down the fibers in textiles, causing them to weaken and eventually disintegrate. Some bacteria and fungi also cause discoloration and staining on the textiles. This can lead to significant damage to the textiles over time, making it important to identify and address any microorganisms that may be present even in some kind of preserved conditions. In addition to identifying the types of microorganisms that are present, studying the microflora of preserved textiles can also provide information about the environmental conditions that are conducive to microbial growth. This information can be used to develop a preservation strategy that addresses these factors.

4.2.1 Selection of the degraded textiles

The fabrics chosen for analysis comprised of cotton and silk which were more than 60 years old and had been preserved by wrapping them in mulmul fabric along with naphthalene balls by one of the textile collectors. These fabrics had become weak and were disintegrating even with light handling. Additionally, wool fabric which had been kept in a storage area for clothing and textiles for more than 30 years that had previously undergone moth infestation and had holes in them, but later exposed to naphthalene balls was also selected for the study. The objective was to identify the fungi and bacteria that had grown on these materials.

4.2.2 Isolating and identifying the microorganisms present on the preserved cellulosic and protein fabrics undergone deterioration

The suspension was spread on six separate plates for each fabric, with three rounds of spreading done. After that, the plates were placed in an incubator for 24 hours. The resulting colonies were identified with labels consisting of both letters and numbers. Figure 4.1 displays the colonies that were grown on nutrient agar plates from cotton fabric.

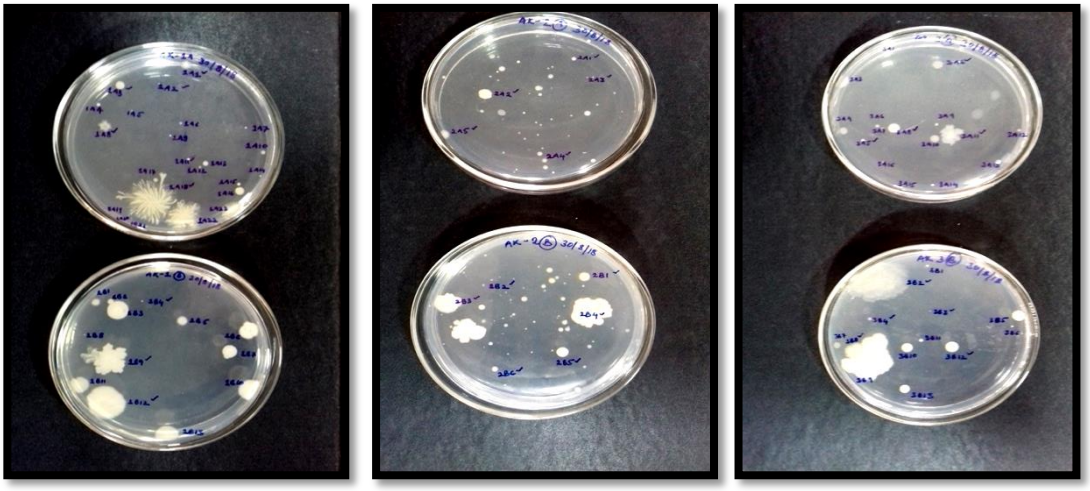

Fig. 4.1: Colonies developed on Agar plates

The isolated bacteria were observed for visually identical colonies and the non-identical ones from each plate were then sub-cultured individually into new plates and preceded for its identification. Table 4.2 shows the bacterial load for each fabric grown on their plates.

Table 4.2: Bacterial load on nutrient agar for the three fabrics

Number of plates/ samples	**Name of the plates/ sample**	**Number of colonies in each plate for cotton fabric**	**Number of colonies in each plate for silk fabric**	**Number of colonies in each plate for wool fabric**
1	1A	23	2	0
2	1B	13	7	1
3	2A	49	2	3
4	2B	60	2	5
5	3A	19	4	4
6	3B	13	9	1
Total number of colonies		177	26	14
Visually non-identical colonies		32	08	06

The data presented in Table 1 indicated that the amount of bacteria present was highest on the cotton fabric, followed by the silk and wool fabrics. To further identify these bacteria, a total

of 32 non-identical colonies were isolated from the cotton fabric, 8 from silk, and 6 from wool fabric, and sub-cultured onto new plates for further analysis.

4.2.3 Characterization and identification of bacterial isolates

4.2.3.1 Morphological characterization

The colonies that were not identical from all the three fabrics were classified based on their shape, structure, size, and colour. The table 4.3, 4.4 and 4.5 below shows the categorization.

Table 4.3: Colony appearance of the non-identical bacteria isolated from cotton fabric

Colonies	Form	Elevation	Margin	Size	Pigmentation
1A1	Filamentous	Umbonate	Erose	Small	White
1A2	Punctiform	Pulvinate	Entire	Pinpoint	White
1A3	Circular	Pulvinate	Entire	Small	Yellow
1A8	Irregular	Umbonate	Curled	Large	White
1A11	Circular	Pulvinate	Entire	Pinpoint	Off White
1A18	Filamentous	Pulvinate	Filamentous	Large	White
1B4	Punctiform	Pulvinate	Entire	Pinpoint	White
1B9	Irregular	Umbonate	Curled	Large	White
1B12	Circular	Pulvinate	Entire	Large	White
2A1	Circular	Pulvinate	Entire	Small	White
2A2	Irregular	Umbonate	Curled	Moderate	White
2A3	Circular	Pulvinate	Entire	Small	Transparent
2A4	Circular	Pulvinate	Entire	Small	White
2A5	Circular	Pulvinate	Entire	Moderate	Transparent
2A6	Circular	Pulvinate	Entire	Small	White
2B1	Circular	Pulvinate	Entire	Moderate	White
2B2	Punctiform	Pulvinate	Entire	Pinpoint	White
2B3	Irregular	Umbonate	Curled	Large	White
2B4	Irregular	Umbonate	Curled	Large	Off White
2B5	Circular	Pulvinate	Entire	Moderate	Off White
2B6	Circular	Pulvinate	Entire	Moderate	Yellow
3A2	Circular	Pulvinate	Entire	Moderate	White
3A5	Circular	Pulvinate	Entire	Small	White

3A8	Circular	Pulvinate	Entire	Moderate	White
3A11	Irregular	Umbonate	Lobate	Large	Translucent
3A12	Circular	Pulvinate	Entire	Moderate	White
3A13	Punctiform	Pulvinate	Entire	Pinpoint	Transparent
3A14	Irregular	Pulvinate	Curled	Moderate	Yellow
3B2	Irregular	Umbonate	Curled	Large	Transparent
3B4	Irregular	Umbonate	Curled	Large	White
3B8	Filamentous	Umbonate	Filamentous	Moderate	Off white
3B12	Circular	Pulvinate	Entire	Small	Off white

Table 4.4 : Colony appearance of the non-identical bacteria isolated from silk fabric

Colonies	**Form**	**Elevation**	**Margin**	**Size**	**Pigmentation**
1B1	Irregular	Umbonate	Curled	Moderate	White
2A1	Irregular	Umbonate	Curled	Large	White
2B2	Irregular	Umbonate	Curled	Large	White
3A1	Circular	Pulvinate	Entire	Small	White
3A3	Irregular	Umbonate	Curled	Large	White
3B2	Irregular	Umbonate	Curled	Large	White
3B3	Irregular	Umbonate	Curled	Moderate	White
3B6	Irregular	Umbonate	Curled	Moderate	White

Table 4.5 : Colony appearance of the non-identical bacteria isolated from wool fabric

Colonies	**Form**	**Elevation**	**Margin**	**Size**	**Pigmentation**
1A1	Irregular	Umbonate	Curled	Large	White
2A1	Irregular	Umbonate	Curled	Large	White
2B2	Circular	Pulvinate	Entire	Small	White
3A1	Irregular	Umbonate	Curled	Large	White
3A3	Irregular	Umbonate	Curled	Large	White
3A4	Irregular	Umbonate	Curled	Large	White

4.2.3.2 Biochemical characterization

The sub-cultured colonies from all three fabrics were further studied for their morphological characteristics like their appearance in terms of their form, elevation, margin, size, pigmentation, and gram stain. The colonies were further studied for their biochemical tests like catalase, oxidase test, Indole, and motility tests which are presented in Tables 4.6, 4.7, and 4.8.

Colonies 1A1, 1A2, 1A8, 1B12, 2A2, 2A5, 2B1, 2B3, 2B4, 2B5, 2B6, 3A8, 3A11, 3B2, 3B4, 3B8, 3B12 from cotton; 1A1, 2A1, 3A1, 3A3, 3A4 from wool and 2A1, 2B2, 3A3, and 3B2 from silk fabric showed gram-positive stain with bacilli shaped colonies. They showed positive responses towards catalase test, positive oxidase test, and motility test. Thus, they were categorized as *Bacillus cereus* species.

The cocci shaped isolates that presented gram-positive stain with positive catalase test, negative for oxidase test, helped in categorizing the isolates as *Micrococcus* species. Its specific morphological features of being circular form, small in size with yellow pigmentation further confirmed its species.

The colonies appearing circular in form, with the entire margin, pinpoint to small in size, and white pigmentation when observed under a microscope were identified as Gram-positive bacteria with Cocci in shape. These colonies tested positive towards the catalase test and negative towards the oxidase test, they also showed negative in the motility test, pointing these characteristics towards *Staphylococcus aureus* species. Further, to confirm its identification, these colonies were transferred to a sterile tube of phenol red mannitol broth showing positive results with a change of color from reds to yellow, indicating the pH change to acidic.

The colonies which were identified as Gram-negative bacteria were further sub-cultured and grown on MacConkey agar using the streak plate method. MacConkey Agar is a type of culture medium that is designed to be both selective and differential which is composed of lactose, bile salts, neutral red, and crystal violet. (Bergey et al., 1974). Bile salts and crystal violet inhibit the growth of Gram-positive and allow for the selection and isolation of Gram-negative bacteria, differentiating them based on lactose fermentation. Neutral red dye is a pH indicator that is colourless above a pH of 6.8 and red at a pH below 6.8. When acid is produced as a result of lactose fermentation, it causes the dye to turn red. Lactose-fermenting bacteria produce a red color on MacConkey agar, while lactose non-fermenters maintain the original yellow color of the medium.

Colonies 1A18, 1B9, 2A4, 2A6, 2B2, 3A2, 3A12, and 3A13 from cotton fabric, 1B1 from wool and 3B3, and 3B6 from silk fabric were identified as Gram-negative and rod-shaped. They resulted positive for both catalase and oxidase test. These colonies had a typical odour of grape-like and had a swarming growth on MacConkey agar and were unable to ferment lactose and so formed un-dyed colonies on the MacConkey medium pointing it towards *Pseudomonas species.* Later on, these colonies were grown on Pseudomonas agar with positive growth which resulted in its verification.

Table 4.6: Biochemical characteristics of bacteria's isolated from cotton fabric

Sr. No	Colonies	Gram stain	Colony Shape	Catalase	Oxidase	Motility	Mannitol fermentation	Bacteria Species
1	1A1	Gram +ve	Bacilli	+ve	+ve	+ve	-	*Bacillus cereus*
2	1A2	Gram +ve	Bacilli	+ve	+ve	+ve	-	*Bacillus cereus*
3	1A3	Gram +ve	Cocci	+ve	-ve	-ve	-	*Micrococcus*
4	1A8	Gram +ve	Bacilli	+ve	+ve	+ve	-	*Bacillus cereus*
5	1A11	Gram +ve	Cocci	+ve	-ve	-ve	+ve	*Staphylococcus aureus*
6	1A18	Gram -ve	Rod- shaped	+ve	+ve	+ve	-	*Pseudomonas*
7	1B4	Gram +ve	Cocci	+ve	-ve	-ve	+ve	*Staphylococcus aureus*
8	1B9	Gram –ve	Rod- shaped	+ve	+ve	+ve	-	*Pseudomonas*
9	1B12	Gram +ve	Bacilli	+ve	+ve	+ve	-	*Bacillus cereus*
10	2A1	Gram +ve	Cocci	+ve	-ve	-ve	+ve	*Staphylococcus aureus*
11	2A2	Gram +ve	Bacilli	+ve	+ve	+ve	-	*Bacillus cereus*
12	2A3	Gram +ve	Cocci	+ve	-ve	-ve	+ve	*Staphylococcus aureus*
13	2A4	Gram -ve	Rod- shaped	+ve	+ve	+ve	-	*Pseudomonas*
14	2A5	Gram +ve	Bacilli	+ve	+ve	+ve	-	*Bacillus cereus*
15	2A6	Gram -ve	Rod- shaped	+ve	+ve	+ve	-	*Pseudomonas*
16	2B1	Gram +ve	Bacilli	+ve	+ve	+ve	-	*Bacillus cereus*
17	2B2	Gram -ve	Rod- shaped	+ve	+ve	+ve	-	*Pseudomonas*
18	2B3	Gram +ve	Bacilli	+ve	+ve	+ve	-	*Bacillus cereus*
19	2B4	Gram +ve	Bacilli	+ve	+ve	+ve	-	*Bacillus cereus*
20	2B5	Gram +ve	Bacilli	+ve	+ve	+ve	-	*Bacillus cereus*
21	2B6	Gram +ve	Bacilli	+ve	+ve	+ve	-	*Bacillus cereus*
22	3A2	Gram -ve	Rod- shaped	+ve	+ve	+ve	-	*Pseudomonas*

23	3A5	Gram +ve	Cocci	+ve	-ve	-ve	+ve	*Staphylococcus aureus*
24	3A8	Gram +ve	Bacilli	+ve	+ve	+ve	-	*Bacillus cereus*
25	3A11	Gram +ve	Bacilli	+ve	+ve	+ve	-	*Bacillus cereus*
26	3A12	Gram -ve	Rod- shaped	+ve	-ve	+ve	-	*Pseudomonas*
27	3A13	Gram -ve	Rod- shaped	+ve	+ve	+ve	-	*Pseudomonas*
28	3A14	Gram +ve	Cocci	+ve	-ve	-ve	-	*Micrococcus*
29	3B2	Gram +ve	Bacilli	+ve	+ve	+ve	-	*Bacillus cereus*
30	3B4	Gram +ve	Bacilli	+ve	+ve	+ve	-	*Bacillus cereus*
31	3B8	Gram +ve	Bacilli	+ve	+ve	+ve	-	*Bacillus cereus*
32	3B12	Gram +ve	Bacilli	+ve	+ve	+ve	-	*Bacillus cereus*

Table 4.7: Biochemical characteristics of bacteria's isolated from Wool fabric

Sr. No	Colonies	Gram stain	Colony Shape	Catalase	Oxidase	Motility	Mannitol fermentation	Bacteria Species
1	1A1	Gram +ve	Bacilli	+ve	+ve	+ve	-	*Bacillus cereus*
2	2A1	Gram +ve	Bacilli	+ve	+ve	+ve	-	*Bacillus cereus*
3	2B2	Gram –ve	Rod-shaped	+ve	+ve	+ve	-	*Pseudomonas*
4	3A1	Gram +ve	Bacilli	+ve	+ve	+ve	-	*Bacillus cereus*
5	3A3	Gram +ve	Bacilli	+ve	+ve	+ve	-	*Bacillus cereus*
6	3A4	Gram +ve	Bacilli	+ve	+ve	+ve	-	*Bacillus cereus*

Table 4.8: Biochemical characteristics of bacteria's isolated from Silk fabric

Sr. No	Colonies	Gram stain	Colony Shape	Catalase	Oxidase	Motility	Mannitol fermentation	Bacteria Species
1	1B1	Gram –ve	Rod-shaped	+ve	+ve	+ve	-	*Pseudomonas*
2	2A1	Gram +ve	Bacilli	+ve	+ve	+ve	-	*Bacillus cereus*
3	2B2	Gram +ve	Bacilli	+ve	+ve	+ve	-	*Bacillus cereus*
4	3A1	Gram +ve	Cocci	+ve	-ve	-ve	+ve	*Staphylococcus aureus*

5	3A3	Gram +ve	Bacilli	+ve	+ve	+ve	-	*Bacillus cereus*
6	3B2	Gram +ve	Bacilli	+ve	+ve	+ve	-	*Bacillus cereus*
7	3B3	Gram – ve	Rod-shaped	+ve	+ve	+ve	-	*Pseudomonas*
8	3B6	Gram – ve	Rod-shaped	+ve	+ve	+ve	-	*Pseudomonas*

Based on the preceding three tables, it can be noted that the cotton fabric had the highest number of colonies, followed by silk and then wool fabric. Additionally, it was observed that the number of Gram-positive bacterial isolates exceeded the number of Gram-negative bacterial isolates in all three types of fabric. Bacillus cereus was the most frequently identified Gram-positive isolate, while Pseudomonas species was the predominant Gram-negative bacteria found on cotton, silk, and wool fabric. Gutarowska & Michalski (2012) in their study has also reported Bacillus species to be found majorly on the cotton fabric while Bacillus and Pseudomonas species both majorly on silk and wool fabric.

4.2.3.3 Identification of fungal isolates

From the isolated fungi, *Aspergillus* was found as dominating fungi. The genus refers to a group of molds that has been identified to contain around 300 different species of fungi. *Aspergillus Niger,* and *Aspergillus fumigatus* were identified under a compound microscope seen in figure 4.2. *Aspergillus Niger* is filamentous fungi, which means that they tend to form filaments (hyphae) and thus resemble the structure of a plant. It produced dark brown spores from their conidial heads which makes them distinguishable. When viewed under the microscope, *Aspergillus Niger* consists of smooth and colourless conidiophores and spores. Whereas, *Aspergillus fumiga*tus had branching hyphae (long, branching filaments) that form a complex network called a mycelium. The hyphae have septa (cell walls that divide the hyphae into individual cells) with small pores that allow the movement of organelles and molecules between the cells. The hyphae may also produce spores called conidia, which are typically round and have a distinctive rough or bumpy surface. These conidia can be seen as clusters on the tips of the hyphae or as individual structures that are released into the air for dispersal.

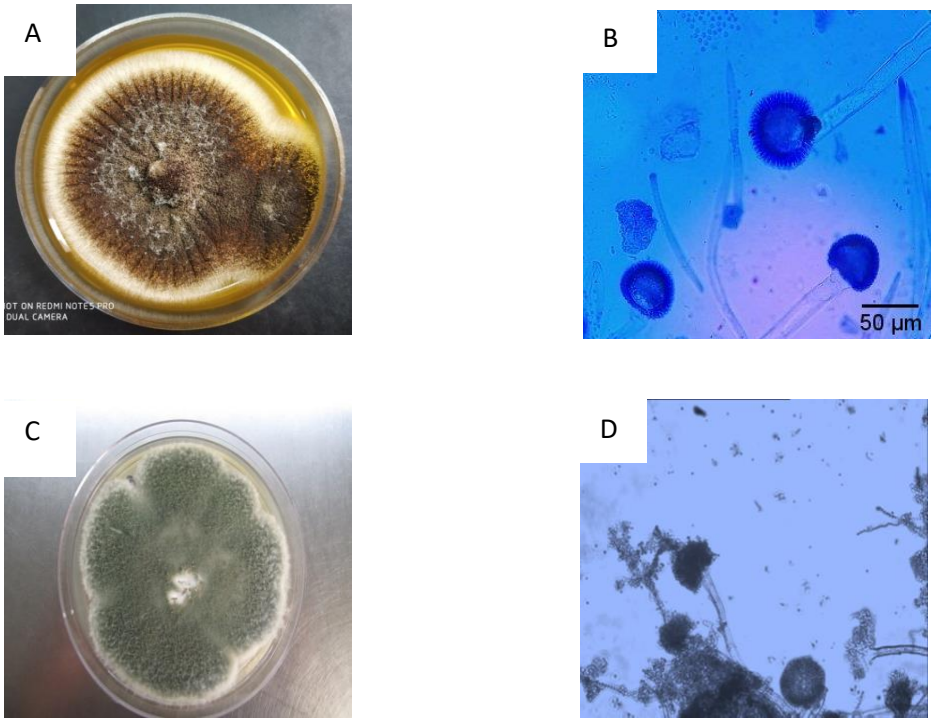

Fig. 4.2: Fungal growth on media and spore morphologies:
A, B- *Aspergillus Niger* and C, D- *Aspergillus Fumigatus*

4.3 Preparation of nanoparticles (NPs)

4.3.1 Selection of core and wall material

From the results of the first objective (Section 4.1) after interacting with the conservators, curators and after an extensive literature study, essential oils like cinnamon oil, clove oil, carom seed oil and neem oil were selected under the study. Chitosan being widely used for entrapping essential oils. Tripolyphosphate (TPP) was used as a cross-linking agent as it has been widely used and proved to provide better stability and formation of nanoparticles. Apart from being water soluble it is versatile and can cross link wide range of polymers. It is non-toxic and cost effective as well.

4.3.2 Preparation of essential oil chitosan nanoparticles (CNPs)

4.3.2.1 Pilot work

The preparation of essential oil chitosan nanoparticles involved two methods: first, the creation of a nano-emulsion, and second, the use of ionic gelation. Chitosan was chosen as the material to encase the essential oil due to its biodegradability, cationic charge, and muco-adhesive nature, making it the most suitable choice for encapsulation. The cross-linking agent, TPP, which has a negative charge, was utilized to generate the nanoparticles. The use of

surfactants such as Tween 80 and Poloxamer 188 were chosen as an effective strategy for developing stable and functional nanoparticles. These surfactants help to improve the stability, solubility, and bioavailability of the nanoparticles. The success of the nanoparticle system relies on its high entrapment efficiency, which enables the drug to be administered at lower or more effective doses while reducing the amount of matrix components. Loading capacity, on the other hand, is a measure of the amount of drug that can be loaded into the nanoparticles. Therefore, the optimization of the amount of chitosan, amount of essential oil, percentage and type of surfactant suitable according to the type of oil, TPP concentration, stirring rate and the method of nanoparticle preparation was selected based on achieving the highest entrapment efficiency of the essential oil in the nanoparticles.

4.3.2.1.1 Screening the parameters for developing neem essential oil nanoparticles

Table 4.9 : Screening of Chitosan for Neem oil nanoparticles

Neem oil Nanoparticles			**Results**		
Chitosan Concentration	Surfactant %	TPP %	Size (nm)	% Entrapment efficiency	% Loading capacity
0.5	0.75	1	285 ± 21	72.63 ± 1.89	7.40 ± 0.56
1	0.75	1	**168 ± 24**	**79.24 ± 2.34**	**13.4 ± 0.91**
1.5	0.75	1	244 ± 13	63.57 ± 3.37	9.9 ± 1.21
2	0.75	1	308 ± 19	59.46 ±2.45	8.61 ± 0.98

TPP: Sodium tripolyphosphate

Table 4.10 : Screening of the two Surfactants for Neem oil nanoparticles

Neem oil Nanoparticles				**Results**					
% Chitosan	Tween 80 %	Poloxamer 188 %	TPP %	Size (nm)	Size (nm)	% EE	% EE	% LC	% LC
1	0.5	0.5	1	268 ± 24	291 ± 19	71.55 ± 2.1	65.11± 3.3	14.0 ± 0.68	14.0 ± 0.71
1	**0.75**	0.75	1	**172 ± 27**	322 ± 23	**81.36 ± 2.56**	58.11± 5.13	**13.6 ± 0.52**	9.85 ± 0.67
1	1	1	1	236 ± 21	351 ± 29	64.61 ± 1.45	49.17 ± 2.56	9.03 ± 0.51	6.87 ± 0.43
1	2	2	1	289 ± 19	409 ± 35	54.38 ± 1.67	41.34 ± 5.23	4.47 ± 0.58	3.40 ± 0.47

TPP: Sodium tripolyphosphate, EE: Entrapment efficiency, LC: Loading capacity

Table 4.11 : Screening of Chitosan: Oil for Neem oil nanoparticles

Neem oil Nanoparticles			**Results**		
Polymer: Oil Concentration	Surfactant %	TPP %	Size (nm)	% Entrapment efficiency	% Loading capacity
1:1	0.75	1	**184 ± 16**	**78.65 ± 1.28**	**12.99 ± 0.77**
1:2	0.75	1	256 ± 19	69.36 ± 2.54	20.10 ± 0.64
1:3	0.75	1	312 ± 21	62.12 ± 2.71	23.58 ± 0.60

TPP: Sodium tripolyphosphate

Table 4.12: Screening of Cross-linking agent for Neem oil nanoparticles

Neem oil Nanoparticles			**Results**		
Chitosan Concentration	Surfactant %	TPP %	Size (nm)	% Entrapment efficiency	% Loading capacity
1	0.75	**1**	**165 ± 29**	**76.56 ± 0.34**	**12.80 ± 0.87**
1	0.75	2	226 ± 25	68.31 ± 1.26	11.58 ± 0.81
1	0.75	3	284 ± 27	51.32 ± 1.23	8.70 ± 0.69

TPP: Sodium tripolyphosphate

Table 4.13: Screening of type of method and RPM used for Neem oil nanoparticles

Neem oil Nanoparticles			**Results**							
Polymer: Oil	Tween 80 %	TPP %	RPM Method I	RPM Method II	Size (nm)	Size (nm)	% EE	% EE	% LC	% LC
1:1	0.75	1	1200	10,000	320± 21	262 ± 29	48.23 ± 4.89	62.41 ± 1.34	8.16 ± 0.31	10.57 ± 0.38
1:1	0.75	1	1500	**13,000**	291 ± 37	**189 ± 26**	57.61 ± 2.91	**78.42 ± 1.56**	8.91 ± 0.38	**12.28 ± 0.34**
1:1	0.75	1	1800	16,000	267 ± 21	141 ± 26	52.83 ± 1.80	56.79 ± 1.1	9.8 ± 0.12	9.61 ± 0.49

TPP: Sodium tripolyphosphate, EE: Entrapment efficiency, LC: Loading capacity

Table 4.9- 4.13 represents the entrapment efficiency, loading capacity and the size of the neem oil chitosan nanoparticles at different concentration of the parameters. The most efficient entrapment of chitosan, oil, and TPP was achieved at 1% respectively. When comparing surfactants, Tween 80 at 0.75% yielded better results than poloxamer, in terms of both entrapment efficiency and size. Neem essential oil chitosan nanoparticles were created using

two methods, emulsification + Ionic gelation and nano-emulsification + Ionic gelation. The latter method resulted in the highest entrapment efficiency and loading capacity of 78.42 ± 1.56% and 12.28 ± 0.34% with the smallest nanoparticle size of 189 ± 26nm. The optimized conditions for creating these nanoparticles involved using 1% chitosan, 1% oil, 1% TPP, and 0.75% Tween 80, with the nano-emulsification + Ionic gelation method. This included stirring at 13,000 RPM using a high shear homogenizer for 10 minutes, followed by stirring at 1800 rpm for 2 hours, as stated in the methodology chapter.

4.3.2.1.2 Screening the parameters for developing cinnamon essential oil nanoparticles

Table 4.14: Screening of Chitosan for Cinnamon oil nanoparticles

Cinnamon oil Nanoparticles			**Results**		
Chitosan Concentration (%)	Surfactant Poloxamer 188 %	TPP %	Size (nm)	% Entrapment efficiency	% Loading capacity
0.5	0.5	1	256 ± 23	63.45 ± 2.23	15.28 ± 0.89
1	0.5	1	**224 ± 17**	**76.58 ± 1.23**	**16.46 ± 0.91**
1.5	0.5	1	312 ± 16	56.67 ± 1.37	11.00 ± 0.61
2	0.5	1	328 ± 17	49.54 ± 1.69	8.76 ± 0. 65

TPP: Sodium tripolyphosphate

Table 4.15: Screening of Cross-linking agent for Cinnamon oil nanoparticles

Cinnamon oil Nanoparticles			**Results**		
% Chitosan	Surfactant %	TPP %	Size (nm)	% EE	% LC
1	0.5	**1**	**219 ± 11**	**75.66 ± 3.41**	**16.26 ± 0.88**
1	0.5	2	264 ± 19	68.24 ± 2.75	14.66 ± 0.76
1	0.5	3	326 ± 17	61.44 ± 2.67	13.30 ± 0.69

TPP: Sodium tripolyphosphate, EE: Entrapment efficiency, LC: Loading capacity

Table 4.16: Screening of Chitosan: Oil for Cinnamon oil nanoparticles

Cinnamon oil Nanoparticles			**Results**		
Polymer: Oil Concentration	Surfactant %	TPP %	Size (nm)	% EE	% LC
1:1	0.5	1	**231 ± 12**	**73.68 ± 2.35**	**15.83 ± 0.90**
1:2	0.5	1	288 ± 23	62.37 ± 2.46	20.08 ± 0.83
1:3	0.5	1	326 ± 20	53.46 ± 2.06	24.11 ± 0.81

TPP: Sodium tripolyphosphate, EE: Entrapment efficiency, LC: Loading capacity

Table 4.17: Screening of Surfactants for Cinnamon oil nanoparticles

Cinnamon oil Nanoparticles				**Results**					
% Chitosan	Tween 80 %	Poloxamer 188 %	TPP %	Size (nm)	Size (nm)	% EE	% EE	% LC	% LC
1	0.5	**0.5**	1	362 ± 42	**236 ± 31**	61± 2.45	**75.44 ± 2.28**	13.17 ± 0. 67	**16.21 ± 0.71**
1	0.75	0.75	1	329 ± 29	386 ± 24	63.48 ± 3.66	66.72 ± 2.12	10.75 ± 0. 57	11.30 ± 0.33
1	1	1	1	381 ± 21	258 ± 28	59.10 ± 3.25	62.35 ± 1.62	8.26 ± 0.49	8.86 ± 0.53
1	2	2	1	409 ± 36	314 ± 29	53.01 ± 2.69	54.82 ± 2.93	6.92 ± 0.51	7.16 ± 0.45

TPP: Sodium tripolyphosphate, EE: Entrapment efficiency, LC: Loading capacity

Table 4.18: Screening of type of method and RPM used for Cinnamon oil nanoparticles

Cinnamon oil Nanoparticles			**Results**							
Polymer: Oil	Poloxamer %	TPP %	RPM Method I	RPM Method II	Size (nm)	Size (nm)	% EE	% EE	% LC	% LC
1:1	0.5	1	1200	10,000	363 ± 17	404 ± 19	53.18 ± 3.06	59.23 ± 2.19	9.0 ± 0.24	10.0 ± 0.37
1:1	0.5	1	1500	13,000	289 ± 28	364 ± 19	66.65 ± 1.23	53.56 ± 2.72	11.29 ± 0.53	9.07 ± 0.45
1:1	0.5	1	**1800**	16,000	**226 ± 25**	381 ± 36	**74.23 ± 2.77**	49.13 ± 4.58	**12.57 ± 0.55**	8.32 ± 0.39

TPP: Sodium tripolyphosphate, EE: Entrapment efficiency, LC: Loading capacity

To obtain maximum entrapment efficiency of cinnamon oil nanoparticle; chitosan, oil, and TPP of 1% of each were found to be the most effective. In terms of surfactants, Poloxamer at 0.50% concentration resulted in better entrapment efficiency and smaller particle size compared to other surfactants. Two methods were used to create cinnamon essential oil chitosan

nanoparticles, namely emulsification + Ionic gelation (Method I) and nano-emulsification + Ionic gelation (Method II). The former method showed the highest entrapment efficiency and loading capacity of 74.23 ± 2.11% and 12.57 ± 0.55% with a nanoparticle size of 226 ± 25 nm as seen in table 4.15. As observed from table 4.14 – 4.18, the optimized conditions for creating these nanoparticles involved using 1% chitosan, 1% oil, 1% TPP, and 0.50% Poloxamer 188, with the emulsification+ Ionic gelation method. The nanoparticles were stirred at 1800 rpm for 2 hours, as mentioned in the methodology section.

4.3.2.1.3 Screening the parameters for developing clove essential oil nanoparticles

Table 4.19 : Screening of Chitosan for Clove oil nanoparticles

Clove oil Nanoparticles			**Results**		
Chitosan Concentration	Surfactant (Tween 80) %	TPP %	Size (nm)	% EE	% LC
0.5	0.75	1	324 ± 17	36.17 ± 2.11	6.69 ± 0.22
1	0.75	1	**287 ± 21**	**48.64 ± 2.08**	**8.23 ± 0.13**
1.5	0.75	1	364 ± 26	42.08 ± 1.36	6.57 ± 0.17
2	0.75	1	366 ± 27	37.65 ± 2.19	5.45 ± 0.35

TPP: Sodium tripolyphosphate, EE: Entrapment efficiency, LC: Loading capacity

Table 4.20: Screening of Chitosan: Oil for Clove oil nanoparticles

Clove oil Nanoparticles			**Results**		
Polymer: Oil Concentration	Surfactant (Tween80) %	TPP %	Size (nm)	% EE	% LC
1:1	0.75	1	**294 ± 18**	**51.62 ± 1.56**	**9.5 ± 0.44**
1:2	0.75	1	341 ± 27	35.71 ± 1.79	10.34 ± 0.38
1:3	0.75	1	402 ± 25	29.67 ± 1.71	11.26 ± 0.31

TPP: Sodium tripolyphosphate, EE: Entrapment efficiency, LC: Loading capacity

Table 4.21 : Screening of Surfactants for Clove oil nanoparticles

Clove oil Nanoparticles				**Results**					
% Chitosan	Tween 80 %	Poloxamer 188 %	TPP %	Size (nm)	Size (nm)	% EE	% EE	% LC	% LC
1	0.5	0.5	1	401 ± 22	408 ± 23	39.14 ± 1.45	39..21 ± 2.31	8.41 ± 0.13	8.43 ± 0.24
1	**0.75**	0.75	1	**294 ± 21**	321 ± 38	**46.84 ± 3.34**	40.73 ± 1.07	**7.93 ± 0.36**	6.90 ± 0.21
1	1	1	1	318 ± 15	343 ± 25	44.34 ± 2.56	39.58 ± 1.14	6.20 ± 0.31	5.53 ± 0.19
1	2	2	1	342 ± 18	371 ± 31	36.42 ± 2.09	34. 31 ± 3.23	3.0 ± 0.22	2.82 ± 0.17

TPP: Sodium tripolyphosphate, EE: Entrapment efficiency, LC: Loading capacity

Table 4.22: Screening of Cross-linking agent for Clove oil nanoparticles

Clove oil Nanoparticles			**Results**		
Chitosan Concentration	Surfactant (Tween 80) %	TPP %	Size (nm)	% Entrapment efficiency (EE)	% Loading capacity (LC)
1	0.75	**1**	**287 ± 12**	**48.64 ± 3.11**	**8.24 ± 0.24**
1	0.75	2	366 ± 09	44.36 ± 2.33	7.51 ± 0.33
1	0.75	3	436 ± 11	38.25 ± 2.45	6.48 ± 0.27

TPP: Sodium tripolyphosphate

Table 4.23: Screening of type of method and RPM used for Clove oil nanoparticles

Clove oil Nanoparticles			**Results**							
Polymer: Oil	Tween 80 %	TPP %	RPM Method I	RPM Method II	Size (nm)	Size (nm)	% EE	% EE	% LC	% LC
1:1	0.75	1	1200	10,000	363 ± 32	381 ± 19	42.68 ± 2.12	38.21 ± 2.31	7.23 ± 0.13	6.47 ± 0.11
1:1	0.75	1	1500	13,000	324 ± 35	320 ± 35	46.84 ± 2.34	39.73 ± 2.46	7.93 ± 0.26	6.72 ± 0.17
1:1	0.75	1	**1800**	16,000	**294 ± 33**	302 ± 21	**51.62 ± 3.1**	36.58 ± 3.01	**8.7 ± 0.31**	6.1 ± 0.25

TPP: Sodium tripolyphosphate, EE: Entrapment efficiency, LC: Loading capacity

Table 4.19- 4.23 suggests that to achieve maximum entrapment efficiency for clove oil nanoparticle, 1% of each component such as chitosan, oil, and TPP were determined to be the most effective. Among the surfactants tested, Tween 80 at a concentration of 0.75% resulted in higher entrapment efficiency and smaller particle size. Emulsification+ Ionic gelation method of nanoparticle preparation produced the highest entrapment efficiency and loading capacity of 51.62 ± 3.1% and 8.7 ± 0.31% with a nanoparticle size of 294 ± 33 nm. For these optimal conditions, the nanoparticles were stirred at 1800 rpm for 2 hours, as stated in the methodology section.

4.3.2.1.4 Screening the parameters for developing Carom essential oil nanoparticles

Results from the below table 4.24- 4.28 suggests that the maximum entrapment efficiency of carom oil was obtained at 1% chitosan, oil, and TPP respectively. Among the surfactants, Tween 80 at a concentration of 0.75% using Emulsification+ Ionic gelation resulted in higher entrapment efficiency and loading capacity of 70.66 ± 2.24 % and 11.9 ± 0.64 %, and smaller particle size of 294 ± 33 nm. The nanoparticles were stirred at 1800 rpm for 2 hours, as stated in the methodology section.

Table 4.24: Screening of Chitosan for Carom oil nanoparticles

Carom oil Nanoparticles			**Results**		
Chitosan Concentration	Surfactant %	TPP %	Size (nm)	% EE	% LC
0.5	0.75	1	489 ± 17	63.16 ± 1.95	11.6 ± 0.43
1	0.75	1	**369 ± 22**	**72.32 ± 2.61**	**12.25 ± 0.53**
1.5	0.75	1	421 ± 37	61.18 ± 2.85	9.5 ± 0.61
2	0.75	1	468 ± 31	56.31 ± 2.59	8.16 ± 0.6

TPP: Sodium tripolyphosphate, EE: Entrapment efficiency, LC: Loading capacity

Table 4.25: Screening of Chitosan: Oil for Carom oil nanoparticles

Carom oil Nanoparticles			**Results**		
Polymer: Oil Concentration	Surfactant %	TPP %	Size (nm)	% EE	% LC
1:1	0.75	1	**318 ± 19**	**69.27 ± 2.89**	**11.07 ± 0.46**
1:2	0.75	1	389 ± 24	53.12 ± 2.99	15.39 ± 0.29
1:3	0.75	1	466 ± 27	41.68 ± 2.36	15.82 ± 0.71

TPP: Sodium tripolyphosphate, EE: Entrapment efficiency, LC: Loading capacity

Table 4.26: Screening of Surfactants for Carom oil nanoparticles

Carom oil Nanoparticles				**Results**					
% Chitosan	Tween 80 %	Poloxamer 188 %	TPP %	Size (nm)	Size (nm)	% EE	% EE	% LC	% LC
1	0.5	0.5	1	528 ± 31	456 ± 11	56.82 ± 2.57	59.11± 2.19	12.21 ± 0.55	12.71 ± 0.67
1	**0.75**	0.75	1	**346 ± 23**	491 ± 23	**70.25 ± 3.45**	58.11± 3.13	**11.09 ± 0.31**	9.8 ± 0.22
1	1	1	1	403 ± 17	509 ± 31	63.14 ± 2.78	47.17 ± 3.78	8.83± 0.56	6.5 ± 0.62
1	2	2	1	436 ± 21	562 ± 29	51.68 ± 2.23	44.34 ± 4.24	4.25 ± 0.78	3.6 ± 0.71

TPP: Sodium tripolyphosphate, EE: Entrapment efficiency, LC: Loading capacity

Table 4.27: Screening of Cross-linking agent for Carom oil nanoparticles

Carom oil Nanoparticles			**Results**		
Chitosan Concentration	Surfactant %	TPP %	Size (nm)	% EE	% LC
1	0.75	**1**	**356 ± 29**	**73.45 ± 2.73**	**12.44 ± 0.68**
1	0.75	2	426 ± 23	64.03 ± 2.92	10.3 ± 0.51
1	0.75	3	468 ± 37	54.36 ± 3.73	9.21 ± 0.61

TPP: Sodium tripolyphosphate, EE: Entrapment efficiency, LC: Loading capacity

Table 4.28 : Screening of type of method and RPM used for Carom oil nanoparticles

Carom oil Nanoparticles			**Results**							
Polymer: Oil	Tween 80 %	TPP %	RPM Method I	RPM Method II	Size (nm)	Size (nm)	% EE	% EE	% LC	% LC
1:1	0.75	1	1200	10,000	496 ± 35	491 ± 11	46.18 ± 2.55	47.09 ± 1.89	7.82 ± 0.4	7.9 ± 0.58
1:1	0.75	1	1500	13,000	443 ± 28	452 ± 38	56.29 ± 2.86	48.34 ± 1.13	9.5 ± 0.32	8.19 ± 0.54
1:1	0.75	1	**1800**	16,000	**349 ± 23**	403 ± 41	**70.66 ± 2.24**	42.35 ± 2.33	**11.9 ± 0.64**	7.17 ± 0.61

TPP: Sodium tripolyphosphate, EE: Entrapment efficiency, LC: Loading capacity

After evaluating the parameters for all four essential oils based on their highest entrapment efficiency in the pilot work, the method for preparing nanoparticles was selected. The nano-emulsion+ ionic gelation method was chosen for neem oil chitosan nanoparticles, while the emulsion+ ionic gelation method was selected for clove, cinnamon, and carom essential oil nanoparticles. The choice of surfactant varied depending on the highest entrapment efficiency observed in the type of essential oil nanoparticles, with Poloxamer 188 selected for cinnamon nanoparticles and Tween 80 selected for neem, clove, and carom essential oil nanoparticles. The effects of different concentrations of chitosan, selected surfactant, oil, and TPP, as well as stirring rate, were evaluated in order to optimize the conditions for developing the nanoparticles. Further details on these optimization efforts are provided in the next section.

4.4 Optimizing nanoparticle formulation and process parameters to maximize the Entrapment Efficiency and Loading capacity

The efficacy of nanoparticle-based drug delivery systems depends largely on the entrapment efficiency, which is the percentage of drug that is successfully incorporated into the nanoparticles during the preparation process and loading capacity, which refers to the amount of essential oil that can be loaded into the chitosan nanoparticles.

Achieving high entrapment efficiency and loading capacity is essential for maximizing the efficacy of the nanoparticles. In this section, we will discuss the various parameters that have been investigated and optimized to enhance the entrapment efficiency and loading capacity of chitosan nanoparticles for effective drug delivery. Below are the graphs illustrating the entrapment efficiency at different parameters under the nanoparticle formulation highlighting the bar showing the highest entrapment efficiency for each parameter in a darker shade.

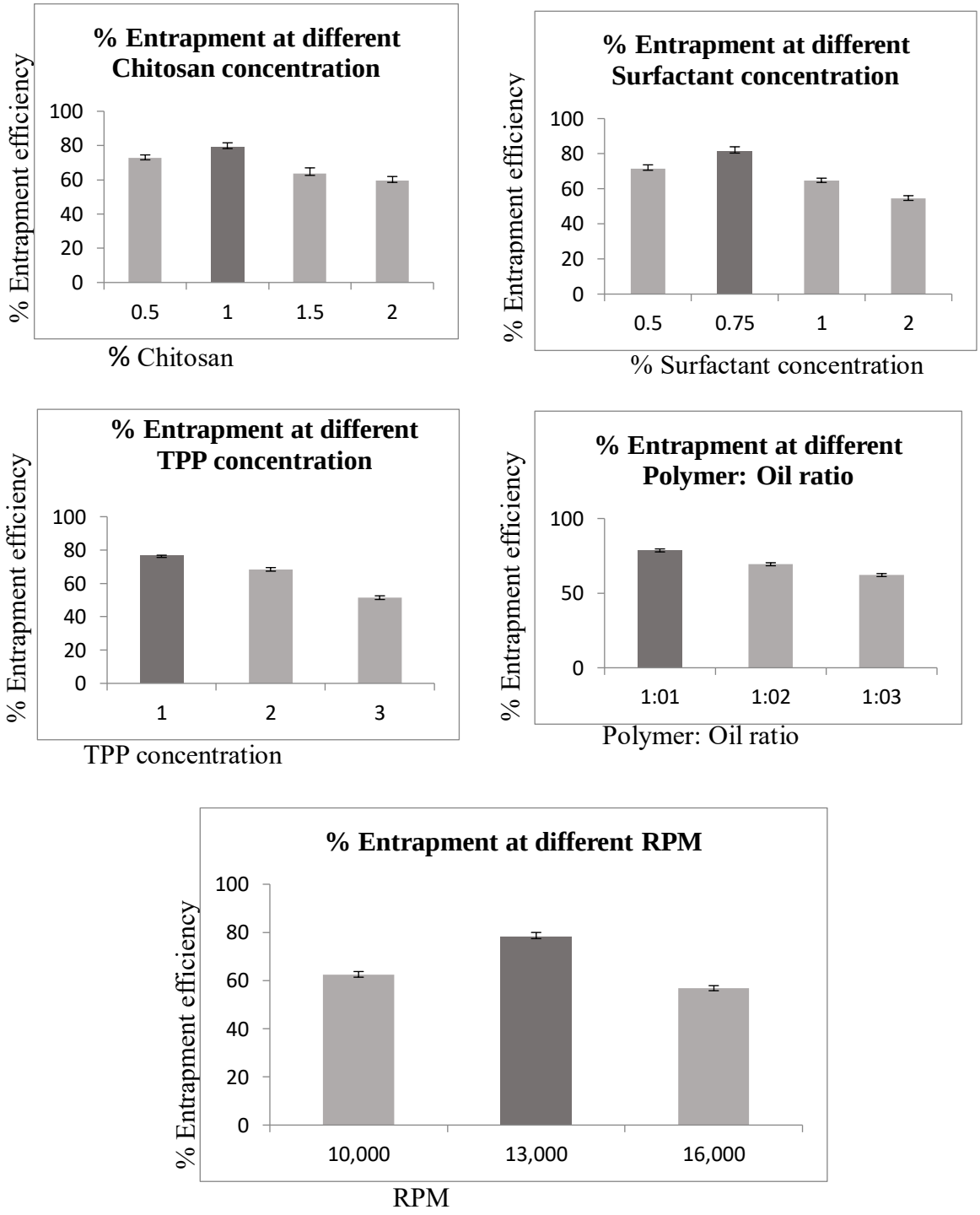

Graph 4.1: % Entrapment efficiency of neem oil chitosan nanoparticles at different parameters

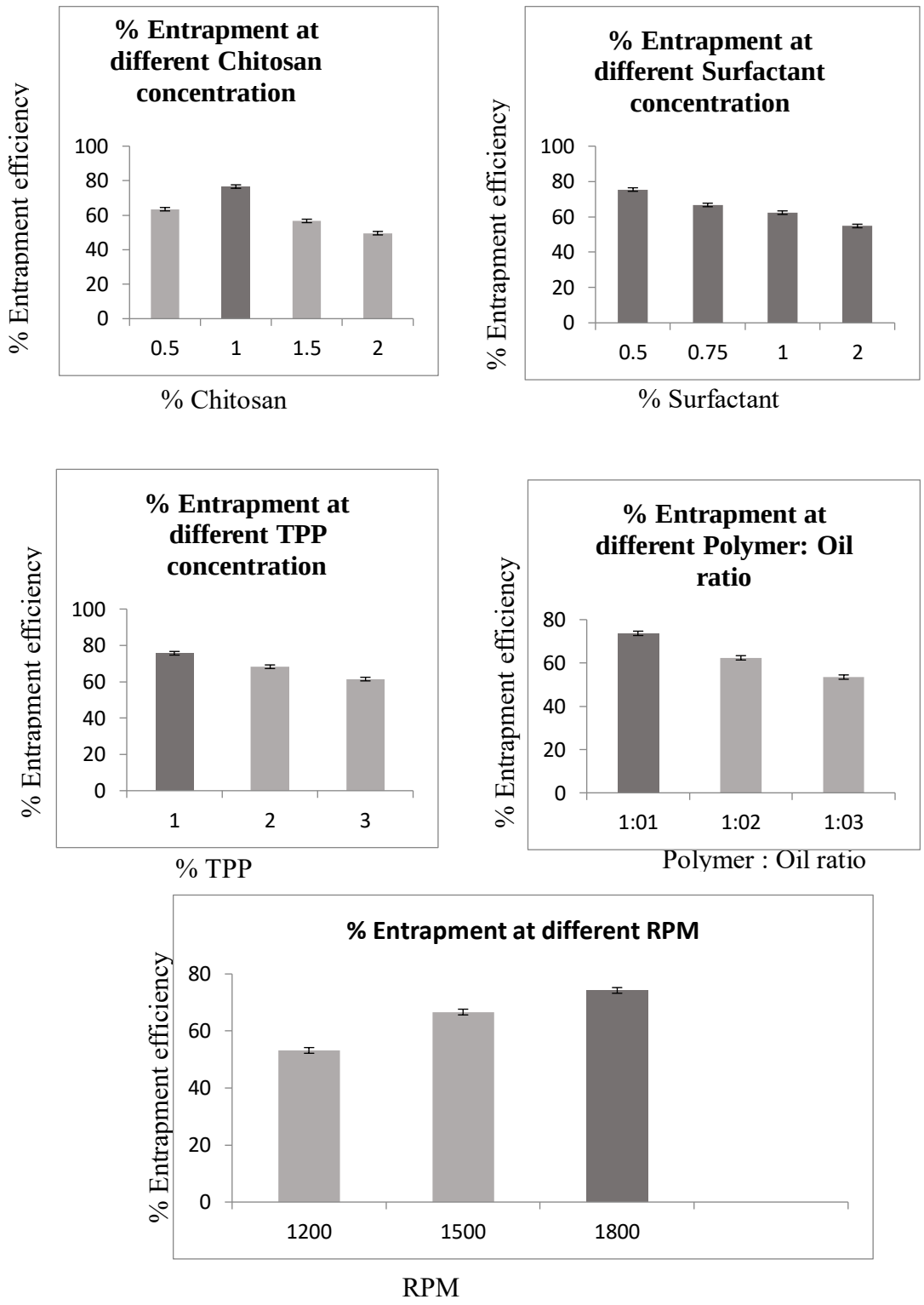

Graph 4.2: % Entrapment efficiency of cinnamon oil chitosan nanoparticles at different parameters

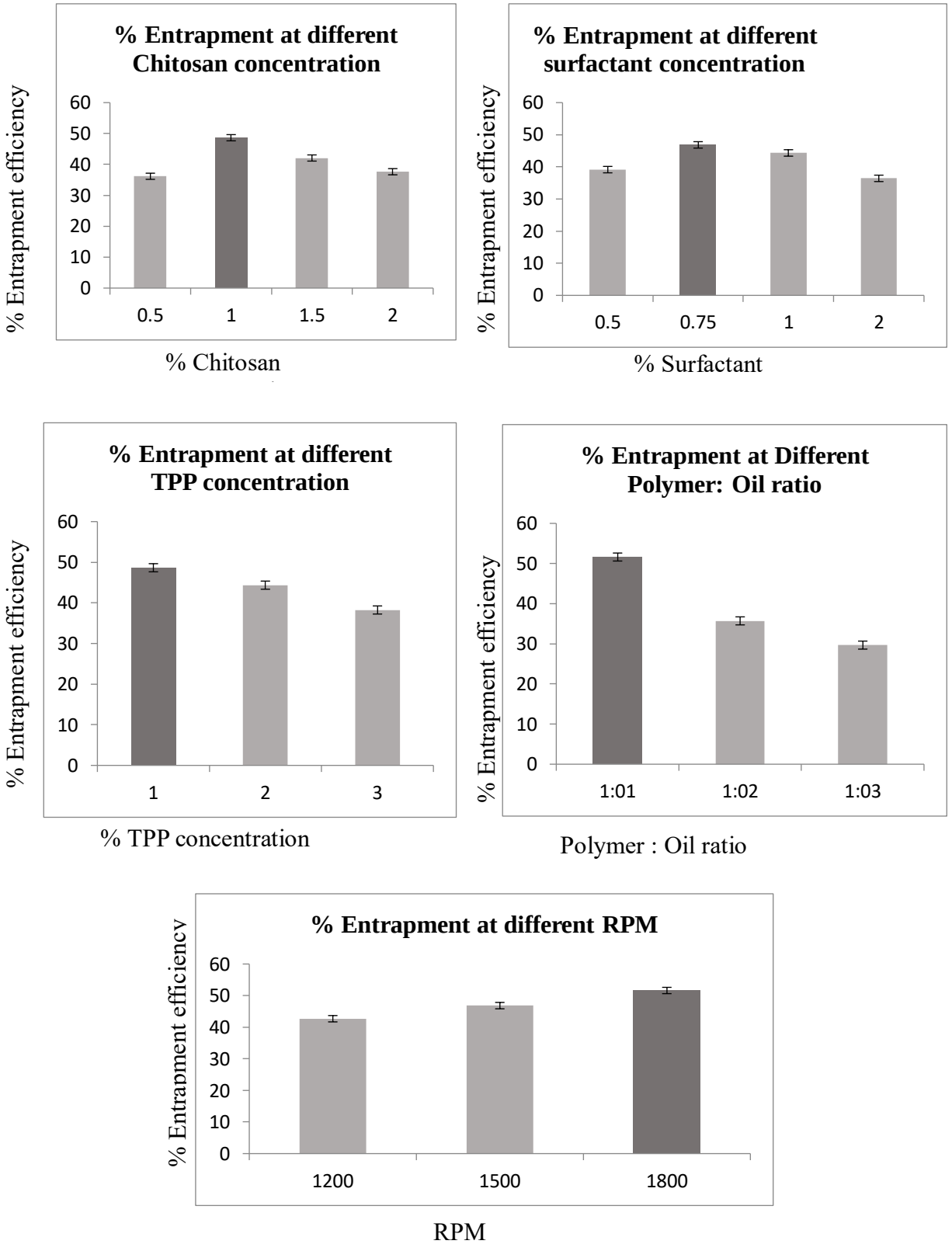

Graph 4.3: % Entrapment efficiency of clove oil chitosan nanoparticles at different parameters

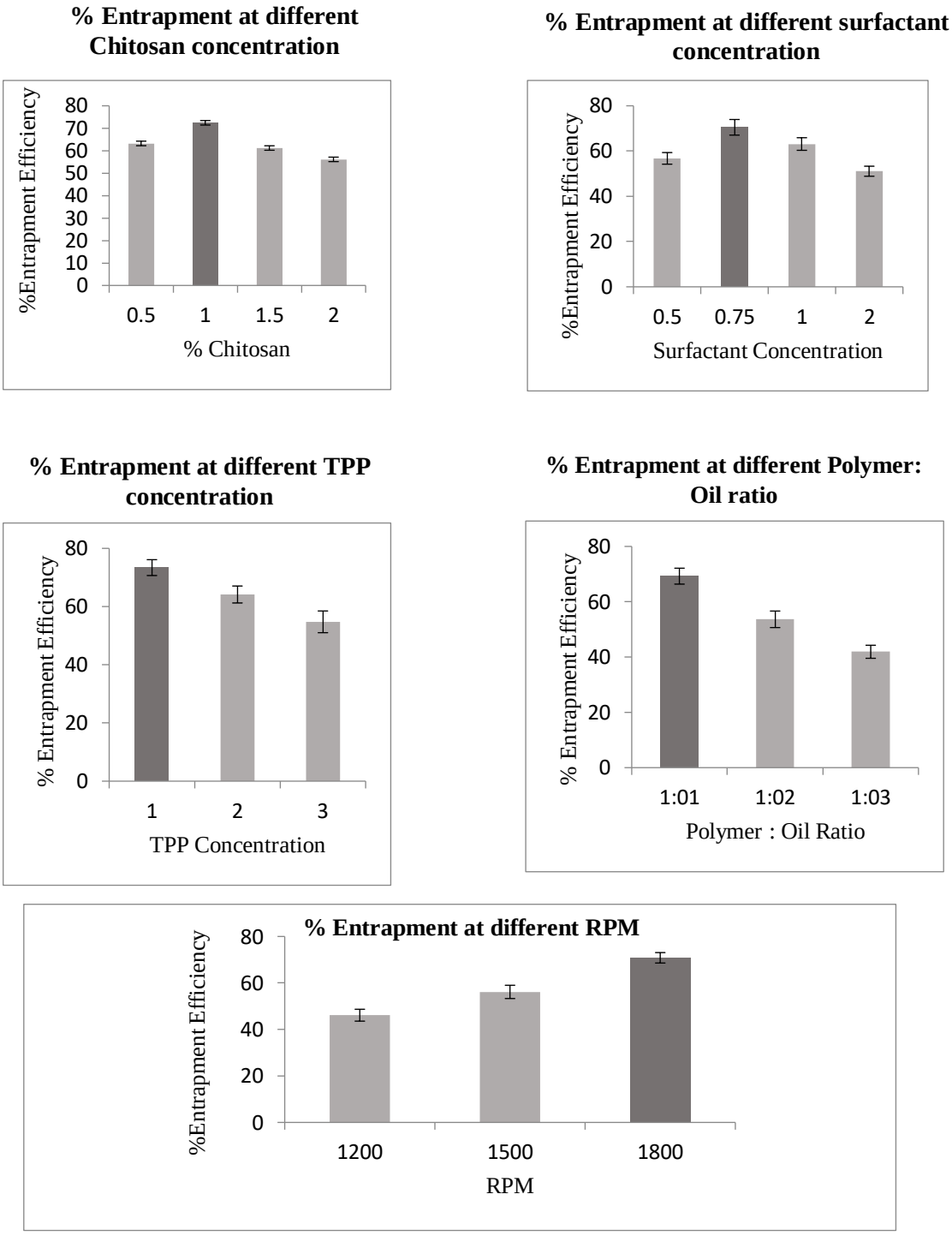

Graph 4.4: % Entrapment efficiency of carom oil chitosan nanoparticles at different parameters

4.4.1 Effect of Chitosan concentration on the entrapment efficiency, loading capacity and nanoparticle size

To optimize chitosan for the greatest entrapment efficiency, the concentration was adjusted to 0.5, 1, 1.5, and 2 % while maintaining a constant concentration of surfactant Tween 80 at 0.75% and TPP at 1% for neem, clove, and carom essential oil, and surfactant poloxamer at 0.50% for cinnamon oil as seen in table 4.9-4.28. The percentage that resulted in the highest entrapment efficiency was selected.

The percent entrapment efficiency and loading capacity of all the essential oils were seen to be highest at 1% concentration of chitosan with 79.24 ± 2.34% and 13.4 ± 0.91% in neem oil nanoparticles, 76.58 ± 1.23% and 16.46 ± 0.91 % in cinnamon oil nanoparticles, 48.64 ± 2.08% and 8.23 ± 0.13 % in clove oil nanoparticles; and 72.32 ± 2.61% and 12.25 ±0.53 in carom oil nanoparticles, respectively. There was an increase of 7% in entrapment when compared to 0.5 % concentration in neem oil, whereas 13%, 12%, and 9% increase in cinnamon oil, clove oil, and carom oil. This suggests that with the increase of polymer, more oil was encapsulated in the nanoparticles. However, further increase of chitosan concentration led to decreased entrapment efficiency. A reduction of 15% was observed in neem oil nanoparticle, 20% in cinnamon oil nanoparticles, and 6% and 11% in clove and carom oil nanoparticles at 1.5% chitosan.

The increase in entrapment efficiency from 0.5% to 1% chitosan concentration can be attributed to the fact that as the chitosan concentration increases, there is an increase in the available surface area for interaction with TPP, leading to the formation of smaller particles with a higher surface area-to-volume ratio. This provides more opportunities for the essential oils to be encapsulated within the nanoparticles, resulting in increased entrapment efficiency.

However, when the chitosan concentration was further increased beyond 1%, the entrapment efficiency decreased. This could be due to several reasons. One possible reason could be the formation of larger particles or aggregates, which reduces the surface area available for interaction with TPP and thus limits the amount of essential oil that can be encapsulated within the nanoparticles. The tables show that the average size of the nanoparticle increased when chitosan concentration was increased beyond 1%.

It was noticed that the loading capacity varies in accordance with the changes in entrapment efficiency, whereby an increase in entrapment efficiency causes an increase in loading capacity, while a decrease in entrapment efficiency results in a decrease in loading capacity. Entrapment efficiency refers to the proportion of oil that is successfully trapped by the chitosan. If the entrapment efficiency is high, it means that most of the oil is bound to the chitosan, and there is less free oil in the system. In this case, the chitosan has reached its maximum binding capacity, and the loading capacity is also high. On the other hand, if the entrapment efficiency is low, it means that there is more free oil in the system that can potentially be bound to the chitosan. In this case, the chitosan is not yet fully saturated with oil, and the loading capacity is also low. So, in general, as the entrapment efficiency increases, the loading capacity also tends to increase because the chitosan is binding more oil molecules. Conversely, as the entrapment efficiency decreases, the loading capacity also tends to decrease because the chitosan is binding fewer oil molecules. (Hanafy et al., 2015) also observed similar trend of increase in loading capacity with an increase in entrapment efficiency with the change in chitosan concentration.

Interestingly, the nanoparticles observed to have higher size at 0.5% chitosan compared to 1%, which could be attributed to the aggregation of oils caused by insufficient chitosan available to form a wall layer for all the essential oils. For instance, the size of the neem essential oil nanoparticle was 285 ± 21 nm, when the chitosan percent was 0.5%. It decreased at 1% to 168 ± 24 nm and further again increased to 244 ± 13 nm and 308 ± 19 nm when the percentage of chitosan was increased to 1.5 and 2. Therefore, 1% chitosan is considered to be the optimized condition for the nanoparticles. Another possible reason could be the high concentration of chitosan, which can result in increased viscosity of the solution and hinder the diffusion of neem essential oil into the nanoparticles. (Nguyen & Le, 2021) noted a similar trend for Palmarosa essential oil encapsulated with chitosan; the efficiency of encapsulation increased from 22.8% to 34.0% when the concentration of chitosan ranged from 5.0 to 10.0 g/L, then decreased to 26.1% at 12.5 g/L. (Javid et al., 2014) in their studies also reported that when the % chitosan was lower than this, the oil particles aggregated because there was not enough chitosan available to form a shell around them. Conversely, when the ratio was higher, the chitosan was able to form layers around the oil particles, leading to an increase in the overall size of the microcapsules.

4.4.2 Effect of % surfactant on the entrapment efficiency, loading capacity and nanoparticle size

According to the study conducted by Sun et al. (2021), the addition of tween 80 leads to an improvement in the efficiency of encapsulation. Results from the pilot study from tables 4.9-4.28 suggested using Tween 80 for developing neem, clove and carom essential oil as they yielded more entrapment of oil as compared to poloxamer 188. Whereas, cinnamon oil was entrapped to its highest with the presence of poloxamer when compared to Tween 80. Hence, tween 80 was added at different concentrations (0.5, 0.75, 1, and 2%) to the chitosan solution for developing neem, clove, and carom essential oil nanoparticles and poloxamer 188 (0.5, 0.75, 1, and 2%) for cinnamon oil nanoparticles. Both Tween 80 and Poloxamer 188 are non-ionic surfactant that aids in the formation of a uniform oil dispersion by reducing the interfacial tension between the oil and the aqueous phase. They allow for a greater degree of oil droplet formation and stabilization, resulting in improved entrapment efficiency. The data showed that for all three oils, there was a pattern of increasing entrapment efficiency at a concentration of 0.75% of Tween 80, followed by a decline when the surfactant concentration was further increased to 1% and 2%. For instance, the encapsulation efficiency initially increased from 71.55% to 80.36% at concentrations of 0.50% and 0.75% Tween 80 in neem essential oil nanoparticles. At the same time, the loading capacity of the nanoparticle decreased slightly from 14.0 ± 0.68% to 13.6 ± 0.52% when the surfactant concentration was increased. This could be because a higher surfactant concentration may have occupied some of the binding sites on the surface of the nanoparticles, thereby reducing the overall capacity of the system to bind target material. On the other hand, for cinnamon essential oil nanoparticles, the highest entrapment efficiency of 75.44 ± 2.28% was observed at 0.50% of Poloxamer 188, and a decrease in entrapment efficiency was noted from 0.75-2%. This trend can be explained by the fact that Tween 80 and poloxamer 188 are a non-ionic surfactant that must have reduced the surface tension of the oil phase, leading to better wetting and dispersion of the oil droplets in the aqueous phase, which ultimately resulted in higher encapsulation efficiency. However, when the concentration of Tween 80 was increased beyond 0.75% and poloxamer beyond 0.50%, the encapsulation efficiency decreased to 64.61% and 54.38% at concentrations of 1% and 2%, respectively, for neem essential oil nanoparticles, and a 9% reduction was observed in cinnamon essential oil nanoparticles. This decreased encapsulation efficiency suggests that, the excess surfactant could have created unfavourable conditions for the formation and stabilization of oil droplets. This could have happened due to several factors, such as the

formation of micelles or the depletion of surfactant at the oil-water interface. These factors could have led to the disruption of the droplet structure, resulting in lower encapsulation efficiency. Formation of foam on the surface of the solution was noted by the researcher with the increase in 2% of Tween 80. This formation of foam can be an indication of excessive surfactant, which can lead to unfavourable conditions for the formation and stability of oil droplets, ultimately resulting in lower encapsulation efficiency.

The surfactant plays a significant role in controlling the size of nanoparticles. As observed in the tables, the data demonstrates that size of the neem, carom and clove essential oil nanoparticles decreased at 0.75% of Tween 80 and increased at higher concentrations of 1% and 2%. This trend can be explained by the effect of surfactant concentration on the emulsion droplet size. Also, at low concentration of Tween 80 (0.5%), the surfactant molecules were not as abundant, leading to the formation of larger oil droplets in the emulsion. As a result, the nanoparticles are larger in size. When the concentration of Tween 80 is increased to 0.75%, the surfactant molecules become more abundant and can more effectively coat the oil droplets, leading to the formation of smaller and more uniform droplets resulting in smaller nanoparticles. For example, smaller size of neem oil nanoparticles of an average size of 172 ± 27 nm was observed at 0.75% Tween 80. However, at higher concentrations of 1% and 2%, the excess surfactant may begin to accumulate and form micelles in the emulsion. These micelles act as additional barriers to the coalescence of the oil droplets, leading to larger nanoparticle sizes. This is consistent with the increase in nanoparticle size to 236 ± 21 nm and 289 ± 19 nm at 1% and 2% Tween 80 concentrations, respectively. (Sukmawati et al., 2018) in her paper mentioned that the addition of 0.5% v/v Tween 80 resulted in the formation of smaller nanoparticles compared to when 0.1% v/v Tween 80 was used. This suggests that Tween 80 may act as a stabilizing agent during nanoparticle formation by reducing surface energy and inhibiting growth. However, in a previous study, researchers reported that increasing the concentration of Tween 80 further, resulted in the amphiphilic molecule depositing on the surface of the particles, leading to an increase in particle size. Therefore, it can be concluded that the range of Tween 80 concentrations used during nanoparticle preparation can have varying effects on the particle size (Hanafy et al., 2015).

4.4.3 Effect of oil concentration on entrapment efficiency, loading capacity and nanoparticle size

Oil concentration is also one of the factors that affect the entrapment efficiency of oil-loaded nanoparticles. Three different concentrations of all the essential oils were used to encapsulate with 1% chitosan concentration. According to the graphs 4.1- 4.4, the highest entrapment efficiency was observed at 1% oil concentration. 78.65 ± 1.28% in neem oil nanoparticles, 73.68 ± 2.35% in cinnamon oil nanoparticles, 51.62 ± 1.56% in clove oil nanoparticles, and 69.27 ± 2.89% in carom oil nanoparticles. However, it was observed that as the oil concentration increased to 2% and 3%, the entrapment efficiency drastically decreased in all the nanoparticles. For instance, neem nanoparticle showed reduction in entrapment efficiency to 69.36 ± 2.54% and 62.12 ± 2.71% at 2 and 3%, respectively. Whereas, both clove and carom oil nanoparticles showed highest reduction of 16% in entrapment efficiency at 2% oil concentration.

This decrease in efficiency at higher oil concentrations can be attributed to the oil droplets becoming more difficult to encapsulate within the nanoparticle matrix. With higher oil concentrations, the likelihood of oil droplets coalescing or merging increases, leading to larger droplets that are more challenging to encapsulate. This ultimately reduces the overall efficiency of the encapsulation process, resulting in lower entrapment efficiency. Several studies have investigated the effect of oil concentration on the entrapment efficiency of oil-loaded nanoparticles. The researchers found that an increase in the initial essential oil content resulted in a decrease in entrapment efficiency (EE). This decrease could be attributed to the saturation of essential oil loading into the wall material during the encapsulation process (Agustinisari et al., 2020).

However, when it came to loading capacity, an increase of % loading capacity was observed with an increase in percentage of oil in all the essential oil chitosan nanoparticles. Thus might be because as the oil content increases, the available surface area for chitosan to form a stable complex with oil molecules decreases, leading to a lower entrapment efficiency. However, the amount of oil that can be loaded onto the chitosan also increases due to an increase in the oil-to-chitosan ratio, leading to a higher loading capacity. (Shetta, 2017) in her study found a similar trend where the loading capacity increased with the increase in green tea oil and the peppermint oil concentration with the decrease in entrapment efficiency. Similar

results were also observed by (Nguyen et al., 2021) where the loading capacity increased with the increase percentage of Palmarosa essential oil.

The impact of the percentage of oil on the size of nanoparticles can be significant. When the percentage of oil in the formulation increases, the size of the resulting nanoparticles generally tends to increase as well. This is because the oil droplets can coalesce and form larger particles during the emulsification and gelation process. The data obtained while screening the oil percent found that the size of the nanoparticles increases with the increase in oil percent.

For example, in table 4.11, of neem essential oil chitosan nanoparticles, is observed that the size of the nanoparticles increased with increasing oil content. The smallest nanoparticle size of 184 ± 16 nm was obtained at an oil content of 1%. When the oil content was increased to 2%, the nanoparticle size increased to 256 ± 19 nm. Similarly, when the oil content was further increased to 3%, the nanoparticle size increased to 312 ± 21 nm.

Similarly, there is a size increase of 57 nm cinnamon oil nanoparticles, 71 nm carom oil nanoparticles, and 46 nm in clove oil nanoparticles. The size further increases with the oil increases to 3%. In their review, (Javed et al., 2014) stated that an increase in the concentration of essential oil encapsulated in fixed concentration sodium alginate led to a significant increase in microcapsule size.

4.4.4 Impact of % TPP on the entrapment efficiency, loading capacity and nanoparticle size

TPP was used as a crosslinking agent to create chitosan nanoparticles with essential oils. TPP is a negatively charged polyanion that can interact with the positively charged amino groups of chitosan, resulting in the formation of a complex between the two polymers. This complexation reaction leads to the formation of a gel-like structure that entraps the drug molecules within the nanoparticle matrix. It is commonly used in nanoparticle synthesis to improve stability, control size, and enhance the entrapment efficiency of the nanoparticles. It works by crosslinking with chitosan molecules and forming a network structure, which leads to the entrapment of essential oil within the nanoparticles. Three different concentrations of TPP (1%, 2%, and 3%) were added as a crosslinking agent to the chitosan essential oil solution. They found that the highest entrapment efficiency and loading capacity was observed in neem nanoparticles (76.56 ± 0.34%), followed by cinnamon oil nanoparticles (75.66 ± 3.41%), carom

oil nanoparticles (73.45 ± 2.73 %), and clove nanoparticles (48.68 ± 3.11%) when 1% TPP solution was added. This is because a higher number of cross-linking units leads to better stability and stronger binding between the drug and chitosan, resulting in a higher entrapment efficiency and slower drug release rate. However, as the concentration of TPP increased beyond a certain point (2% and 3%), the encapsulation efficiency decreased significantly in all the nanoparticles. This is because too much TPP can make the nanoparticles too tightly bound, hindering the interaction between TPP and the core material for chitosan binding, resulting in a decrease in entrapment efficiency.

It also appeared that the loading capacity of essential oil nanoparticles was highest at 1% TPP, regardless of the type of oil used. Additionally, the highest loading capacity was observed in cinnamon nanoparticles (16.26 ± 0.88%) followed by neem nanoparticles (12.80 ± 0.87%). However, despite the fact that the entrapment efficiency was highest for neem oil nanoparticles (76.56 ± 0.34%), followed by cinnamon oil nanoparticles (73.45 ± 2.73%), the loading capacity was higher for cinnamon oil nanoparticles. This suggests that it might be possible that the higher loading capacity of the cinnamon oil nanoparticles was due to their ability to bind more tightly to the TPP or other components of the nanoparticle system, which could allow them to retain more of the target material. At the same time, the higher entrapment efficiency of the neem oil nanoparticles suggests that they were better able to capture the target material initially, before binding it to the nanoparticle system.

Moreover, the relationship between entrapment efficiency and loading capacity seems to be direct. As the entrapment efficiency increased, the loading capacity also increased and conversely, as the entrapment efficiency decreased, the loading capacity decreased as well. This could be because the nanoparticles with higher entrapment efficiency are better able to trap and retain the essential oil, resulting in a higher loading capacity.

The size of nanoparticles is mainly influenced by the concentration of TPP in the chitosan solution. Results show that the addition of a 1% TPP promoted the formation of smaller nanoparticles due to the increased stability of the chitosan-TPP complex. As the concentration of TPP was increased to 2 and 3%, the size of the nanoparticles tends to increase as well. This is because higher concentrations of TPP lead to the formation of larger chitosan-TPP complexes, which resulted in the formation of larger nanoparticles. Moreover, the addition of TPP can also control the size of nanoparticles by affecting the degree of cross-linking

between chitosan molecules. The degree of cross-linking can influence the mechanical properties and stability of nanoparticles, which can in turn affect their size. By controlling the degree of cross-linking, TPP can be used to create nanoparticles with specific sizes and properties. (Kim et al., 2022) in their study mentioned that beyond a certain point of increase of TPP, the entrapment efficiency decreases because the chitosan and TPP form a more compact structure, which hinders the drug's interaction with the core material. They also mentioned that, the size of the nanoparticles can be affected by the amounts of charged particles in the solution, and if there is too much or too little TPP, the particles may become too big or small. This is because the extra TPP can cause the particles to become larger. The researchers selected a ratio of 1:1 between CS and TPP because the nanoparticles produced with this ratio had the highest entrapment efficiency and a satisfactory particle size and distribution.

4.4.5 Impact of stirring rate on the entrapment efficiency, loading capacity and nanoparticle size

The stirring rate plays a crucial role in the preparation of nanoparticles as it affects the size and entrapment efficiency of the particles. For emulsification and ionic gelation, out of 1200, 1500 and 1800 rpm, the optimized stirring rate was found to be 1800. At this rate, the entrapment efficiency and loading capacity was found to be high, and the size of the particles were lowest and also within the acceptable range. This is because at this rate, the emulsion droplets are effectively broken down, and the ionic gelation process occurs uniformly, leading to the formation of well-defined particles. Below 1800 rpm, the nanoparticles aggregates leading to higher size of nanoparticles and less entrapment efficiency. Cinnamon oil chitosan nanoparticles exhibited an entrapment efficiency of 74.23 ± 2.11% and a loading capacity of 12.57 ± 0.55%. In comparison, clove and carom nanoparticles showed lower entrapment efficiencies of 51.62 ± 3.1% and 70.66 ± 2.24%, respectively, and lower loading capacities of 8.7 ± 0.31% and 11.9 ± 0.6%, respectively. Moreover, it was observed that the change in loading capacity was directly proportional to the change in entrapment efficiency. This means that when the entrapment efficiency increased, the loading capacity also increased and vice versa.

In the case of nano-emulsion and ionic gelation, the process was carried out in two stages. In the first stage, high shear homogenization at 13000 rpm for 10 minutes was used to create a fine emulsion, followed by stirring at 1800 rpm on a magnetic stirrer. This two-stage process resulted in the formation of nanoparticles with higher entrapment efficiency and

loading capacity and smaller size compared to other stirring rates. This is because the high shear homogenization at a high speed creates a fine emulsion with smaller droplets, and the subsequent stirring at a lower speed facilitates the ionic gelation process, resulting in the formation of nanoparticles with smaller size and higher entrapment efficiency. Neem essential oil nanoparticles gave the highest entrapment efficiency and loading capacity of 78.42 ± 1.56% and of 12.28 ± 0.34% using this method as compared to the emulsion and ionic gelation method. This could be as the density and the viscosity of the neem essential oil was higher than the other essential oils. This may have influenced the formation of nanoparticles. Generally, oils with lower density form smaller nanoparticles due to their ability to disperse more easily in the aqueous phase and interact more effectively with the polymer matrix. The table 4.13 also shows that the further increase in the homogenization speed beyond 13000, the entrapment efficiency decreases. The loading capacity also decreases with a decrease in entrapment efficiency. High sheer might have result in too much energy being transferred to the medium causing the essential oils to evaporate, and result in particle aggregation. A similar study by (Shetta, 2017) showed highest entrapment efficiency of peppermint oil) for 10 minutes stirring at 14000 rpm.

Below Table 4.29 represents the results of the optimized conditions of all the essential oil nanoparticles**:**

Table 4.29: Optimized conditions of the nanoparticles selected under the study

Optimized conditions of the essential oil nanoparticles					**Results**		
Oil	Polymer: Oil	Surfactant %	TPP %	RPM	Size (nm)	% EE	LC %
Neem	1:1	0.75 (Tween 80)	1	13000	189 ± 26	78.42 ± 1.56	12.28 ± 0.34
Cinnamon	1:1	0.5 (Poloxamer 188)	1	1800	226 ± 25	74.23 ± 2.11	12.57 ± 0.55
Clove	1:1	0.75 (Tween 80)	1	1800	294 ± 33	51.62 ± 3.1	8.7 ± 0.31
Carom	1:1	0.75 (Tween 80)	1	1800	349 ± 23	70.66 ± 2.24	11.9 ± 0.64

Based on the data presented in the above table 4.29 , it was observed that the neem essential oil chitosan nanoparticle had the highest oil entrapment efficiency, with the cinnamon, carom, and clove oil nanoparticles following closely behind. The entrapment efficiency of the nanoparticles is influenced by various factors such as the properties of the oils, the method of preparation, and the physicochemical properties of the chitosan, surfactant, and crosslinking agent used. In the case of neem oil nanoparticles, a high entrapment efficiency and loading capacity of 78.42 ± 1.56% and 12.28 ± 0.34% was achieved using a combination of nano-emulsion and ionic gelation methods with 0.75% surfactant (Tween 80) and 1% TPP at 13000 rpm. This high entrapment efficiency can be attributed to the presence of various active compounds such as azadirachtin, nimbin, and nimbidin in neem oil, which can form strong electrostatic interactions with chitosan and TPP resulting in the formation of stable nanoparticles.

Similarly, for clove oil nanoparticles, a 1:1 ratio of clove oil and chitosan, along with 0.75% Tween 80 and 1% TPP at 1800 rpm resulted in a size of 294 ± 33 nm and an entrapment efficiency and loading capacity of 51.62 ± 3.1% and 8.7 ± 0.31%. Clove oil contains eugenol, which has a phenolic group that can form hydrogen bonds with chitosan and TPP, resulting in a relatively low entrapment efficiency as compared to neem oil nanoparticles.

Cinnamon oil nanoparticles showed a size of 226 ± 25 nm and an entrapment efficiency and loading capacity of 74.23 ± 2.11% and 12.57 ± 0.55% using 1:1 ratio of cinnamon oil and chitosan, 0.5% Poloxamer 188 and 1% TPP at 1800 rpm. Cinnamon oil contains cinnamaldehyde, which has a double bond that can form covalent bonds with TPP, resulting in a stable cross-linked matrix and higher entrapment efficiency.

Finally, carom oil nanoparticles had a size of 349 ± 23 nm and an entrapment efficiency and loading capacity of 70.66 ± 2.24% and 11.9 ± 0.64% using a 1:1 ratio of carom oil and chitosan, 0.75% Tween 80 and 1% TPP at 1800 rpm. Carom oil contains thymol, which has a phenolic group that can form hydrogen bonds with chitosan and TPP, resulting in a relatively high entrapment efficiency.

4.5 Characterization of the nanoparticles

The characterization of nanoparticles is an essential step in the development of effective and safe drug delivery systems. The physicochemical properties of nanoparticles play a critical role

in their action, and durability. Therefore, a comprehensive characterization of nanoparticles is necessary to ensure the reproducibility and quality control of their preparation and to evaluate their potential.

4.5.1 Determining the calibration curve of the essential oils

The percent entrapment efficiency and the loading capacity of the nanoparticles in the study was calculated by determining the calibration curve of essential oils at first. It provides a standard reference point for measuring the amount of oil that has been encapsulated within the nanoparticles. A series of standard solutions by diluting the standard compound in a suitable solvent were prepared and the standard solutions were analyzed for its absorbance using a UV-Vis Spectrophotometer. Dichloromethane was used for clove essential oil. Methanol was used for carom essential oil. Cinnamon essential oil was dissolved in 70:30 methanol and water. Whereas, DCM: Methanol at 54: 46 dissolved neem essential oil. A linear calibration curve was plotted with the concentration of the standard solutions on the x-axis and the absorbance on the y-axis. A regression coefficient (R2) was calculated to generate the calibration curve equation.

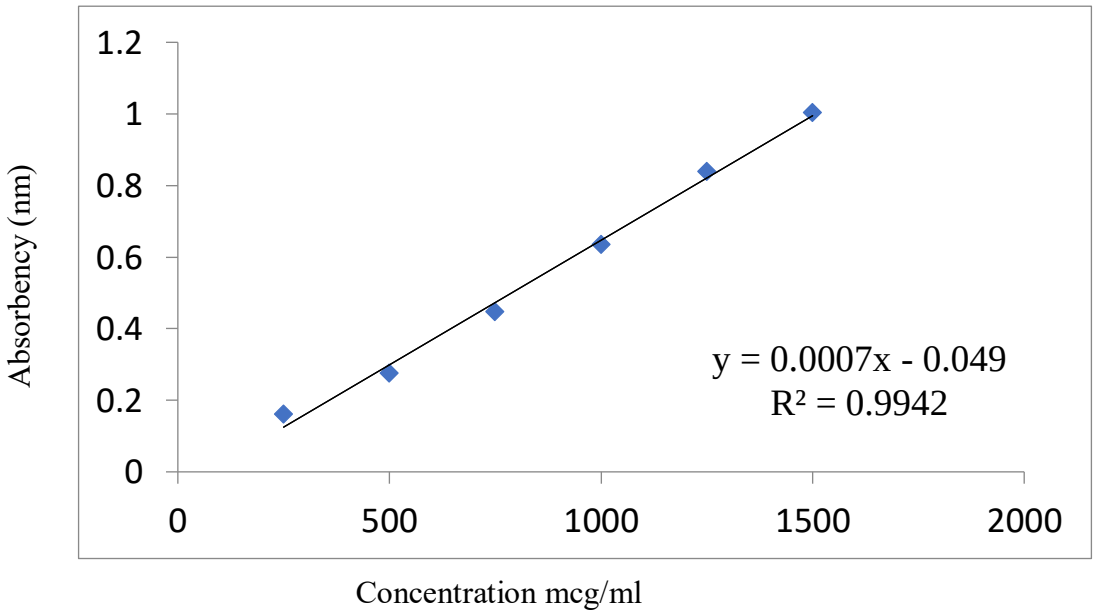

Graph 4.5: Calibration curve of neem essential oil

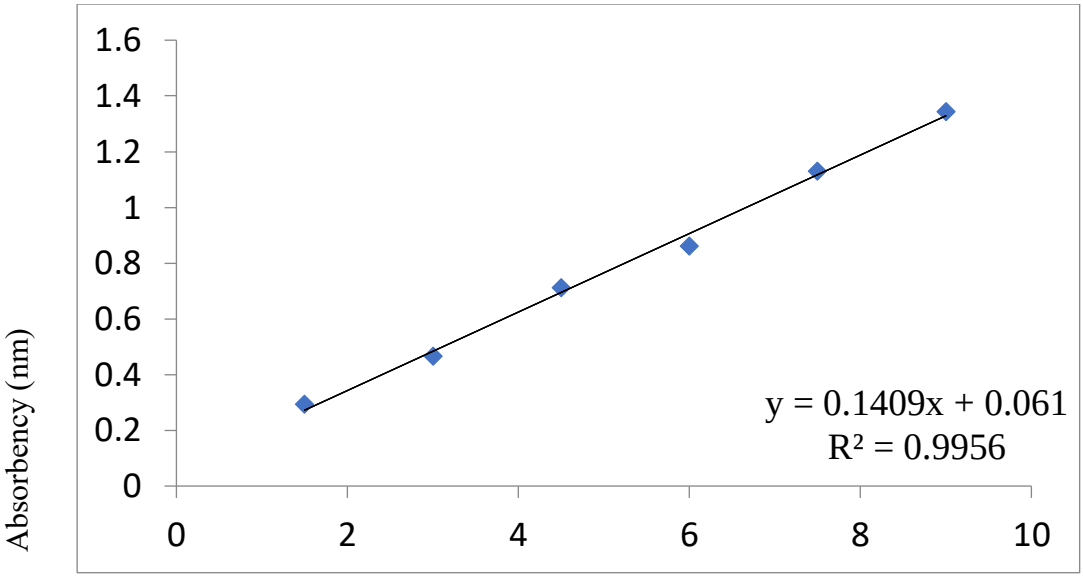

Graph 4.6: Calibration curve of cinnamon essential oil

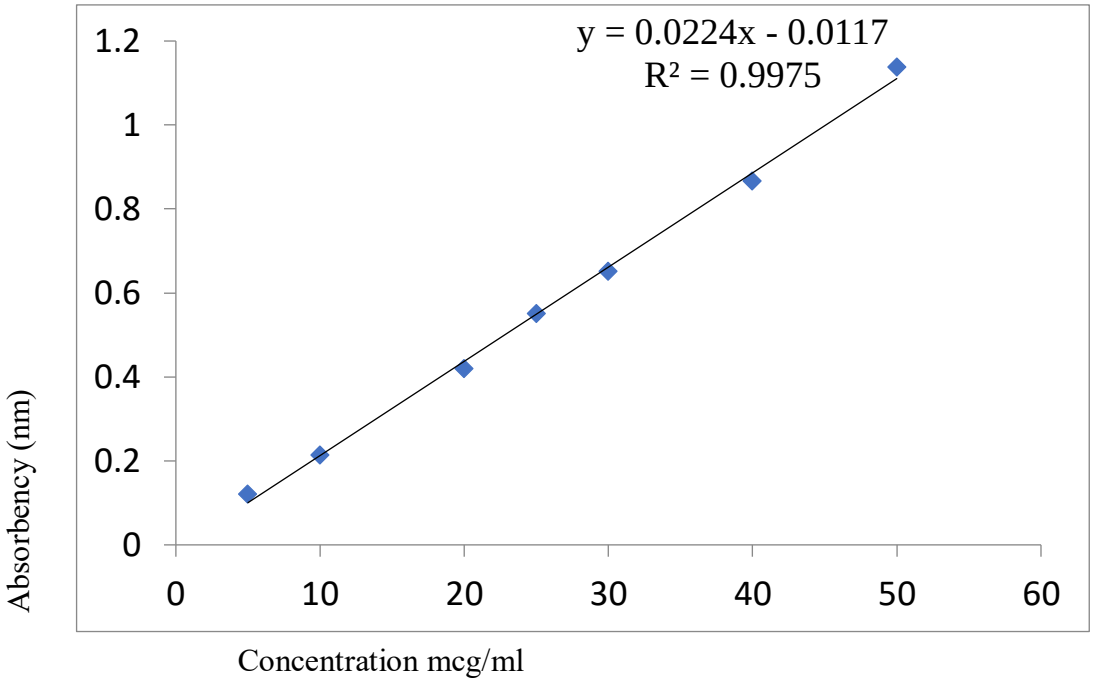

Graph 4.7: Calibration curve of clove essential oil

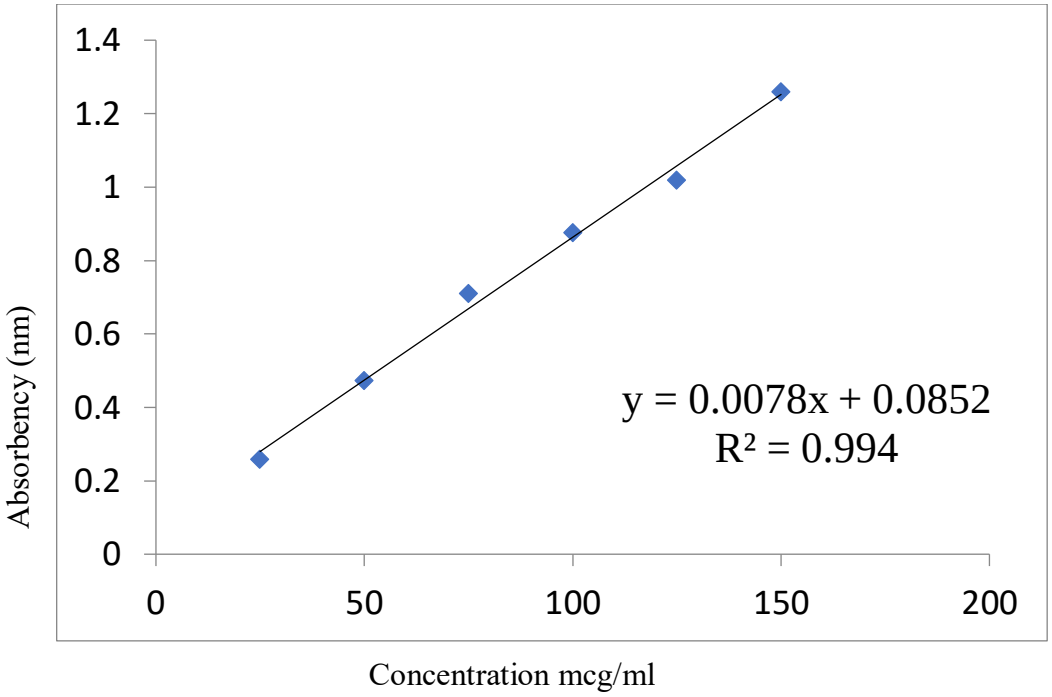

Graph 4.8: Calibration curve of carom essential oil

The absorbance spectrum of neem essential oil showed a peak at 278nm, cinnamon oil at 287 nm, clove oil at 278 nm, and carom at 277nm. The calibration curve in the graphs above shows the relationship between the concentration of the selected essential oils and their corresponding absorbance or response. Using this curve, the regression coefficient equation was derived to relate the absorbance or response to the oil concentration as seen in graph 4.5- 4.8. To calculate the entrapment efficiency of the essential oils in the nanoparticles, the absorbance value obtained from each nanoparticle sample was used with the regression coefficient equation to determine the oil concentration. This concentration value was then converted to a percentage based on the weight of the nanoparticle sample to calculate the entrapment efficiency of the nanoparticles.

4.5.2 Determining the particle size and the polydispersity index (PDI) of the prepared nanoparticles.

Nanoparticle size and size distribution are crucial factors that determine the efficacy and safety of nanoparticle-based drug delivery systems. Particle size affects the biodistribution, cellular uptake, and drug release kinetics of nanoparticles, while the size distribution reflects the uniformity of the particle population. Therefore, determining the particle size and the polydispersity index (PDI) of the prepared nanoparticles is essential to evaluate their quality and performance.

The PDI is a measure of the width of the size distribution, where a PDI value close to zero indicates a narrow size distribution, while a value closer to one indicates a broad size distribution. The PDI is affected by various factors, including the preparation method, the properties of the drug and the carrier material, and the processing conditions. Thus, controlling the PDI is crucial to ensure a consistent and uniform particle size distribution, which is important for reproducibility and batch-to-batch consistency. The test was performed using a zeta sizer which uses the technique of dynamic light scattering (DLS) to measure the Brownian motion of nanoparticles in a liquid medium. The results of the average size and the PDI of the optimized neem, cinnamon, and clove chitosan nanoparticles obtained from the zeta sizer are shown in the figure 4.3- 4.6.

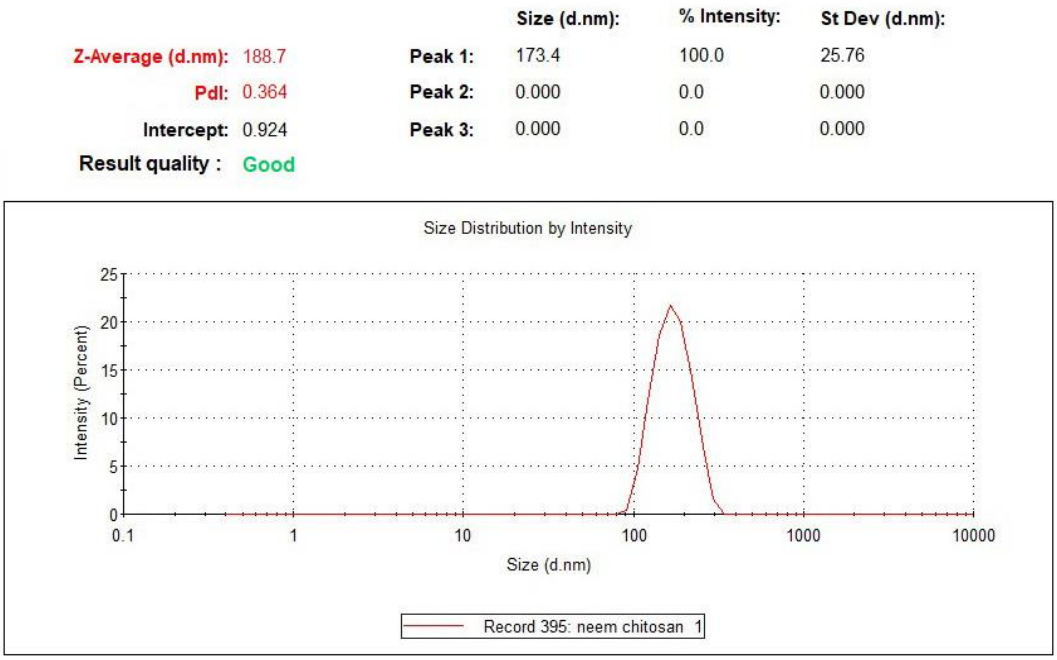

Fig. 4.3: PDI of the optimized Neem essential oil chitosan nanoparticles

		Size (d.nm):	% Intensity:	St Dev (d.nm):
Z-Average (d.nm): 226.0	Peak 1:	221.4	100.0	25.40
PdI: 0.241	Peak 2:	0.000	0.0	0.000
Intercept: 0.914	Peak 3:	0.000	0.0	0.000
Result quality : Good				

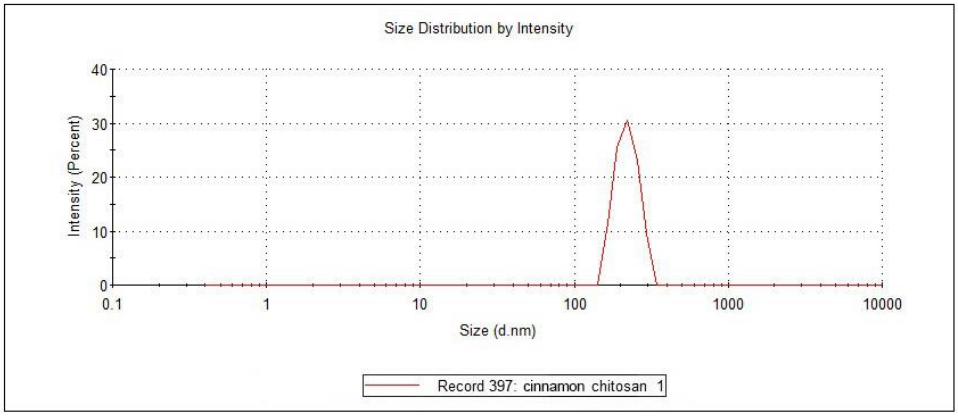

Fig. 4.4: PDI of the optimized Cinnamon essential oil chitosan nanoparticles

		Size (d.nm):	% Intensity:	St Dev (d.nm):
Z-Average (d.nm): 293.9	Peak 1:	311.3	95.1	35
PdI: 0.287	Peak 2:	4837	4.9	708.4
Intercept: 0.960	Peak 3:	0.000	0.0	0.000
Result quality : Good				

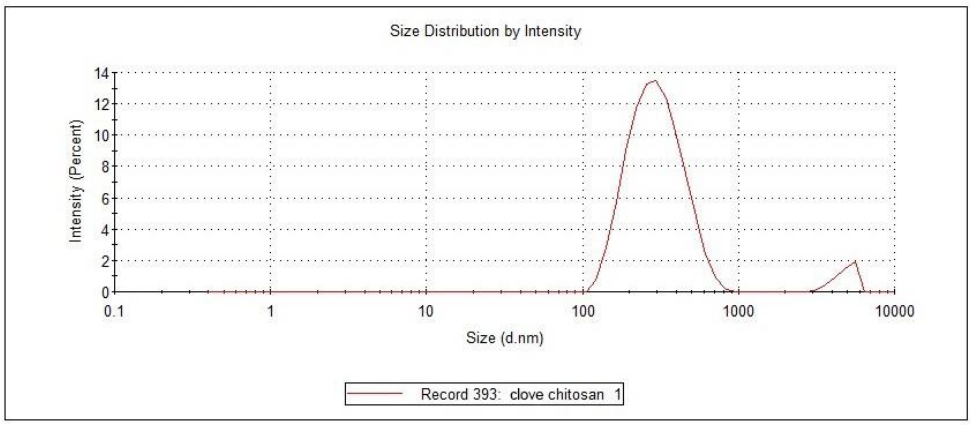

Fig. 4.5: PDI of the optimized Clove essential oil chitosan nanoparticles

		Size (d.nm):	% Intensity:	St Dev (d.nm):
Z-Average (d.nm): 349.7	Peak 1:	208.7	54.4	28.59
PdI: 0.540	Peak 2:	0.000	0.0	0.000
Intercept: 0.696	Peak 3:	0.000	0.0	0.000
Result quality : Good				

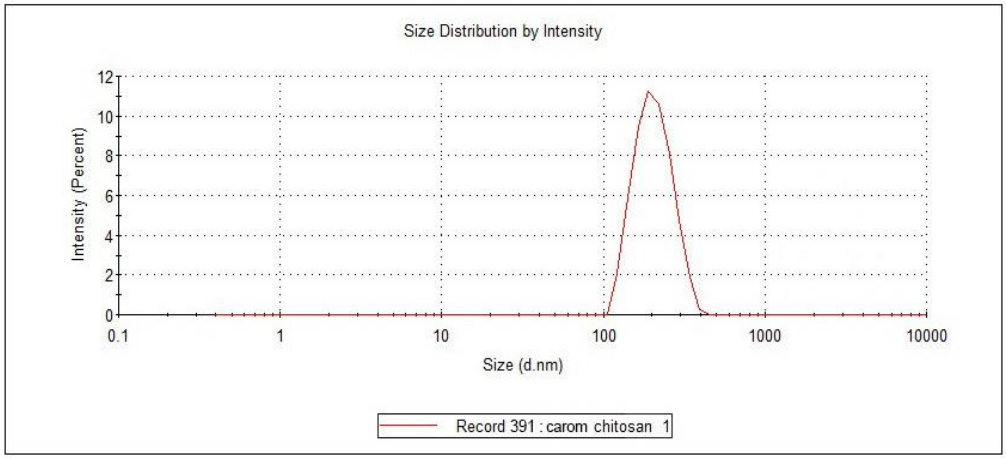

Fig. 4.6: PDI of the optimized Carom essential oil chitosan nanoparticles

The results of the study showed that the size and polydispersity index (PDI) of the neem chitosan, cinnamon chitosan, and clove chitosan nanoparticles were different. The neem chitosan nanoparticles had the smallest size of 189 nm, while the cinnamon chitosan nanoparticles had a slightly larger size of 226 nm, and the clove chitosan nanoparticles had the largest size of 294 nm.

In terms of size distribution, the cinnamon chitosan nanoparticles had the narrowest size distribution, with a PDI of 0.241. The neem chitosan nanoparticles had a higher PDI of 0.364, indicating a broader size distribution. The clove chitosan nanoparticles had the widest size distribution, with a PDI of 0.287. The PDI values indicate the degree of uniformity of the particle size distribution, with a lower PDI value indicating a more uniform particle size distribution. The values obtained for all three types of optimized nanoparticles were relatively low, indicating that the particle size distributions were relatively narrow.

The observed differences in particle size and PDI values can be attributed to various factors such as the concentration and properties of the chitosan and essential oils used, the type and concentration of cross-linking agents, surfactants, and the processing conditions such as stirring rate.

4.5.3 Determining the minimum inhibitory concentrations (MIC) of the nanoparticles

The MIC test involved analyzing the lowest concentration of a substance that effectively inhibits the growth of a microorganism. To perform the test, a series of dilutions of optimized nanoparticles were created using a 2-fold dilution system, with initial concentrations of neem oil at 1476 µg/mL, cinnamon oil at 1412 µg/mL, clove oil at 1436 µg/mL, and carom oil at 1469 µg/mL. For example, a 2-fold dilution series of neem essential oil-chitosan nanoparticle solution with a concentration of 1476 µg/mL would be 738, 369, 184.5, 92.25, 46.12, 20.06, 11.59, and so on in µg/mL. The bacterial species selected for observation were *Bacillus cereus, Staphylococcus aureus, Pseudomonas*, and *Escherichia coli,* while the fungal species was *Aspergillus fumigatus*. The below tables 4.30-4.34 represents the bacterial and fungal growth observed at a particular dilution of each nanoparticle along with the combination of the nanoparticles.

Table 4.30: MIC of nanoparticles against *Bacillus cereus*

Dilution	MIC against *Bacillus cereus*					
	NNPs	C1NPs	C2NPs	C3NPs	C1NPs + C2NPs	NNPs + C2NPs
1	NG	NG	NG	NG	NG	NG
2	NG	NG	NG	**Growth**	NG	NG
4	**Growth**	**Growth**	NG	Growth	NG	NG
8	Growth	Growth	**Growth**	Growth	NG	**Growth**
16	Growth	Growth	Growth	Growth	**Growth**	Growth
32	Growth	Growth	Growth	Growth	Growth	Growth
64	Growth	Growth	Growth	Growth	Growth	Growth
128	Growth	Growth	Growth	Growth	Growth	Growth

NG: No Growth

Table 4.31: MIC of nanoparticles against *Staphylococcus aureus*

Dilution	MIC against *Staphylococcus aureus*					
	NNPs	C1NPs	C2NPs	C3NPs	C1NPs + C2NPs	NNPs + C2NPs
1	NG	NG	NG	NG	NG	NG
2	NG	NG	NG	**Growth**	NG	NG
4	**Growth**	**Growth**	NG	Growth	NG	NG
8	Growth	Growth	**Growth**	Growth	NG	**Growth**
16	Growth	Growth	Growth	Growth	**Growth**	Growth
32	Growth	Growth	Growth	Growth	Growth	Growth
64	Growth	Growth	Growth	Growth	Growth	Growth
128	Growth	Growth	Growth	Growth	Growth	Growth

NG: No Growth

Table 4.32: MIC of nanoparticles against *Pseudomonas*

Dilution	MIC against *Pseudomonas*					
	NNPs	C1NPs	C2NPs	C3NPs	C1NPs + C2NPs	NNPs + C2NPs
1	NG	NG	NG	**Growth**	NG	NG
2	**Growth**	**Growth**	NG	Growth	NG	NG
4	Growth	Growth	**Growth**	Growth	NG	**Growth**
8	Growth	Growth	Growth	Growth	**Growth**	Growth
16	Growth	Growth	Growth	Growth	Growth	Growth
32	Growth	Growth	Growth	Growth	Growth	Growth
64	Growth	Growth	Growth	Growth	Growth	Growth
128	Growth	Growth	Growth	Growth	Growth	Growth

NG: No Growth

Table 4.33: MIC of nanoparticles against *Escherichia coli*

Dilution	MIC against *Escherichia coli*					
	NNPs	C1NPs	C2NPs	C3NPs	C1NPs + C2NPs	NNPs + C2NPs
1	NG	NG	NG	**Growth**	NG	NG
2	**Growth**	**Growth**	NG	Growth	NG	NG
4	Growth	Growth	**Growth**	Growth	NG	**Growth**
8	Growth	Growth	Growth	Growth	**Growth**	Growth
16	Growth	Growth	Growth	Growth	Growth	Growth
32	Growth	Growth	Growth	Growth	Growth	Growth
64	Growth	Growth	Growth	Growth	Growth	Growth
128	Growth	Growth	Growth	Growth	Growth	Growth

NG: No Growth

Table 4.34: MIC of nanoparticles against *Aspergillus fumigatus*

Dilution	MIC against *Aspergillus fumigatus*					
	NNPs	C1NPs	C2NPs	C3NPs	C1NPs + C2NPs	NNPs + C2NPs
1	NG	NG	NG	**Growth**	NG	NG
2	**Growth**	**Growth**	**Growth**	Growth	NG	**Growth**
4	Growth	Growth	Growth	Growth	**Growth**	Growth
8	Growth	Growth	Growth	Growth	Growth	Growth
16	Growth	Growth	Growth	Growth	Growth	Growth
32	Growth	Growth	Growth	Growth	Growth	Growth
64	Growth	Growth	Growth	Growth	Growth	Growth
128	Growth	Growth	Growth	Growth	Growth	Growth

NG: No Growth

Data from table 4.30 and table 4.31 presents the MIC results for six different types of nanoparticles, including single essential oil nanoparticles and combinations of two essential oil nanoparticles, against two gram-positive bacteria, *Bacillus cereus* and *Staphylococcus aureus*. The results indicate that all the nanoparticle samples have the same MIC values for both bacteria, which suggests a broad-spectrum antimicrobial activity. However, there are

differences in the MIC values for the different types of nanoparticles which could indicate a broad-spectrum antimicrobial activity. When looking at the individual essential oil nanoparticles, Clove essential oil nanoparticles (C2NPs) had the highest MIC between dilutions 4 and 8, which means that it was the most effective at inhibiting bacterial growth at a lower concentration compared to other single essential oil nanoparticles. Furthermore, when Cinnamon and Clove nanoparticles were combined (C1NPs+C2NPs), they showed the highest MIC value at dilution 16 of all the combinations tested, including neem and clove combination (NNPs+C2NPs), as well as single nanoparticles. This suggests that combining the two essential oil nanoparticles enhances their antimicrobial activity which could be likely due to synergistic effects. In contrast, the MIC values for neem essential oil nanoparticles (NNPs) and Cinnamon essential oil (C1NPs) were likely between dilutions of 2 and 4, since there was growth at a dilution of 4. For carom oil nanoparticles (C3NPs), growth was observed at dilution 2, indicating that the MIC was likely between the original concentration and dilution 2 which is the lowest antibacterial activity compared to other essential oil nanoparticles.

The tables 4.32 and 4.33 display the MIC values for Pseudomonas and E. coli, which are gram-negative bacteria. All the nanoparticles demonstrated a comparable pattern of effectiveness against these bacteria, except for the fact that the dilutions required for gram-negative bacteria were lower than those needed for gram-positive bacteria. This suggests that the nanoparticles acted similarly against all four types of bacteria, but a higher concentration was needed to inhibit the growth of gram-negative bacteria than gram-positive ones.

When looking at the individual essential oil nanoparticles, the most effective at inhibiting bacterial growth at a lower concentration was observed with Clove essential oil nanoparticles (C2NPs) having the highest MIC between dilutions 2 and 4. In combination of nanoparticles, Cinnamon and Clove nanoparticles (C1NPs+C2NPs), showed the highest MIC value at dilution 8 when compared to neem and clove combination (NNPs+C2NPs), as well as single nanoparticles.

The results from the tables showed that Carom essential oil nanoparticles (C3NPs) did not exhibit any antibacterial activity against both gram-negative bacteria when compared to other nanoparticles. Additionally, it was observed that Carom essential oil nanoparticles exhibited antibacterial activity at a very low dilution of 2, even though the nanoparticles had a high entrapment efficiency of 70.66 ± 2.24%. Furthermore, carom essential oil nanoparticles

did not demonstrate any anti-fungal properties against *Aspergillus fumigatus* (table 4.34). This indicates that Carom essential oil nanoparticles had the least to zero activity towards bacteria and fungi and was therefore excluded from further study.

Based on the data presented in table 4.34, it can be observed that all single oil nanoparticles and neem-clove oil nanoparticle combinations had similar MIC results against *Aspergillus fumigatus* at dilution 2. On the other hand, the combination of cinnamon and clove oil nanoparticles exhibited the highest MIC value at dilution 4. These results suggest that the nanoparticles were effective in inhibiting the growth of Aspergillus fumigatus, but required higher concentrations (i.e. less dilution) as compared to bacteria. It is important to note that the nanoparticles showed better antimicrobial activity against bacteria than fungi.

Overall, the results suggest that essential oil chitosan nanoparticles have potential as antimicrobial agents, especially when used in combination. However, the concentration required to inhibit the growth of gram-negative bacteria was higher than that needed for gram-positive bacteria. This could be attributed to the differences in the cell walls of these two types of bacteria. Gram-negative bacteria have an additional outer membrane that acts as a barrier, making them less susceptible to antimicrobial agents. Therefore, a higher concentration of nanoparticles is needed to penetrate this barrier and exert their antimicrobial activity. The differences in MIC values for the different types of nanoparticles can be attributed to the differences in the types and concentrations of bioactive compounds present in the essential oils used to prepare the nanoparticles.

4.5.4 Surface analysis of the prepared NPs using Scanning electron microscope (SEM)

The final optimized nanoparticles that were selected for the study were individually developed from neem, cinnamon, and clove essential oil. These selected nanoparticles were observed under SEM.

Figure 4.7, 4.8, and 4.9 shows the SEM images of neem, cinnamon and clove essential oil nanoparticles which exhibit spherical and uniform shaped essential oil chitosan nanoparticles, which suggests that the synthesis process was consistent. The particle size, as determined by the scales shown in the images, are similar to the size observed using a Zetasizer. Additionally, no cracks were observed in the particles, indicating that the wall layer formed continuously during the synthesis process. However, a small number of nanoparticles showed inward grooves or dents, which could be due to the diffusion of oil or the lyophilization process.

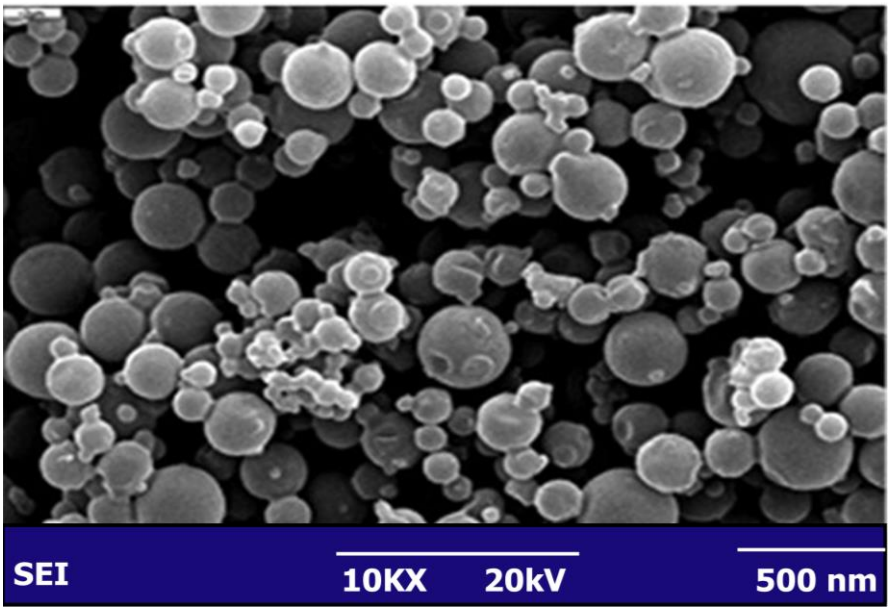

Figure 4.7 : SEM image of optimized neem essential oil chitosan nanoparticles

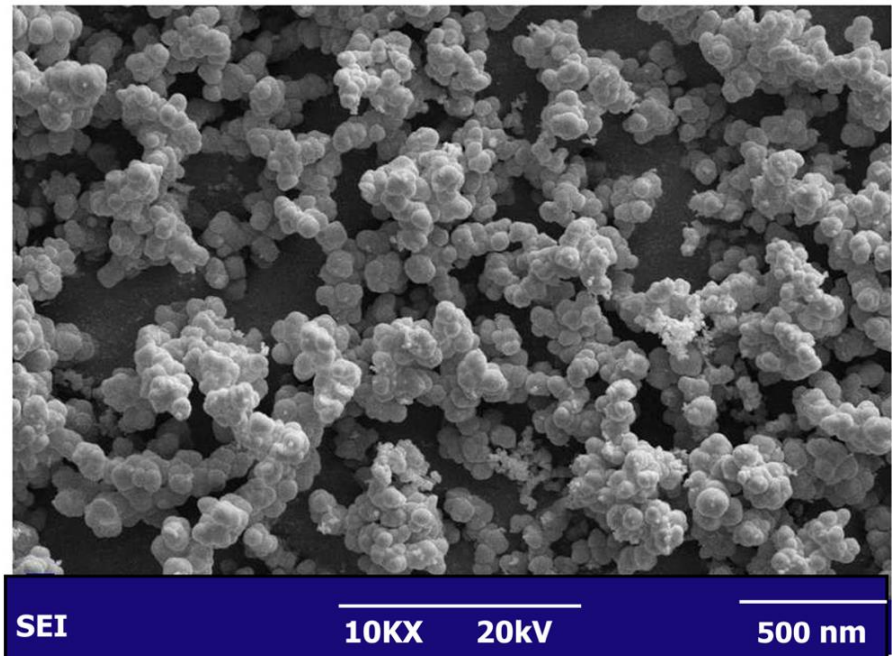

Fig. 4.8 : SEM image of optimized cinnamon essential oil chitosan nanoparticles

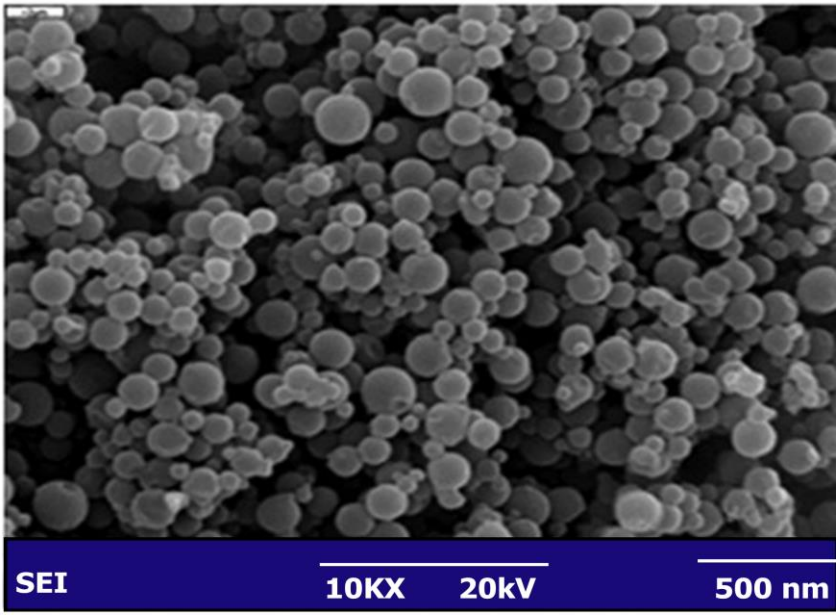

Fig. 4.9 : SEM image of optimized clove essential oil chitosan nanoparticles

4.6 Application of the optimized essential nanoparticles on the substrate

100% cotton and 100% polyester fabric were selected as a substrate under the study. Table 4.35 shows the preliminary data of the selected fabrics.

Table 4.35: Preliminary data of the selected fabric

Fiber content	**Fabric count**		**Weight/Unit area (Gms/mt^2)**	**Fabric thickness (mm)**	**Weave**
	Ends per cm	Picks per cm			
100% cotton	98	62	92	0.27	Plain
100% polyester	82	71	110	0.21	Plain

Based on the MIC results, Neem, clove, cinnamon and combination of clove and cinnamon essential oil nanoparticles were selected for the application on the selected substrates. The MIC results were used to determine the minimum concentration required to prevent visible growth of selected microbes against particular microbes, and the optimized solution was diluted accordingly to obtain the desired concentration for coating the cotton and polyester substrate. To illustrate, when neem oil chitosan nanoparticles at a concentration of 1476 µg/mL were diluted to a 1:4 concentration, growth was observed against both gram-positive bacteria. This

suggested that the nanoparticles could impede growth at a dilution between 2 to 4. Consequently, the solution was optimized by diluting it twice to obtain a concentration of 738 µg/mL for *Bacillus cereus* and *Staphylococcus aureus*. This optimized solution was used to coat cotton and polyester fabric through a padding mangle, with the addition of a 10% citric acid binder that also functioned as a dispersing agent. The presence of citric acid aided in stabilizing the chitosan nanoparticles and preventing them from clumping together. Subsequently, the fabric samples were tested for their antibacterial properties against gram-positive bacteria. Similarly, Cinnamon oil nanoparticles at 1412 µg/mL were diluted twice to achieve 702 µg/mL for application against gram-positive bacteria. On the other hand, clove oil nanoparticles at 1436 µg/mL were diluted six times, as growth was observed at a concentration of 8 when tested against gram-positive bacteria. In the similar fashion, the nanoparticles were diluted for the application on the fabric samples to be tested against gram- negative bacteria. Neem, cinnamon and clove nanoparticles of their original concentration were applied as the growth was observed at dilution 2.

For the combination of cinnamon and clove nanoparticles, growth was observed at the highest dilution of 16 against gram-positive bacteria; thus, the solution was diluted eight times the original. Whereas, the solution was diluted twice against the gram-negative bacteria, respectively. An equal amount of both the cinnamon and clove nanoparticle solution were poured into the bath, and the fabric samples were dipped and padded using a padding mangle as shown in figure 4.10. Three individual samples of all the developed nanoparticles and their combination were padded, dried and cured on the cotton and polyester fabric. The treated fabric samples were further characterized for its antimicrobial, insect repellency, EDX and stability studies.

Fig. 4.10: Padding mangle

4.7 Assessment of the treated fabrics

4.7.1 Assessment of Antibacterial activity of the treated cotton and polyester fabric using standard AATCC 147

The coated cotton and polyester fabric samples were tested against the selected bacterial strains using AATCC 147 parallel streak method. The assessment of the treated fabric against the bacterial colonies are presented below.

A) Assessment of *Bacillus cereus* activity of the treated cotton and polyester fabric

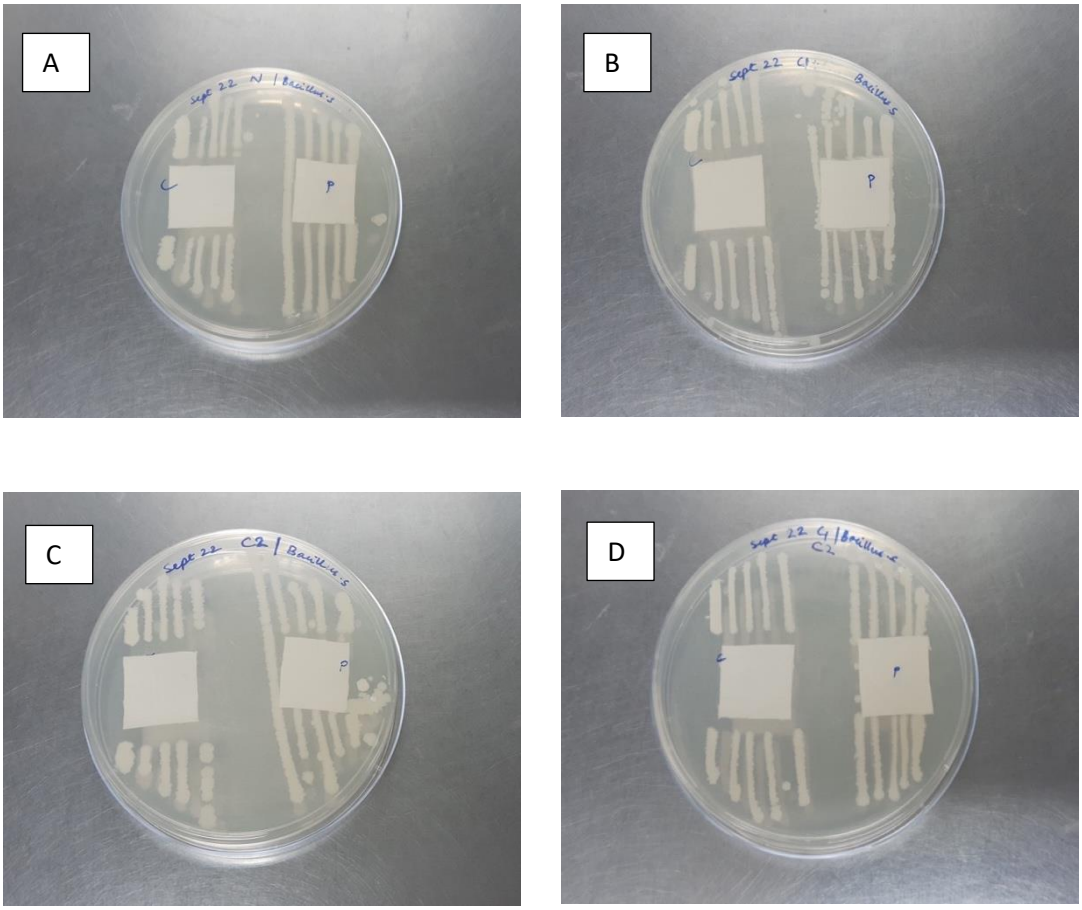

Fig. 4.11: Antibacterial activity of the treated cotton (on the left of the petri dish) and polyester fabric (on the right of the petri dish) against *Bacillus cereus*.
A-Neem oil chitosan nanoparticle, B- Cinnamon oil chitosan nanoparticle, C- Clove oil chitosan nanoparticle, and D- Cinnamon and Clove oil chitosan nanoparticle

Table 4.36: Zone of inhibition of the nanoparticle treated cotton and polyester fabric against *Bacillus cereus*

Sr. No	**Nanoparticles**	**Zone of inhibition (mm) against *Bacillus cereus***	
		Cotton fabric	Polyester fabric
1.	Neem Chitosan Np	2.8 ± 0.2	-
2.	Cinnamon Chitosan Np	3.0 ± 0.3	-
3.	Clove Chitosan Np	4.3 ± 0.3	-
4.	Clove+ Cinnamon Np	4.0 ± 0.5	-

Figure 4.11 and the above table 4.36 represent the effectiveness of different oil nanoparticles against Bacillus cereus on treated cotton and polyester fabric. Bacillus cereus is a Gram-positive, spore-forming bacterium. Zone of inhibition refers to the area around the nanoparticle treatment where bacteria growth is inhibited due to the antimicrobial properties of the nanoparticles.

The results indicate that polyester fabric showed no inhibition towards Bacillus cereus, regardless of the type of nanoparticle treatment used. 4.

Among the different oil nanoparticles tested, clove chitosan nanoparticle showed the highest zone of inhibition with 4.3 ± 0.3 mm. The combined use of clove and cinnamon chitosan nanoparticles resulted in a zone of inhibition of 4.0 ± 0.5 mm. Neem chitosan nanoparticles showed the lowest zone of inhibition with 2.8 ± 0.2 mm.

B) Assessment of *Staphylococcus aureus* activity of the treated cotton and polyester fabric

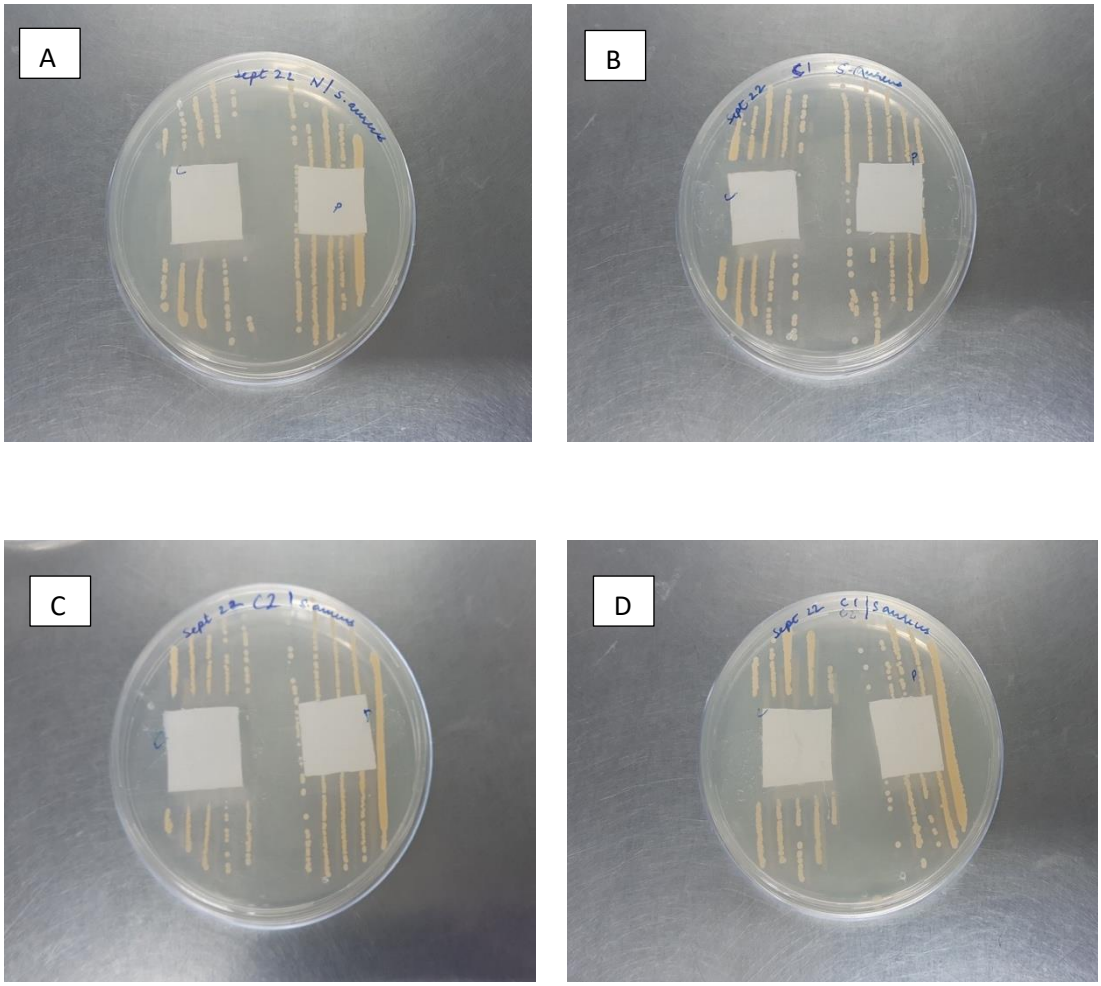

Fig. 4.12: Antibacterial activity of the treated cotton (on the left of the petri dish) and polyester fabric (on the right of the petri dish) against *Staphylococcus aureus.*
A-Neem oil chitosan nanoparticle, B- Cinnamon oil chitosan nanoparticle, C- Clove oil chitosan nanoparticle, and D- Cinnamon and Clove oil chitosan nanoparticle

Table 4.37: Zone of inhibition of the nanoparticle treated cotton and polyester fabric against *Staphylococcus aureus*

Sr. No	**Nanoparticles**	**Zone of inhibition (mm) against *Staphylococcus. Aureus***	
		Cotton fabric	Polyester fabric
1.	Neem Chitosan Np	3.1 ± 0.64	-
2.	Cinnamon Chitosan Np	3.2 ± 0.6	-
3.	Clove Chitosan Np	3.4 ± 0.37	-
4.	Clove+ Cinnamon Np	4 ± 0.4	-

As seen figure 4.12 and the given results in the table 4.37 represent the effectiveness of different oil nanoparticles against *Staphylococcus aureus* on treated cotton and polyester fabric. The results indicate that polyester fabric showed no inhibition towards *Staphylococcus aureus*, regardless of the type of nanoparticle treatment used. On the other hand, cotton fabric showed varying levels of inhibition depending on the type of oil nanoparticle used.

Among the different oil nanoparticles tested, clove+ cinnamon chitosan nanoparticle showed the highest zone of inhibition with 4 ± 0.4 mm. This is similar to the result obtained for *Bacillus cereus*. Clove chitosan nanoparticle showed the second-highest zone of inhibition with 3.4 ± 0.37 mm. Cinnamon chitosan nanoparticle showed a zone of inhibition of 3.2 ± 0.6 mm. Neem chitosan nanoparticle showed the lowest zone of inhibition with 3.1 ± 0.64 mm.

C) Assessment of *Pseudomonas* activity of the treated cotton and polyester fabric

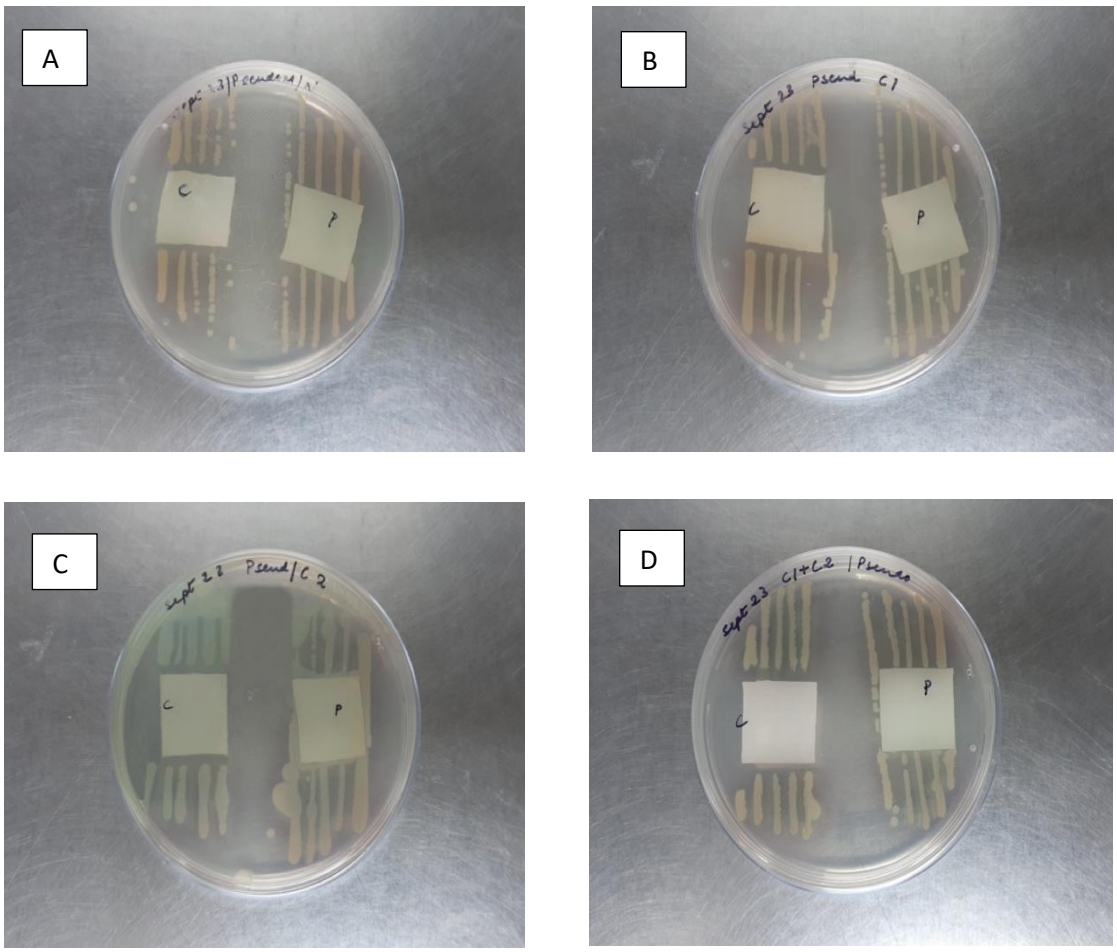

Fig. 4.13: Antibacterial activity of the treated cotton (on the left of the petri dish) and polyester fabric (on the right of the petri dish) against *Pseudomonas.*
A-Neem oil chitosan nanoparticle, B- Cinnamon oil chitosan nanoparticle, C- Clove oil chitosan nanoparticle, and D- Cinnamon and Clove oil chitosan nanoparticle

Table 4.38: Zone of inhibition of the nanoparticle treated cotton and polyester fabric against *Pseudomonas*

Sr. No	**Nanoparticles**	**Zone of inhibition (mm) against *Pseudomonas***	
		Cotton fabric	Polyester fabric
1.	Neem Chitosan Np	1.9 ± 0.2	-
2.	Cinnamon Chitosan Np	1.8 ± 0.2	-
3.	Clove Chitosan Np	2 ± 0.3	-
4.	Clove+ Cinnamon Np	3.2 ±1.3	-

The given results in the figure 4.13 and table 4.38 represent the effectiveness of different oil nanoparticles against *Pseudomonas* on treated cotton and polyester fabric. *Pseudomonas* is a Gram-negative bacterium. The results indicate that polyester fabric showed no inhibition towards *Pseudomonas*, regardless of the type of nanoparticle treatment used. This was similar with the results obtained for *Bacillus cereus* and *Staphylococcus aureus*, indicating that the hydrophobic nature of polyester hinders the interaction of nanoparticles with bacterial cells.

However, cotton fabric showed varying levels of inhibition depending on the type of oil nanoparticle used. Among the different oil nanoparticles tested, clove+ cinnamon chitosan nanoparticles showed the highest zone of inhibition with 3.2 ± 1.3 mm. This is consistent with the results obtained for *Staphylococcus aureus* and *Bacillus cereus*, indicating that the combination of clove and cinnamon oil nanoparticles may have a broad-spectrum antimicrobial effect.

Clove chitosan nanoparticles showed the second-highest zone of inhibition with 2 ± 0.3 mm. This is similar to the results obtained for Staphylococcus aureus, indicating that clove oil nanoparticles possess antimicrobial properties against a broad range of bacteria. Cinnamon chitosan nanoparticles showed a zone of inhibition of 1.8 ± 0.2 mm, which is lower than the results obtained for *Staphylococcus aureus* and *Bacillus cereus.* Neem chitosan nanoparticles showed the lowest zone of inhibition with 1.9 ± 0.2 mm, which is consistent with the results obtained for *Staphylococcus aureus* and *Bacillus cereus.*

D) Assessment of *Escherichia coli* activity of the treated cotton and polyester fabric

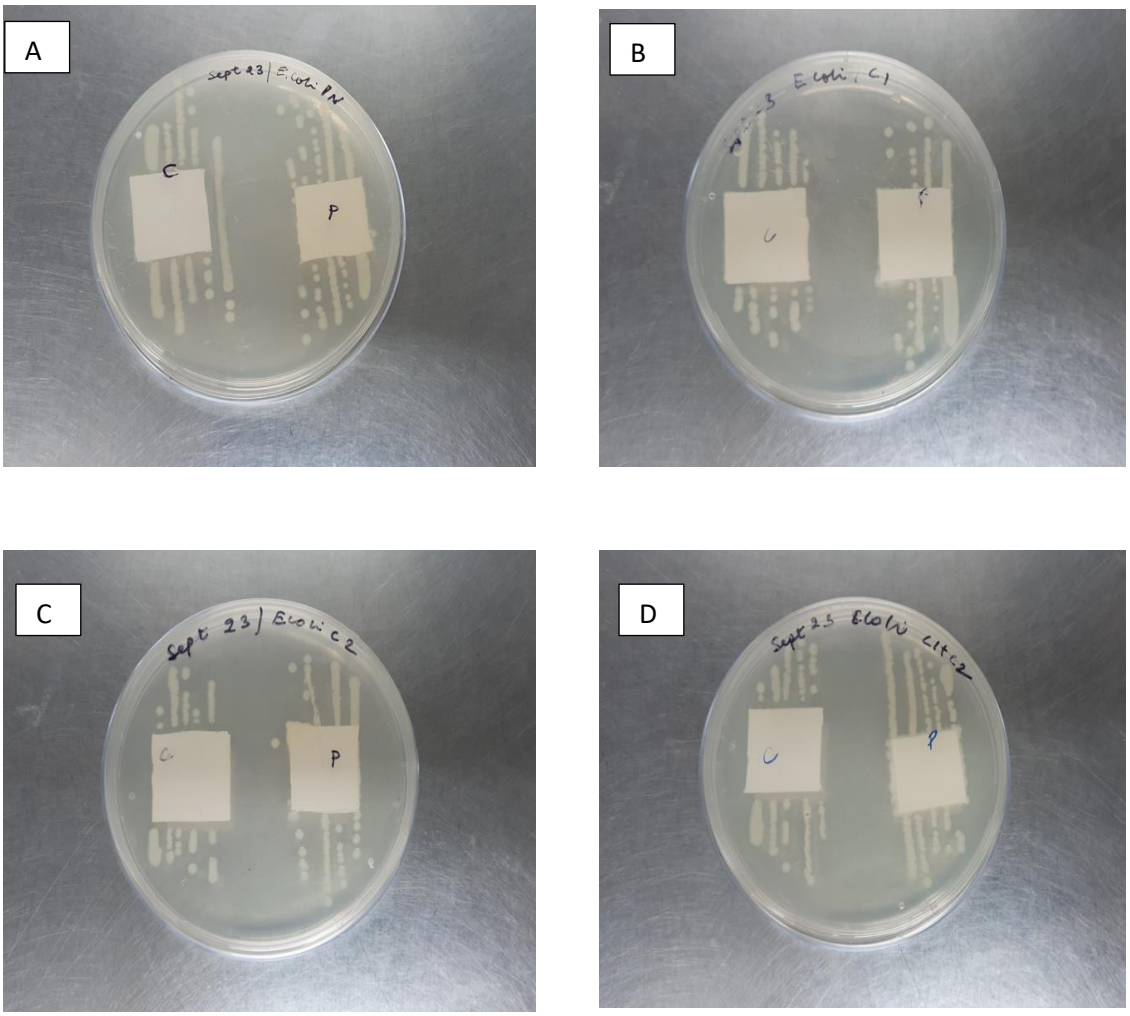

Fig. 4.14: Antibacterial activity of the treated cotton (on the left of the petri dish) and polyester fabric (on the right of the petri dish) against *Escherichia coli.*
A-Neem oil chitosan nanoparticle, B- Cinnamon oil chitosan nanoparticle, C- Clove oil chitosan nanoparticle, and D- Cinnamon and Clove oil chitosan nanoparticle

Table 4.39 : Zone of inhibition of the nanoparticle treated cotton and polyester fabric against *Escherichia coli*

Sr. No	**Nanoparticles**	**Zone of inhibition (mm) against *E. coli***	
		Cotton fabric	Polyester fabric
1.	Neem Chitosan Np	0.8 ± 0.1	-
2.	Cinnamon Chitosan Np	1 ± 0.2	-
3.	Clove Chitosan Np	1.58 ± 0.42	-
4.	Clove+ Cinnamon Np	1.7 ± 0.3	-

Table 4.39 and figure 4.14 represents results showing effectiveness of different oil nanoparticles against *Escherichia coli* (E. coli) on treated cotton and polyester fabric. E. coli is a Gram-negative bacterium. The results indicate that polyester fabric showed no inhibition towards E. coli, regardless of the type of nanoparticle treatment used.

Cotton fabric showed varying levels of inhibition depending on the type of oil nanoparticle used. Clove chitosan nanoparticles showed the highest zone of inhibition with 1.58 ± 0.42 mm. This is lower than the results obtained for *Staphylococcus aureus*, *Pseudomonas*, and *Bacillus cereus*, indicating that E. coli may be less susceptible to clove oil nanoparticles.

Clove+ cinnamon chitosan nanoparticles showed the second-highest zone of inhibition with 1.7 ± 0.3 mm, followed by cinnamon chitosan nanoparticles with 1 ± 0.2 mm. Neem chitosan Np showed the lowest zone of inhibition with 0.8 ± 0.1 mm. These results suggest that cinnamon and clove oil nanoparticles may have a broader spectrum of antimicrobial activity against E. coli compared to neem oil nanoparticles.

E) Antibacterial assessment of blank chitosan nanoparticles treated cotton and polyester fabric against selected bacterial species

Chitosan has been widely studied and recognized for its potential antimicrobial properties. However, to fully evaluate the impact of essential oil-loaded nanoparticles on fabric in terms of its antibacterial activity, it was necessary to explore how blank chitosan affect its effectiveness. Therefore, blank chitosan nanoparticles were prepared using the same optimized conditions and then coated on cotton and polyester fabric to investigate its effect on the bacterial colonies. By comparing the efficacy of essential oil-loaded nanoparticles with that of chitosan on bacterial activity, researcher aimed to understand the combined contribution of chitosan and essential oils to the overall antibacterial activity of the coated fabrics. The test was performes in triplicate to have an average value.

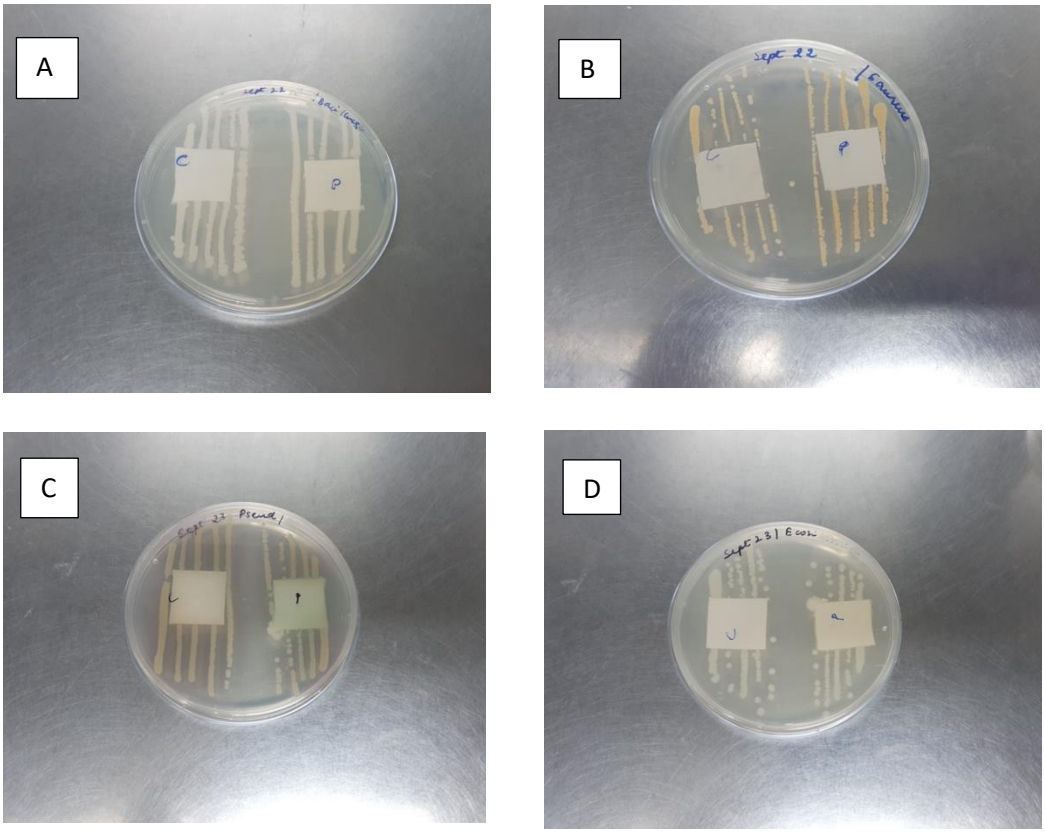

Fig. 4.15: Antibacterial activity of blank chitosan nanoparticles on cotton (on the left of the petri dish) and polyester fabric (on the right of the petri dish) against A-*Bacillus cereus*, B-*Staphylococcus aureus*, C- *Pseudomonas*, and D- *Escherichia coli*.

Figure 4.15 shows the antibacterial activity of the blank chitosan nanoparticles coated on the cotton and polyester fabric. 1% concentration of chitosan, 0.75% tween 80 and, 1% TPP was used to develop the blank chitosan nanoparticle solution which is the same that was used for developing essential oil chiotsan nanoparticles. The results from the figure shows that the prepared blank chitosan nanoparticles had no effect on the bacterial repellency property. No zone of inhibition was observed in any of the samples against all the four bacterial species.

The study investigated the effectiveness of different oil nanoparticles against four different bacterial strains, namely *Staphylococcus aureus, Bacillus cereus, Pseudomonas,* and *E. coli, on* both cotton and polyester fabrics. The results indicate that the hydrophobic nature of polyester hinders the absorption of the finish and interaction of nanoparticles with bacterial cells, leading to no inhibition of all tested bacterial strains on polyester fabric, regardless of the type of nanoparticle treatment used.

The results from the treated cotton fabric indicate that the essential oil-loaded chitosan nanoparticles have a significant effect on the bacterial colonies, while blank chitosan nanoparticles had no effect on bacterial repellency. This suggests that the effectiveness of oil nanoparticles against different bacterial species varied solely depending on the type of oil used in the nanoparticle and the fabric substrate. Neem, clove, and cinnamon essential oils contain several bioactive compounds with antimicrobial properties. When these oils are released from nanoparticles, their mode of action against bacteria attribute to the chemical composition of the oils and their interactions with bacterial cells.

Among the four essential oil nanoparticles tested, combination of clove and cinnamon oil nanoparticles showed the highest zone of inhibition against *Bacillus cereus, Staphylococcus aureus, Pseudomonas*, and *E. coli*. This combination of clove and cinnamon oil nanoparticles showed promising results against these bacterial species, which could be due to their synergistic effect. While in single oil nanoparticles, clove showed the highest zone of repellency against the four bacterial colonies followed by cinnamon oil chitosan nanoparticles.

Clove essential oil contains a high concentration of eugenol, which has been shown to possess antibacterial activity against a variety of bacteria. Eugenol is believed to exert its antimicrobial action by damaging the cell membrane and disrupting the cytoplasmic contents of bacterial cells. Additionally, eugenol can inhibit bacterial enzyme activity and metabolic processes, leading to bacterial cell death (Chouhan et al., 2017).. It is noteworthy that clove oil nanoparticles exhibited the strongest antibacterial properties, despite having the lowest entrapment efficiencies compared to other essential oil nanoparticles. While Cinnamon essential oil contains several bioactive compounds, including cinnamaldehyde, eugenol, and linalool, that have been shown to possess antimicrobial properties. The nanoparticles showed an average repellency when compared to clove and neem oil nanoparticles.

Whereas, Neem essential oil contains a complex mixture of bioactive compounds such as azadirachtin, nimbin, nimbinin, and salannin. These compounds have varying molecular weights and polarities, which can affect their ability to diffuse through the nanoparticle matrix and into bacterial cells. Azadirachtin is a potent insecticide and antifeedant, while nimbin and nimbinin have been reported to possess antifungal and antibacterial activities. Salannin has also been shown to have antibacterial activity. The antimicrobial action of neem oil is thought to be

due to its ability to disrupt bacterial cell membranes and inhibit essential enzymes and metabolic pathways.

Despite of the ability of the bacterial repellency, neem oil nanoparticles consistently showed the lowest zone of inhibition against all bacterial species tested. One of the reasons for the neem chitosan nanoparticles to show the least antimicrobial effect could be the slow release of the oil from the nanoparticles that was observed in the stability and oil release studies. The neem nanoparticles showed high oil retention after one and two months which means the release rate of the bioactive compounds present in neem essential oil from the nanoparticles matrix was slow. On the contrary, the release rate of the clove and cinnamon oil from their nanoparticles was significantly high when compared to that of neem nanoparticles. Therefore, they showed more promising results as compared to that of neem chitosan nanoparticles.

One of the most interesting findings was that the nanoparticles exhibited the highest level of bacterial repellency against *Bacillus cereus* and *Staphylococcus*, which are both gram-positive bacteria, compared to *Pseudomonas* and *E. coli*, which are gram-negative bacteria (E.coli being the lowest). This suggests that gram-positive bacteria may be more susceptible to essential oils compared to gram-negative bacteria. This could be due to the fact that gram-negative bacteria have a rigid outer membrane that is rich in lipopolysaccharide (LPS) and is more complex, making it difficult for hydrophobic compounds to diffuse through it. In contrast, gram-positive bacteria lack this extra complex membrane and are surrounded by a thick peptidoglycan wall that is not dense enough to resist small antimicrobial molecules, making it easier for them to access the cell membrane. Additionally, lipoteichoic acid present in the cell membrane of gram-positive bacteria may facilitate the infiltration of hydrophobic compounds from essential oils due to its lipophilic ends (Chouhan et al., 2017).

In conclusion, the study suggests that clove and cinnamon oil nanoparticles, particularly in combination showed a synergetic broad-spectrum antimicrobial effect against different bacterial species causing highest zone of inhibition of 4mm followed by neem nanoparticles. Thilagavathi & Kannaian (2008) also observed similar results the Prickly Chaff extracts coated cotton fabric. 3 to 5 % of extracts showed between 2.5 - 4.5 mm of zone of inhibition against Staphylococcus aureus and between 0-2.5 mm against E. coli.
While it is also noteworthy that even the lowest amount of essential oil used in the study, which was 1%, resulted in satisfactory antibacterial activity.

4.7.2 Determination of Antifungal test using standard AATCC 30: Antifungal Assessment and Mildew Resistance Test

The treated fabric samples were exposed to the fungal colonies for the period of 14 days. The experiments were conducted three times to obtain an average outcome shown below.

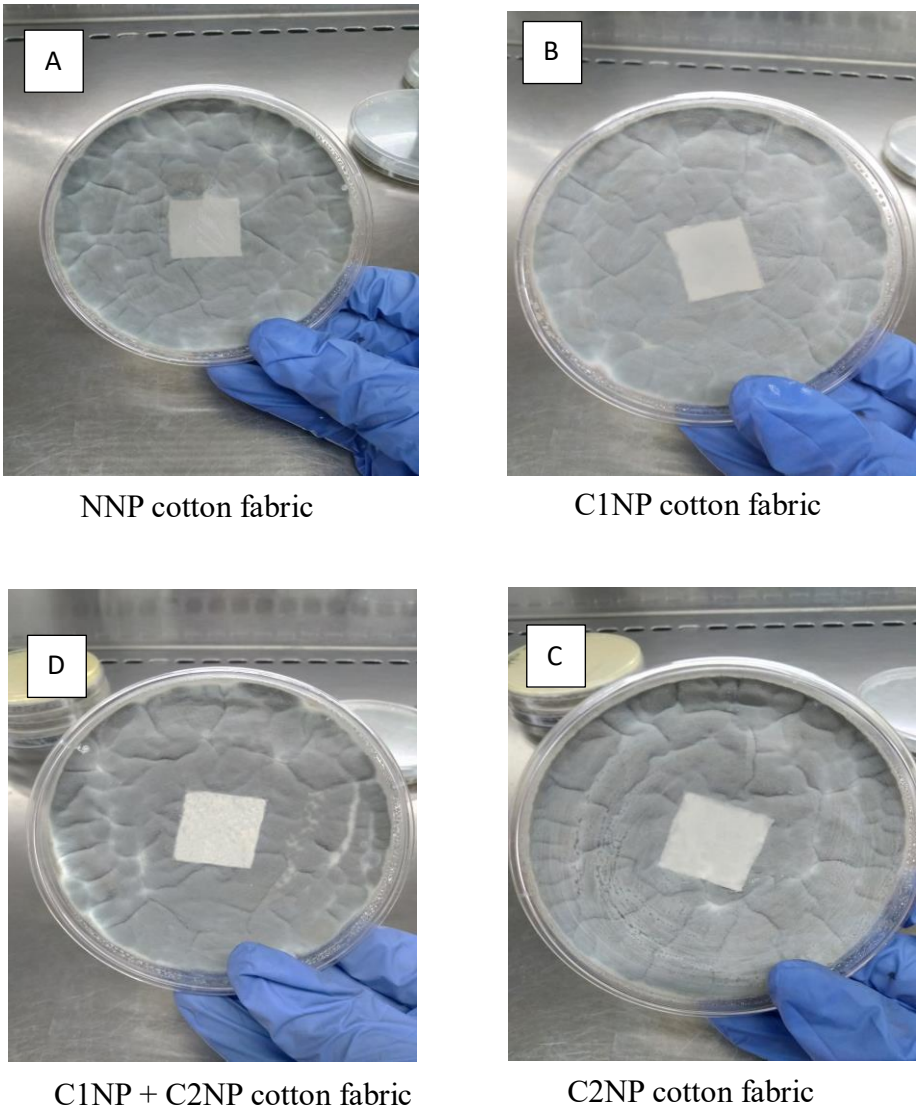

NNP cotton fabric | C1NP cotton fabric

C1NP + C2NP cotton fabric | C2NP cotton fabric

Fig. 4.16: Antifungal activity of the treated cotton fabric against *Aspergillus fumigatus* (A- Neem nanoparticles, B- C1NP- Cinnamon nanoparticles, C- C2NP-Clove nanoparticles, and D- C1NP+C2NP- Cinnamon and Clove nanoparticle)

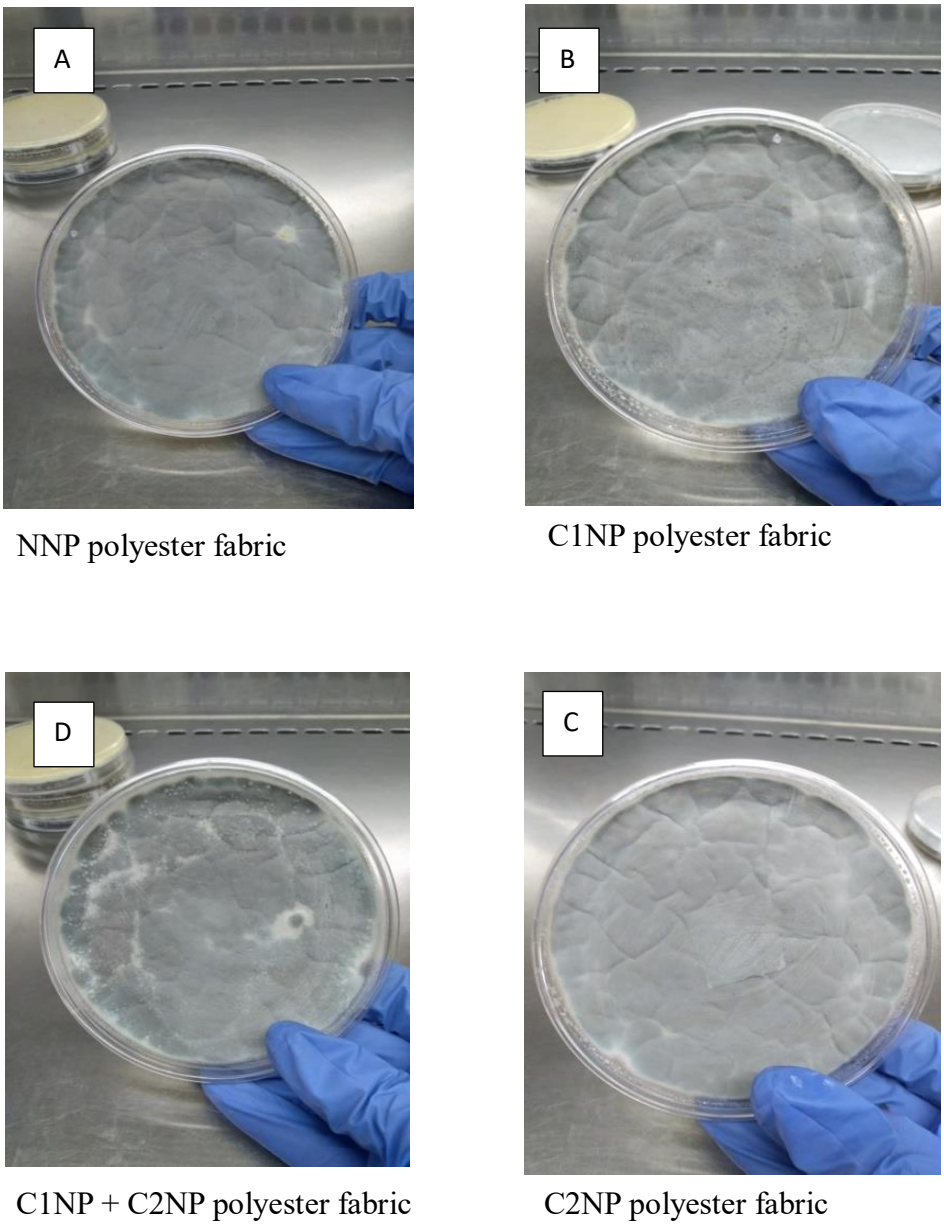

Fig. 4.17: Antifungal activity of the treated polyester fabric against *Aspergillus fumigatus*

(A- NNP-Neem nanoparticles, B- C1NP- Cinnamon nanoparticles, C- C2NP-Clove nanoparticles, and D- C1NP+C2NP- Cinnamon and Clove nanoparticle)

Researcher had also conducted a test on cotton and polyester fabric treated with chitosan nanoparticles that were not infused with any active substance to determine the impact of chitosan on the antifungal property. The outcome indicated that there was no resistance to fungal spores, suggesting that the antifungal ability required more than 1% chitosan.

The figure 4.16 and figure 4.17 represent the results after exposing the treated cotton and polyester fabric to *Aspergillus fumigatus* after incubating the plates at 30°C ± 2°C for 14 days. As seen in the figures, a macroscopic growth was observed in all the plates. All the treated cotton fabric were successful in resisting the growth of fungi on the surface of the fabric. This explains that the finish was successful in repelling the growth of fungi on the cotton fabric. However, the resistance was not widespread across the circumference of the fabric.

On the other hand, the treated samples of polyester fabric did not show any repellency. The treated polyester samples and the entire petri plates were covered with fungal growth. The lack of repellency towards *Aspergillus fumigatus* means that the fungal spores were able to penetrate the fabric and grow on the surface, resulting in the visible fungal growth all over.

A possible explanation for this behaviour could be that the polyester fabric did not absorb or adsorb the finish. Polyester is a synthetic fiber that is made up of long-chain polymers consisting of ester units. Polyester is hydrophobic and does not absorb water. The hydrophobic nature of polyester must have made it difficult for chitosan nanoparticles to adhere to the fabric surface resulting in less effective absorption. Thus, the fungal colonies were easy to spread over the fabric in a closed petri plate for 14 days. On the other hand, cotton fabric is hydrophilic in nature and have a negative charge surface. Along with that citric acid acts as a dispersing agent, it stabilizes the chitosan nanoparticles and help in even coating. When chitosan nanoparticles are applied to cotton fabric, the positively charged nanoparticles are attracted to the negatively charged cotton fibers. The nanoparticles adhere to the cotton fibers through electrostatic interactions resulting in a more effective coating of the fabric with essential oil chitosan nanoparticle.

To confirm that the nanoparticles were coated or not on the polyester fabric, EDX analysis of both the cotton and polyester fabric optimized essential oil nanoparticles was conducted.

4.7.3 Surface analysis of the coated cotton and polyester fabric using Energy dispersive X-ray spectroscopy (EDX)

The results of the antibacterial and antifungal tests indicated that solely the cotton fabric exhibited a noteworthy ability to repel microbes, whereas the polyester fabric did not possess any repellent characteristics towards the chosen bacteria and fungi. This lack of repellency in

the polyester fabric may be attributed to its hydrophobic nature, which prevented it from absorbing or adsorbing the finishing agent. To investigate this further, EDX analysis was conducted to identify the elements present on the surface of the coated cotton and polyester fabrics. The treated samples were trimmed into 2x2 mm dimensions, coated with gold for conductivity, and examined under an EDX microscope. The figure 4.18- 4.21 illustrates the results of an EDX analysis performed on cotton and figure 4.22-4.25 illustrates the results of EDX analysis of polyester fabrics that had been coated with optimized neem, clove, cinnamon and clove + cinnamon essential oil chitosan nanoparticles.

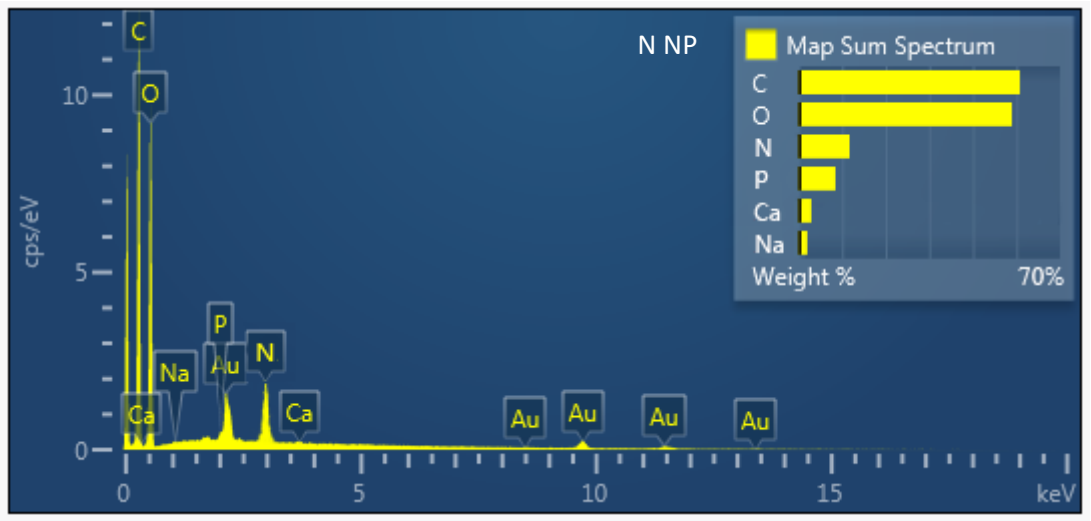

Fig. 4.18 : EDX analysis of neem essential oil chitosan nanoparticle coated cotton fabric

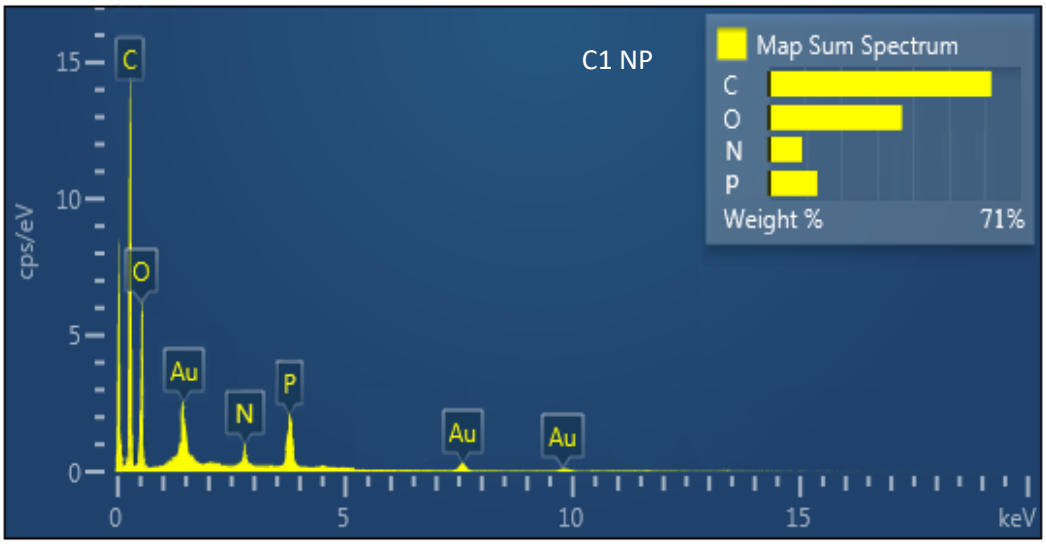

Fig. 4.19 : EDX analysis of Cinnamon essential oil chitosan nanoparticle coated cotton fabric

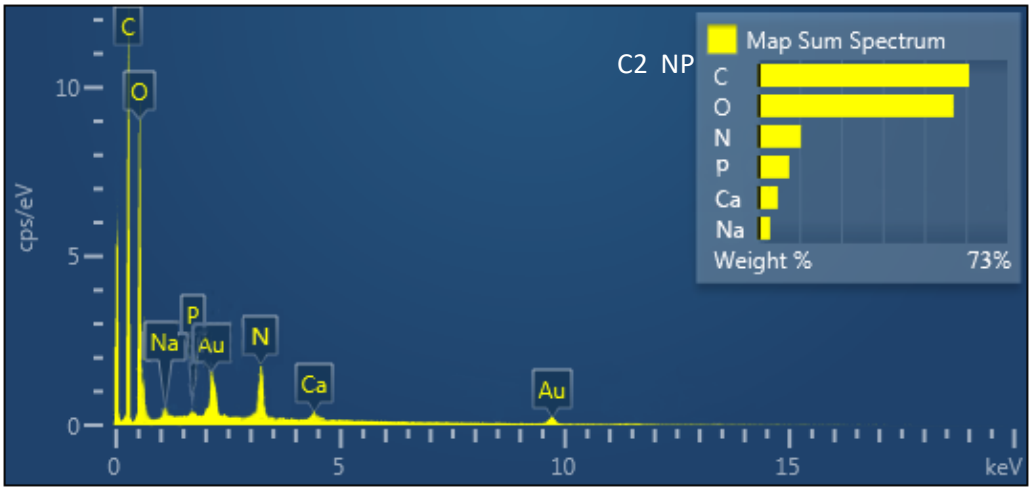

Fig. 4.20: EDX analysis of Clove essential oil chitosan nanoparticle coated cotton fabric

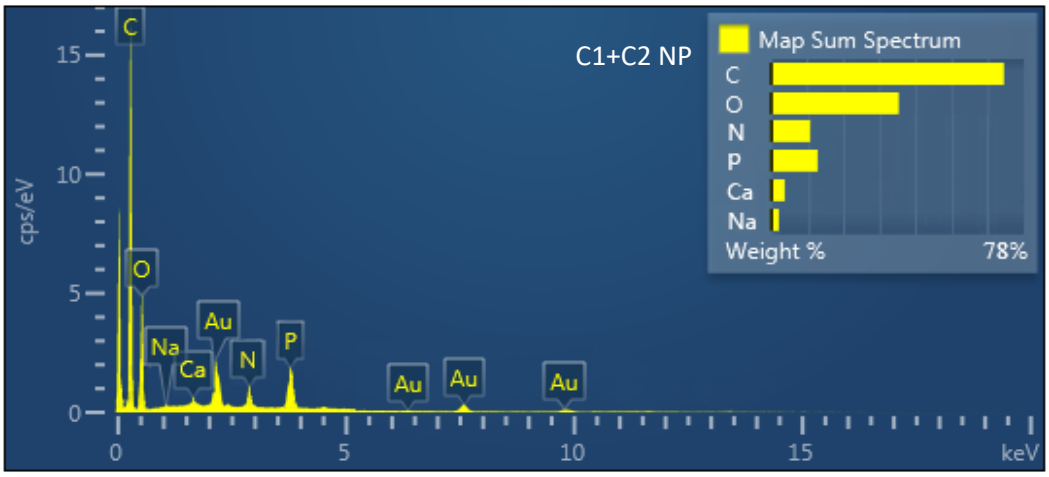

Fig. 4.21: EDX analysis of Cinnamon and Clove essential oil chitosan nanoparticle coated cotton fabric

The above figure 4.18-4.21 illustrates the results of EDX analysis conducted on cotton fabrics treated with nanoparticles of essential oils from neem, cinnamon, clove, and a combination of cinnamon and clove. The EDX analysis reveals the presence of Carbon and Oxygen in all the treated samples, along with minor quantities of Nitrogen, Sodium, Phosphorus, and Calcium.

The peaks of Nitrogen observed in all samples indicate the presence of chitosan and minerals on the treated fabrics. The trace amounts of Sodium and Phosphorus can be attributed to the use of tripolyphosphate as a crosslinking agent during nanoparticle development. These minerals are likely to be present due to the hydrophilic nature of cotton fabric, which facilitates the absorption and coating of the finish on the fabric.

The presence of Calcium in small quantities could be indicative of impurities from chitosan, which is a natural polymer used in the nanoparticle synthesis process. However, the amount of Calcium detected is negligible and not significant enough to impact the overall efficacy of the treated fabric. Based on the EDX analysis results, it can be suggested that the essential oil nanoparticles have been successfully applied to the cotton fabric,

In contrast, the EDX analysis of all essential oil nanoparticles coated on polyester fabric in a figure 4.22- 4.25 showed no signs of any minerals present on any of the samples. This lack of mineral presence could be attributed to the hydrophobic nature of polyester fabric, which inhibits the absorption of the finish onto the fabric.

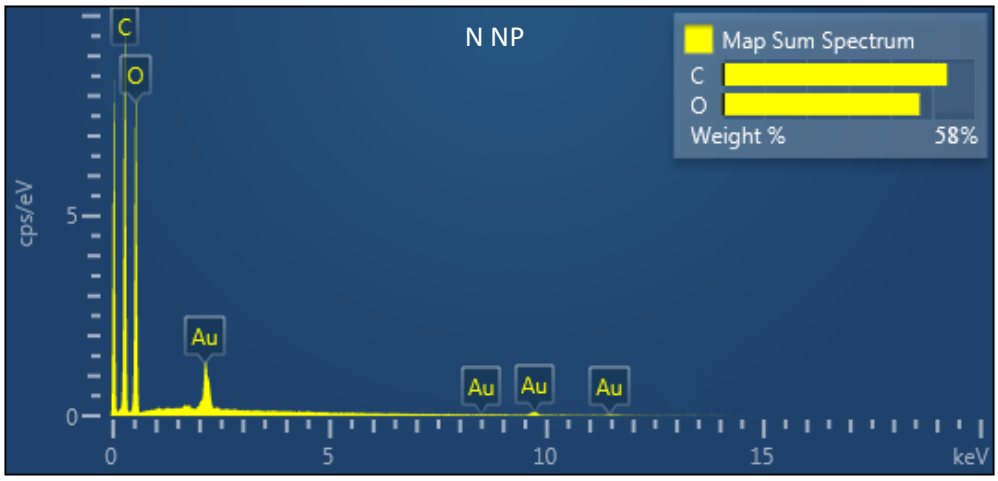

Fig. 4.22 : EDX analysis of neem essential oil chitosan nanoparticle coated polyester fabric

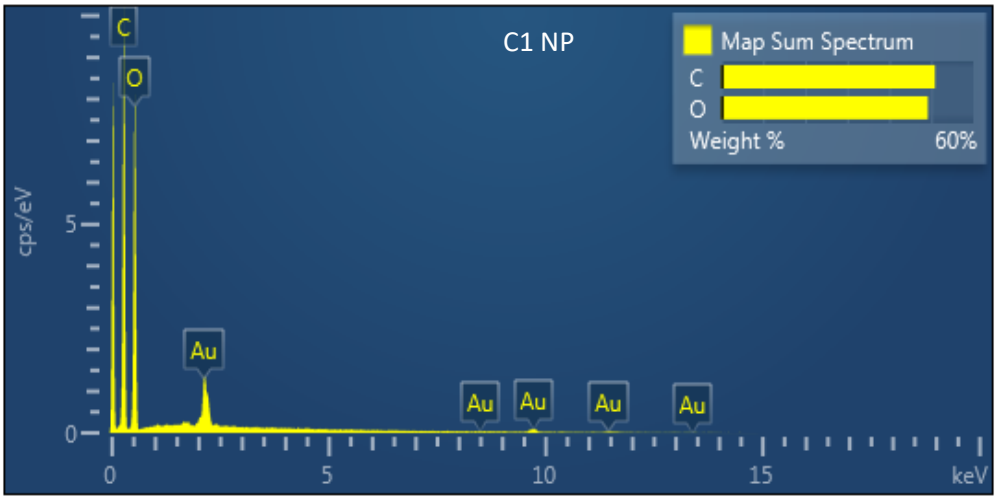

Fig. 4.23: EDX analysis of cinnamon essential oil chitosan nanoparticle coated polyester fabric

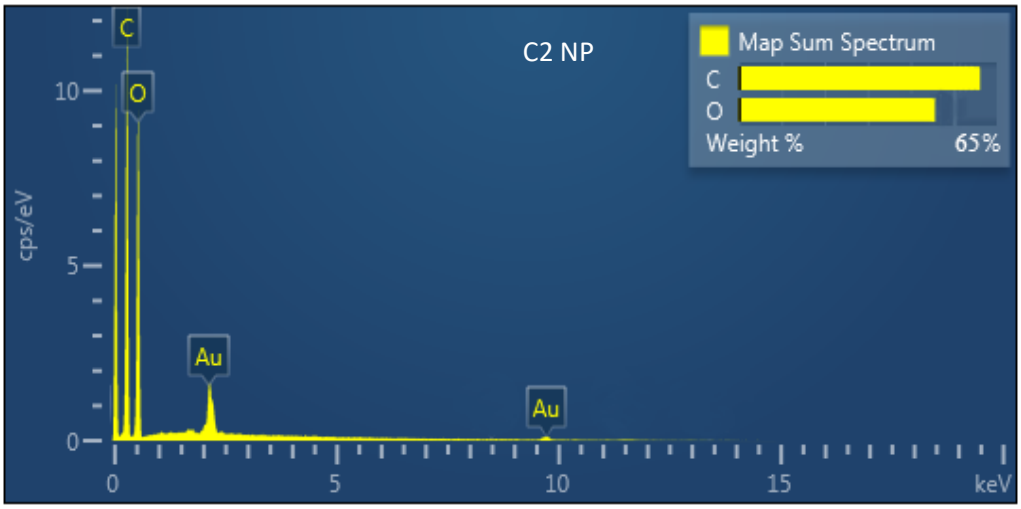

Fig. 4.24 : EDX analysis of clove essential oil chitosan nanoparticle coated polyester fabric

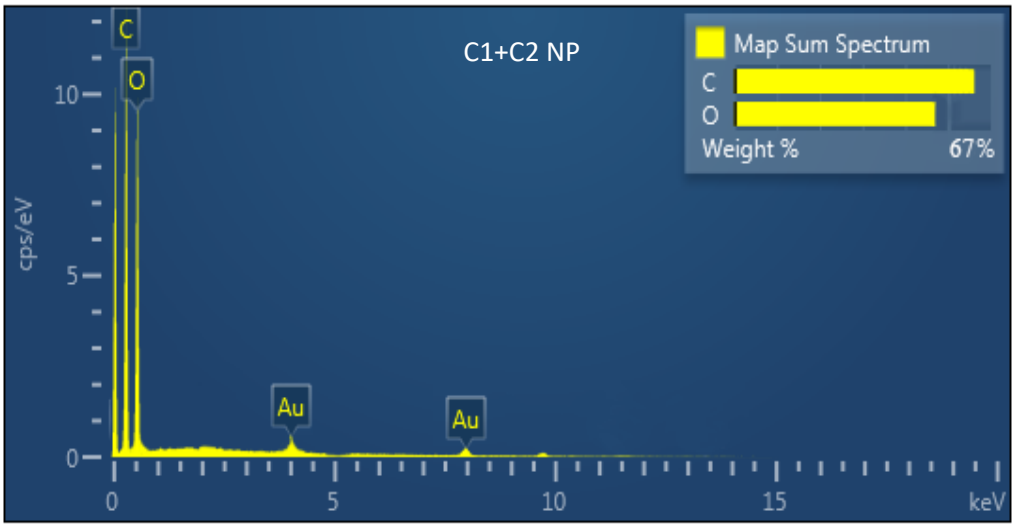

Fig. 4.25: EDX analysis of cinnamon+ clove essential oil chitosan nanoparticle coated polyester fabric

The discussion of these findings can help explain the differences in the antibacterial and antifungal properties observed between the cotton and polyester fabrics, with cotton demonstrating significant repellency against microbes and polyester showing no repellent properties. Therefore, it was concluded that cotton fabric was the optimal substrate and polyester fabric was excluded from further experimentation. Subsequently, only treated cotton fabric was used to conduct the additional tests for all four sets of nanoparticle coating.

4.7.4 Determining the physicochemical stability of the nanoparticles over time and storage conditions

To ensure the effectiveness of the treated fabric in different environmental conditions, the entrapment efficiency of all the treated fabric samples was calculated. One set of samples was kept in a large petri dish at (25°C ± 2) and 65 ± 2% RH, while the other set was exposed to the environment at (25°C ± 2) and 65 ± 2% RH. The entrapment efficiency was calculated for both sets of samples after one month and then again after another month (total two months). By doing so, the percentage of oil retained in the nanoparticles was determined after two months. This helped in evaluating the long-term effectiveness of the treated fabric in different environments. All the samples were exposed to the conditions in triplicates to have an average % retention.

Table 4.40: % retention of oil of covered samples in a petri dish

Sr. No	NP sample	Months	Absorbance (nm)	% Retention	% Change
1.	Neem	0	0.317	100	0
		1	0.314	99.10	0.9
		2	0.308	97.32	2.68
2.	Clove	0	0.613	100	0
		1	0.604	98.56	1.44
		2	0.595	97.13	2.87
3.	Cinnamon	0	0.858	100	0
		1	0.805	93	7
		2	0.794	92	8

The data presented in table 4.40 and table 4.41 indicate the percentage of retained essential oil in nanoparticle-treated fabric under different conditions. Upon comparing all three samples under both conditions, it was observed that the fabric treated with neem essential oil loaded nanoparticles exhibited the highest oil retention of 99.10% after one month and 97.32% after two months in a closed environment. Similarly, it showed the highest oil retention of 93.77% after one month and 87.23% after two months in an open environment. Following neem, clove oil exhibited the highest oil retention of 98.56% after one month and 97.13% after two months

in a closed environment but not in an open environment. Cinnamon oil had the second-highest release rate in an open environment.

Table 4.41: % retention of oil for Uncovered samples (exposed to room temperature)

Sr. No	NP sample	Months	Absorbance (nm)	% Retention	% Change
1.	Neem	0	0.317	100	0
		1	0.296	93.77	6.23
		2	0.274	87.23	12.77
2.	Clove	0	0.613	100	0
		1	0.543	88.55	11.15
		2	0.472	77.66	22.34
3.	Cinnamon	0	0.858	100	0
		1	0.784	90.33	9.67
		2	0.713	81.45	18.55

This could be due to the neem essential oil being high in its density, its release rate from the nanoparticles must be slow as compared to clove and cinnamon oil. This could be due to the fact that neem essential oil has a complex composition, consisting of several bioactive compounds such as azadirachtin, nimbin, nimbinin, and salannin. These compounds have varying molecular weights and polarities, which can affect their ability to diffuse through the nanoparticle matrix. Additionally, neem oil has a higher viscosity and density than clove oil and cinnamon which may also contribute to its slower release rate. (Agustinisari et al., 2020) mentioned that when microcapsules contain a higher amount of essential oil, the chances of release rate of these oils increase. This is caused by a reduction in the thickness of the microcapsule wall, which means that there is not enough wall material to fully encapsulate the oil or in some cases to sustain the essential oil for longer period of time.

On the other hand, clove essential oil is a monoterpenoid-rich oil with low viscosity and lower density. It has a smaller molecular weight than neem oil and can diffuse more easily through the nanoparticle matrix, resulting in a faster release rate. Similarly, cinnamon essential oil is rich in cinnamaldehyde, which has a smaller molecular weight than the compounds found in neem oil and can diffuse through the nanoparticle matrix more quickly. Therefore, clove and

cinnamon essential oils may be released more quickly from chitosan nanoparticles than neem essential oil.

The information gathered from the release rate of the essential oils can be compared to the findings of the antibacterial experiment. The neem oil, which had a slower release rate, showed lower antibacterial activity compared to cinnamon and clove oils that had a faster release rate. The statement suggests that there is a correlation between the release rate of the essential oils and their antibacterial activity. The slower the release rate of the essential oil, the lower the antibacterial activity observed.

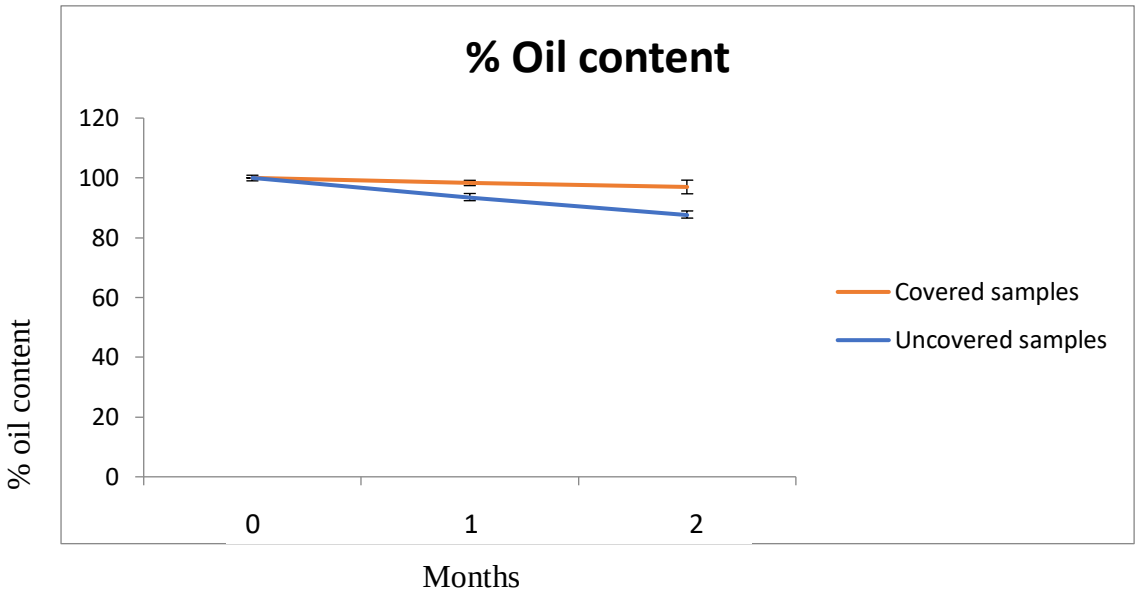

Graph 4.9: Change in % entrapment efficiency of Neem essential oil chitosan nanoparticle treated cotton fabric after exposing to different storage condition for two months

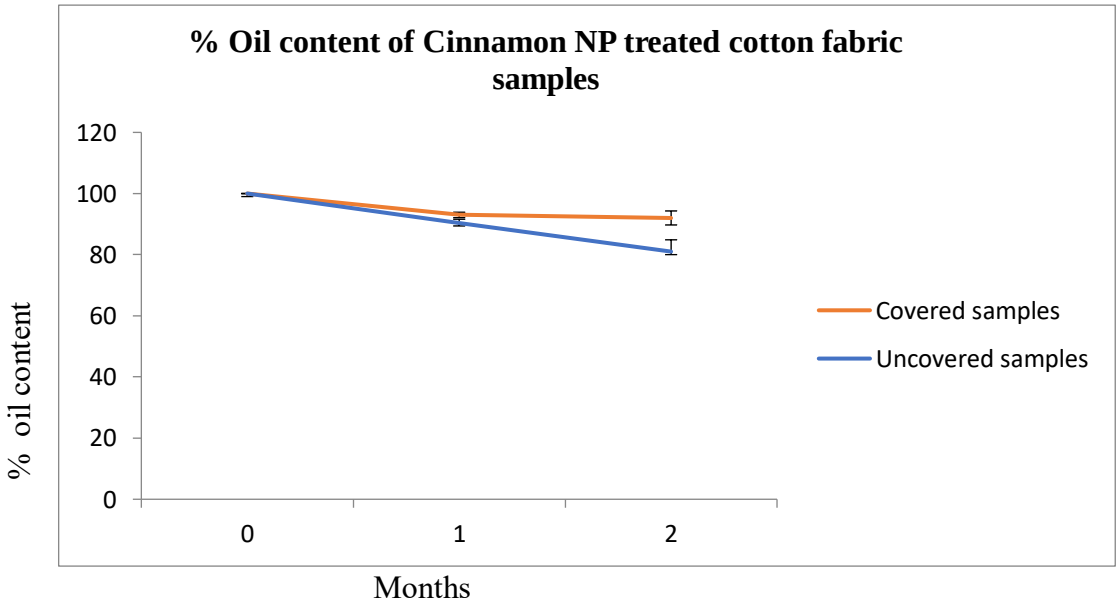

Graph 4.10: Change in % entrapment efficiency of Cinnamon essential oil chitosan nanoparticle treated cotton fabric after exposing to different storage condition for two months

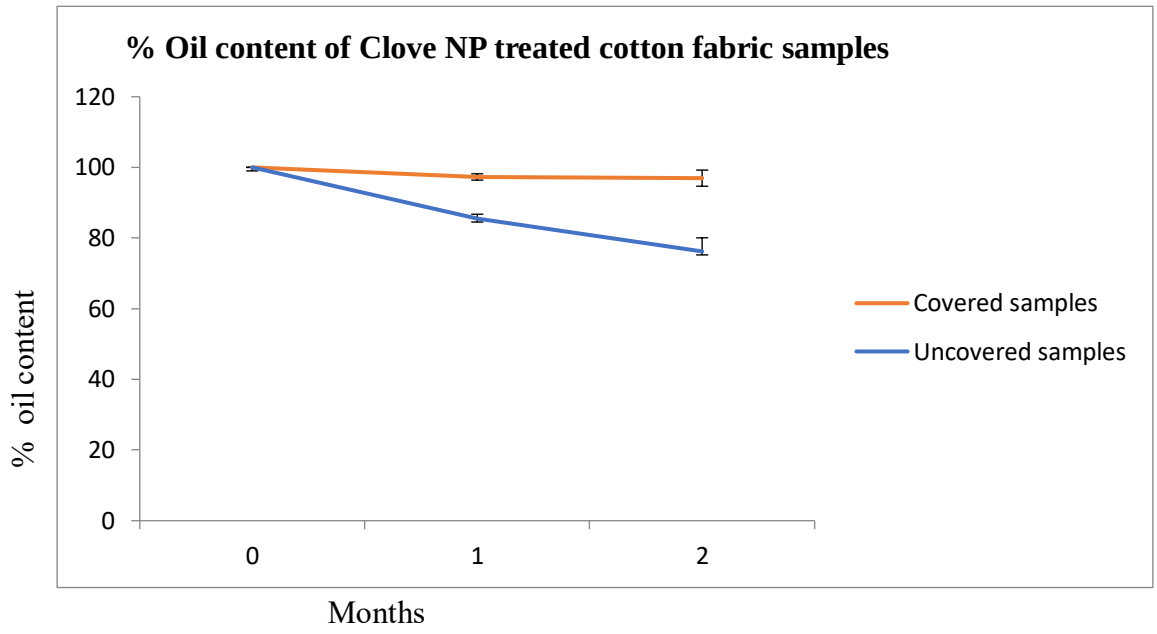

Graph 4.11: Change in % entrapment efficiency of Clove essential oil chitosan nanoparticle treated cotton fabric after exposing to different storage condition for two months

Overall, the % change data from the table 4.39 and table 4.40 indicates that for all three cotton fabric samples treated with essential oil nanoparticles, there was a significant decrease in percent retention as the release rate increased by 50% in the second month compared to the first month as also seen in graph 4.10 and 4.11. This decline was observed in samples that were exposed to the environment. In other words, as the release rate of the essential oils increased, the effectiveness of the treatment in maintaining the antimicrobial and insect repellent properties of the fabric will decrease over time.

It is noteworthy that the percentage of essential oil trapped in the nanoparticle remains above 50% even after being exposed to the environment for two months. The statement highlights the durability of the treated fabric finish, indicating that it can remain effective in trapping essential oils for up to four to five months.

4.7.5 Determination of resistance to insects using standard ISO 3998:1977

Cigarette beetles, scientifically known as Lasioderma serricorne, have the potential to cause damage to textiles that are stored in museums. These insects are known to harm a variety of

objects, including upholstery, plant textiles, mummies, and animal mounts. Infestations of cigarette beetles are more likely to occur in the presence of dried plant materials, such as tobacco leaves, which are often used for preservation in museums as they are a preferred food source for these beetles. Cigarette beetles can also feed on dried animal specimens, such as feathers, fur, and animal hair, which are commonly used in textiles. They are particularly harmful to ethnographic collections, as they reproduce and develop rapidly, causing significant damage to the objects (Querner, 2015).

Additionally, cigarette beetles are attracted to textiles that have been soiled or stained with food, oils, or other organic materials, and their larvae feed on the textile fibers, creating small holes and tunnels in the material. This can lead to weakening of the fabric and permanent damage to the textile. Depositing fecal pellets on the fabric is another way that cigarette beetles can cause damage, staining and weakening the material further. Therefore, it is essential to take measures to prevent infestations of cigarette beetles to safeguard the collections in museums.

Due to their ability to feed on both cellulosic and protein textiles, these insects were selected for testing the repellency of cotton treated with optimized conditions. Figure 4.26 and 4.27 shows glass jars that had been sterilized and fitted with lids containing holes to allow for aeration. The purpose of this setup was to prevent larvae from dying during an experiment. Each jar contained an individual fabric sample that had been optimized with neem essential oil loaded chitosan nanoparticles, clove essential oil loaded chitosan nanoparticles, cinnamon essential oil loaded chitosan nanoparticles, or a combination of clove and cinnamon essential oil loaded chitosan nanoparticles along with scored and washed untreated fabric. Twenty-five larvae were placed on each fabric sample, and the jars were kept in an incubator room with a constant temperature of 24°C and a relative humidity of 70% for 14 days while being monitored occasionally.

Fig. 4.26: Cigarette beetle larvae were laid on the surface of treated and untreated cotton fabric

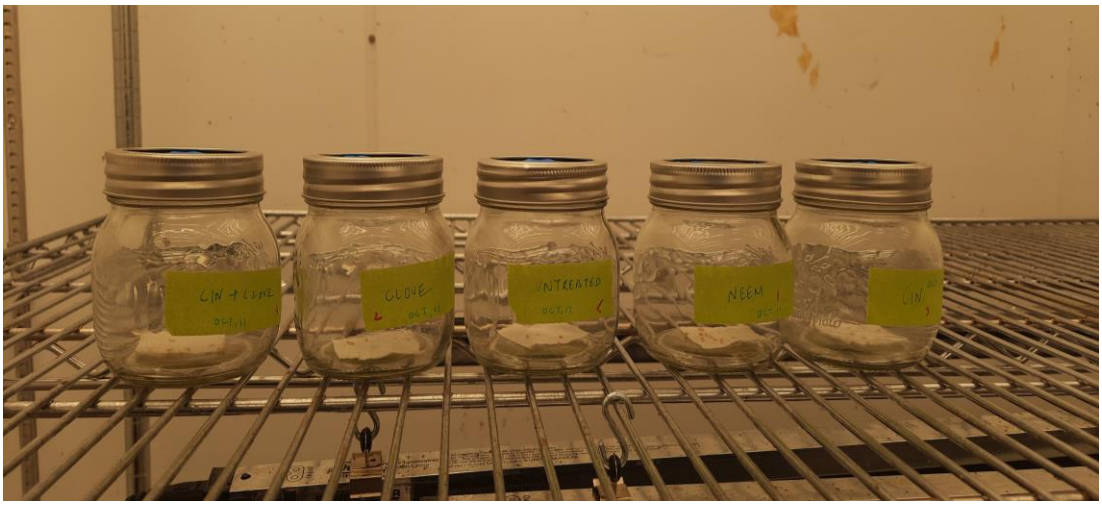

Fig. 4.27: Jars kept in an incubator room at 24C at RH 70% for 14 days

On inspecting after six days, it was observed that all of the larvae in the treated fabric jars had curled up, appeared dark in colour and had moved away from the fabric and towards the edge of the glass. In contrast, some larvae were still on the untreated fabric samples while others were located in the corners of the jars (Figure 4.28).

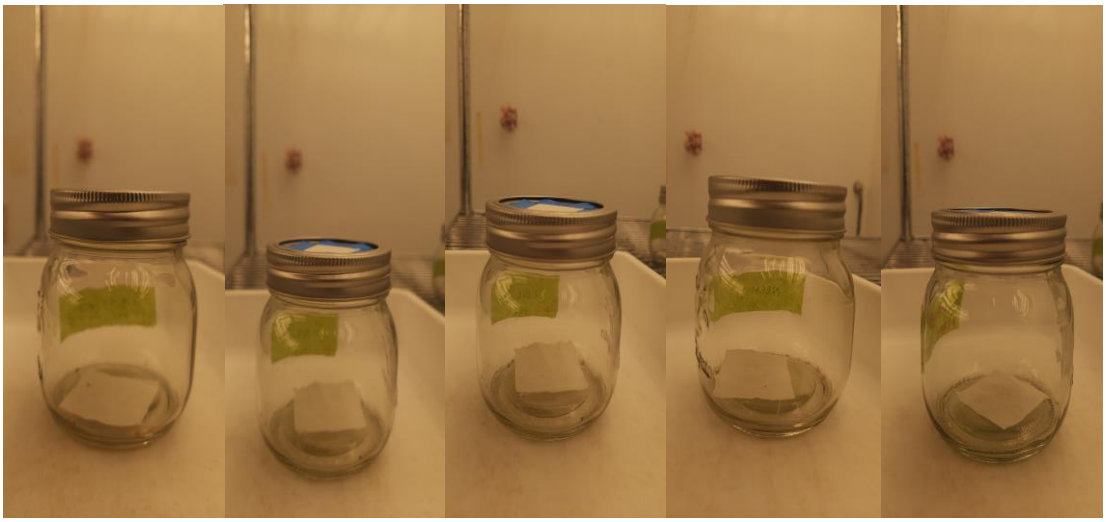

Fig. 4.28: From left- Untreated fabric, C1NP, C2NP, NNP, C1NP + C2NP treated cotton fabrics exposed to cigarette beetle larvae

But, the larvae in the treated fabric jars appeared weak and were barely moving, while those in the untreated fabric jars seemed healthy. By day 12, the larvae in the treated fabric jars had died and turned black indicating its decomposition. Whereas, the larvae in the untreated fabric jars had also died due to a lack of nutrition. Apparently, no holes or surface destruction appeared on the surface of any treated as well as untreated fabric samples. Additionally, the

weight of the fabric samples was noted before and after the test, and there was no loss in weight observed.

One possible explanation of this behavior could be that the essential oil loaded chitosan nanoparticles present in the treated fabric samples were successful in repelling the larvae and eventually causing their demise through prolonged exposure to the volatile compounds. The theory is that the initial rapid release of the volatile compounds from the nanoparticles was sufficient to deter the larvae. In their review paper, (Jasrotia et al., 2022) reported that exposure time to Citrus paradise oil was positively correlated with the mortality rate of T. castaneum (red flour beetle). Additionally, they discussed the effectiveness of various essential oil nanoparticles, such as neem, eucalyptus, and sage, in killing T. castaneum within a 10-12 days exposure period.

While in the previous section (4.7.4), it was observed that the % change of oil or release rate in the first month was low in an enclosed environment condition, it seems that the lower release was still capable of repelling and killing the larvae. Therefore, the use of essential oil loaded chitosan nanoparticles treated cotton fabric can be a potential approach for preventing the infestation of insects and pests.

4.8 SWOC analysis of the developed preservative fabric

Strengths:

- The essential oil loaded chitosan nanoparticles provide a natural and eco-friendly solution for preserving textiles in museums for storage.
- The fabric is effective in repelling insects, which is a major concern in textile preservation.
- The antibacterial and anti-fungal properties of the fabric help prevent microbial growth, which can cause damage to textiles.
- Unlike chemical preservatives, the volatiles releasing from the oils will not cause any side effects on the textiles, on humans and to the environment.
- The control and release mechanism of the essential oil nanoparticles can ensure a sustained and controlled release of the active ingredients, making it more effective and efficient for a longer period of time.
- The range of repellency offered by the essential oil loaded chitosan nanoparticles cotton fabric is much wider compared to the traditional method of using natural ingredients in a sachet, which covers a smaller area.

- Using this fabric eliminates the risk of stains, color fading, and cigarette beetle infestations caused by the use of dried tobacco leaves.
- It simplifies the work of conservators.
- Cotton, being a natural and biodegradable material, makes this fabric a sustainable and affordable option for textile preservation, as it is also breathable.
- The developed finish can be reapplied to the fabric even after its effectivity has reduced.
- Developing the finish requires less complicated technology

Weaknesses:

- The long-term effectiveness of the fabric is up to 5 month and may require replacement after that or reapplication of the finish will be needed.
- The effectiveness of the fabric may vary depending on the extreme change of environment conditions like high temperature.

Opportunities:

- The fabric can be marketed to museums and other organizations that are focused on preserving textiles and artifacts.
- The fabric can also be marketed to individuals at home for storing their textiles in a preserving environment.
- The use of natural and eco-friendly solutions is becoming increasingly popular, which could lead to a higher demand for the fabric.
- The technology could be expanded to other applications, such as home textiles or outdoor fabrics to repel insects and even mosquitoes.

Challenges:

- The effectiveness of the preservative fabric may vary depending on the type and concentration of essential oils used, and the extreme environmental conditions of the textile museum.
- The durability of the preservative fabric may be affected by the exposure to light, moisture, and other environmental factors, which can degrade the essential oils and chitosan nanoparticles over time.
- The fabric may not be effective against all types of insects and microbes, which could limit its usefulness in certain situations.